

**QUANTIFICATION OF GAD67 PROTEIN LEVELS IN AXONAL BOUTONS FROM
DISTINCT SUBTYPES OF GABA NEURONS: REDEFINING CIRCUIT LEVEL
ALTERATIONS IN THE PREFRONTAL CORTEX OF SCHIZOPHRENIA**

by

Brad Ronald Rocco

Bachelor of Science in Neuroscience, Allegheny College, Meadville, PA, 2007

Submitted to the Graduate Faculty of
University of Pittsburgh School of Medicine in partial fulfillment
of the requirements for the degree of
Doctor of Philosophy

University of Pittsburgh

2015

UNIVERSITY OF PITTSBURGH

SCHOOL OF MEDICINE

This dissertation was presented

by

Brad Ronald Rocco

It was defended on

June 4, 2015

and approved by

Patrick Hof, MD, Department of Neuroscience, Icahn School of Medicine at Mount Sinai

Etienne Sibille, PhD, Department of Psychiatry

Tija C. Jacob, PhD, Department of Pharmacology and Chemical Biology

Robert A. Sweet, MD, Department of Psychiatry and Neurology

Committee Chair: J. Patrick Card, PhD, Department of Neuroscience

Dissertation Advisor: Kenneth N. Fish, PhD, Department of Psychiatry

Copyright © by Brad Ronald Rocco

2015

**QUANTIFICATION OF GAD67 PROTEIN LEVELS IN AXONAL BOUTONS FROM
DISTINCT SUBTYPES OF GABA NEURONS: REDEFINING CIRCUIT LEVEL
ALTERATIONS IN THE PREFRONTAL CORTEX OF SCHIZOPHRENIA**

Brad Ronald Rocco, PhD

University of Pittsburgh, 2015

Cognitive impairments are a core feature of schizophrenia, and arise, in part, from deficits in gamma-amino butyric acid (GABA)-releasing neurons within the prefrontal cortex (PFC). ~30% of neurons in the PFC of schizophrenia have markedly reduced mRNA expression for the 67 kDa isoform of the GABA synthesizing enzyme, GAD67. Nearly all GABA neurons in primate neocortex can be classified into non-overlapping subtypes by expressing the calcium-binding proteins parvalbumin (PV), calbindin (CB), and calretinin (CR). About half of all PV neurons, which are subdivided into basket cells and chandelier cells, lack detectable GAD67 mRNA expression in schizophrenia. GAD67 protein levels are lower in axonal boutons from PV basket cells in PFC layers 3-4, and although GAD67 expression has not been assessed in chandelier cells they may also have lower GAD67 levels. Further, GAD67 expression has not been assessed in CB and CR neurons in the illness but correlative evidence suggests that they are differentially affected. For example, CB neurons coexpress somatostatin (SST) and in schizophrenia lower SST mRNA expression is correlated with lower GAD67 mRNA expression at both the tissue and cellular levels. By contrast, CR mRNA expression is unaltered and does not correlate with lower GAD67 mRNA expression. Therefore, lower GAD67 levels in schizophrenia are predicted to be restricted to PV and CB neurons, though this hypothesis has not been directly tested. Accordingly, we assessed GAD67 expression in chandelier, CB, and CR neurons in the PFC of schizophrenia and matched comparison subjects using quantitative confocal microscopy. This

required us to develop a novel technique to identify lipofuscin autofluorescence, which is prominent in human postmortem tissue. We found that the reported marked reduction in GAD67 mRNA expression in only ~30% of neurons in schizophrenia is associated with markedly lower GAD67 protein levels in just a subset of axonal boutons. GAD67 protein levels were trending lower in chandelier cell boutons and were significantly lower in boutons from CB and CR neurons. Our findings suggest that a proportion of PV, CB, and CR neurons have lower GAD67 expression in the PFC of schizophrenia subjects, which may be a consequence of a common mechanism, such as deficits in excitatory drive.

TABLE OF CONTENTS

PREFACE.....	XVII
1.0 INTRODUCTION.....	1
1.1 COGNITIVE CONTROL DEFICITS IN SCHIZOPHRENIA: ROLE OF ALTERED PREFRONTAL CORTEX ACTIVITY	4
1.1.1 Prefrontal cortex and cognitive control	4
1.1.2 Reduced prefrontal cortex activity in schizophrenia.....	4
1.2 EXCITATORY SIGNALING IN THE PREFRONTAL CORTEX: MARKED DEFICITS OF LAYER DEEP 3-4 PYRAMIDAL CELLS IN SCHIZOPHRENIA.....	6
1.2.1 Extrinsic excitatory afferent projections	6
1.2.2 Extrinsic excitatory afferent projections to GABA neurons.....	6
1.2.3 Local excitatory afferent inputs.....	8
1.2.4 Deficits in layers deep 3-4 pyramidal cells.....	10
1.3 GABA NEURONS: REDUCED GAD67 EXPRESSION WITHIN A SUBSET OF NEURONS IN THE PREFRONTAL CORTEX OF SCHIZOPHRENIA	13
1.3.1 Unique functional roles of GABA neuron subtypes in cortical networks.....	13
1.3.1.a PV neurons.....	13

1.3.1.b	CB neurons	13
1.3.1.c	CR neurons	14
1.3.2	Differential expression of the 65 kDa and 67 kDa isoforms of glutamic acid decarboxylase in GABA neuron subtypes	15
1.3.3	GAD67 protein levels report on network activity	16
1.3.4	Lower GAD67 expression in a subset of prefrontal cortex neurons in schizophrenia.....	17
1.3.5	Potential mechanisms for lower GAD67 expression in schizophrenia..	20
1.4	GOALS OF THIS DISSERTATION	22
2.0	QUANTITATIVE METHODS TO ASSESS PROTEIN LEVELS IN AXONAL BOUTONS IN POSTMORTEM HUMAN TISSUE USING FLUORESCENCE CONFOCAL MICROSCOPY TECHNIQUES	23
2.1	INTRODUCTION.....	23
2.2	HUMAN SUBJECTS COHORT	23
2.2.1	Brain collection.....	23
2.2.2	Subject pairing	24
2.3	EXPERIMENTAL METHODS	25
2.3.1	Experimental design	25
2.3.2	Immunohistochemistry	27
2.4	DATA COLLECTION	29
2.4.1	Microscopy equipment	29
2.4.2	Image acquisition	29
2.4.3	Novel method for detecting lipofuscin autofluorescence.....	30

2.4.4	Sampling	34
2.5	DATA SEGMENTATION	36
2.5.1	Image processing.....	36
2.5.2	Masking immunoreactive objects.....	38
2.6	DATA ANALYSES.....	39
2.6.1	Virtual cropping.....	39
2.6.2	Method for defining colocalization.....	40
2.7	CONCLUSION	44
3.0	MARKEDLY LOWER GAD67 PROTEIN LEVELS IN A SUBSET OF BOUTONS IN THE PREFRONTAL CORTEX OF SCHIZOPHRENIA.....	45
3.1	INTRODUCTION.....	45
3.2	MATERIALS AND METHODS	47
3.2.1	Experimental procedures	47
3.2.2	Definitions of vGAT+ and vGAT+/GAD67-IR boutons.....	47
3.2.3	Statistics	49
3.3	RESULTS	50
3.3.1	vGAT+ bouton density and vGAT protein levels are unchanged in schizophrenia.....	50
3.3.2	vGAT+/GAD67-IR bouton density is lower in schizophrenia	51
3.3.3	vGAT+/GAD67-IR bouton GAD67 protein levels are lower in schizophrenia.....	52
3.3.4	Lower vGAT+/GAD67-IR bouton density and GAD67 protein levels are not attributable to comorbid factors	54

3.4	DISCUSSION	56
4.0	GAD67 PROTEIN LEVELS ARE UNCHANGED IN CHANDELIER CELL BOUTONS IN THE PREFRONTAL CORTEX OF SCHIZOPHRENIA.....	59
4.1	INTRODUCTION.....	59
4.2	MATERIALS AND METHODS	61
4.2.1	Experimental Procedures.....	61
4.2.2	Definition of cartridges and vGAT+ cartridge boutons	61
4.2.3	Statistics	64
4.3	RESULTS	65
4.3.1	Cartridge density and vGAT+ boutons per cartridge are unchanged in schizophrenia.....	65
4.3.2	Cartridge bouton GAD67 protein levels are unchanged in schizophrenia.....	65
4.3.3	vGAT+/GAD65+/GAD67+ bouton density is lower in schizophrenia ..	68
4.3.4	vGAT+/GAD65+/GAD67+ bouton GAD67 protein levels are lower in schizophrenia.....	68
4.3.5	vGAT+/GAD67+ bouton density is lower in schizophrenia.....	70
4.3.6	vGAT+/GAD67+ bouton GAD67 protein levels are lower in schizophrenia.....	70
4.3.7	Lower vGAT+/GAD67+ and vGAT+/GAD65+/GAD67+ bouton density and GAD67 protein level measures are not attributable to comorbid factors.....	72
4.4	DISCUSSION	72

5.0	GAD67 PROTEIN LEVELS ARE LOWER IN AXONAL BOUTONS FROM CALBINDIN AND CALRETININ NEURONS IN SCHIZOPHRENIA	78
5.1	INTRODUCTION.....	78
5.2	MATERIALS AND METHODS	80
5.2.1	Experimental procedures	80
5.2.2	Definitions of CB and CR boutons	80
5.2.3	Statistics	84
5.3	RESULTS	85
5.3.1	CB+/vGAT+/GAD67+ and CB+/vGAT+/GAD65+/GAD67+ bouton density is unaltered in schizophrenia	85
5.3.2	CB+/vGAT+/GAD67+ and CB+/vGAT+/GAD65+/GAD67+ bouton GAD67 protein levels are lower in schizophrenia.....	86
5.3.3	CB+/vGAT+/GAD67+ and CB+/vGAT+/GAD65+/GAD67+ bouton CB protein levels are lower in schizophrenia.....	87
5.3.4	CB+/vGAT+/GAD67+ and CB+/vGAT+/GAD65+/GAD67+ bouton vGAT protein levels are unaltered in schizophrenia	89
5.3.5	Differences in CB+/vGAT+/GAD67+ and CB+/vGAT+/GAD65+/GAD67+ bouton GAD67 and CB protein levels in schizophrenia are not attributable to comorbid factors	89
5.3.6	CR+/vGAT+/GAD67+ and CR+/vGAT+/GAD65+/GAD67+ bouton density is lower in schizophrenia	89
5.3.7	CR+/vGAT+/GAD67+ and CR+/vGAT+/GAD65+/GAD67+ bouton GAD67 protein levels are lower in schizophrenia.....	91

5.3.8	CR+/vGAT+/GAD67+ and CR+/vGAT+/GAD65+/GAD67+ bouton CR protein levels are unaltered in schizophrenia.....	92
5.3.9	CR+/vGAT+/GAD67+ and CR+/vGAT+/GAD65+/GAD67+ bouton vGAT protein levels are unaltered in schizophrenia	94
5.3.10	Differences in CR+/vGAT+/GAD67+ and CR+/vGAT+/GAD65+/GAD67+ bouton density and GAD67 protein levels in schizophrenia are not attributable to comorbid factors	94
5.4	DISCUSSION	94
6.0	GENERAL DISCUSSION	100
6.1	SUMMARY OF FINDINGS	100
6.1.1	Lower GAD67 protein levels in a subset of boutons in schizophrenia	100
6.1.2	GAD67 expression in GABA neuron subtypes in schizophrenia.....	101
6.2	LOWER BOUTON GAD67 PROTEIN LEVELS AS A CONSEQUENCE OF REDUCED ACTIVITY IN SCHIZOPHRENIA.....	102
6.2.1	Local excitatory afferent inputs.....	102
6.2.2	Extrinsic excitatory afferent projections	103
6.2.3	Lower expression of several GABA-related markers.....	106
6.3	FUNCTIONAL IMPLICATIONS OF LOWER BOUTON GAD67 PROTEIN LEVELS IN GABA NEURON SUBTYPES IN THE PREFRONTAL CORTEX OF SCHIZOPHRENIA	107
6.3.1	Chandelier cells	107
6.3.2	CB neurons	108
6.3.3	CR neurons.....	109

6.4	EXPERIMENTAL CONSIDERATIONS	110
6.4.1	Data segmentation.....	110
6.4.2	Other microscopy techniques for assessing synaptic protein levels	112
6.5	SUMMARY	113
APPENDIX A	114
APPENDIX B	115
APPENDIX C	116
APPENDIX D	117
APPENDIX E	121
APPENDIX F	128
REFERENCES	130

LIST OF TABLES

Table 2.1. Summary of demographic and postmortem characteristics of human subjects	25
Table 2.2. Experimental design and list of primary antibodies	26
Table B.1. Detailed demographic and postmortem characteristics of human subjects	115

LIST OF FIGURES

Figure 1.1. Schematic diagram of extrinsic excitatory projections from different brain regions to distinct neurons within PFC area 9	8
Figure 1.2. Schematic diagram of relative strength of excitatory drive from local pyramidal cells in different cortical layers to GABA neuron subtypes.....	10
Figure 1.3. Schematic diagram of predicted GAD67 expression alterations in GABA neuron subtypes in response to reduced excitatory drive from layer deep 3-4 pyramidal cells	21
Figure 2.1. Antigen retrieval and vGAT detection in postmortem human tissue	27
Figure 2.2. Custom filter setting to detect lipofuscin.....	32
Figure 2.3. Lipofuscin detection in immunolabeled tissue	33
Figure 2.4. Layer delineation for sampling within total PFC gray matter	35
Figure 2.5. Method to improve discrimination of non-overlapping puncta.....	37
Figure 2.6. GAD content in boutons that were defined using only mask operations	41
Figure 2.7. Classification of GAD content in vGAT+ boutons	43
Figure 3.1. vGAT and GAD67 colocalization in human postmortem tissue	48
Figure 3.2. vGAT+ bouton densities and vGAT protein levels	51
Figure 3.3. vGAT+/GAD67-IR bouton densities and GAD67 protein levels	53
Figure 3.4. Effects of comorbid factors on vGAT+/GAD67-IR bouton density and levels of GAD67 in subjects with schizophrenia.....	55

Figure 4.1. Identification of vGAT-IR cartridges and vGAT+ cartridge boutons	63
Figure 4.2. Cartridge density, vGAT+ boutons per cartridge, and cartridge bouton GAD67 and vGAT protein levels between diagnostic groups	67
Figure 4.3. vGAT+/GAD65+/GAD67+ bouton density, and GAD67 and vGAT protein levels between diagnostic groups	69
Figure 4.4. vGAT+/GAD67+ bouton density and GAD67 and vGAT protein levels between diagnostic groups	71
Figure 5.1. Examples of CB+/vGAT+/GAD67+ and CB+/vGAT+/GAD65+/GAD67+ boutons	82
Figure 5.2. Examples of CR+/vGAT+/GAD67+ and CR+/vGAT+/GAD65+/GAD67+ boutons	83
Figure 5.3. CB+/vGAT+/GAD67+ and CB+/vGAT+/GAD65+/GAD67+ bouton density between diagnostic groups	86
Figure 5.4. CB+/vGAT+/GAD67+ and CB+/vGAT+/GAD65+/GAD67+ bouton GAD67 and CB protein levels between diagnostic groups	88
Figure 5.5. CR+/vGAT+/GAD67+ and CR+/vGAT+/GAD65+/GAD67+ bouton density between diagnostic groups	91
Figure 5.6. CR+/vGAT+/GAD67+ and CR+/vGAT+/GAD65+/GAD67+ bouton GAD67 and CR protein levels between diagnostic groups	93
Figure 6.1. Schematic diagram of GAD67 expression alterations in GABA neuron subtypes of PFC area 9 in response to reduced local excitatory drive from layers deep 3-4 pyramidal cells and extrinsic brain regions	105
Figure A.1. PV neurons are distinguishable by their GAD65 and GAD67 mRNA content.....	114
Figure C.1. vGAT+/GAD67-IR bouton vGAT protein levels	116
Figure D.1. Examples of vGAT+/GAD67+ and vGAT+/GAD65+/GAD67+ boutons.....	118

Figure D.2. Effects of potential comorbid factors on the density and levels of GAD67 from vGAT+/GAD67+ boutons in schizophrenia	119
Figure D.3. Effects of potential comorbid factors on the density and levels of GAD67 from vGAT+/GAD65+/GAD67+ boutons in schizophrenia	120
Figure E.1. CB+/vGAT+/GAD67+ and CB+/vGAT+/GAD65+/GAD67+ bouton vGAT protein levels between diagnostic groups.....	121
Figure E.2. Effects of potential comorbid factors on levels of GAD67 and CB from CB+/vGAT+/GAD67+ boutons in schizophrenia	122
Figure E.3. Effects of potential comorbid factors on levels of GAD67 and CB from CB+/vGAT+/GAD65+/GAD67+ boutons in schizophrenia	123
Figure E.4. CR+/vGAT+/GAD67-, CR+/vGAT+/GAD65+, and CR+/vGAT+/GAD65-IR bouton density between diagnostic groups	124
Figure E.5. CR+/vGAT+/GAD67+ and CR+/vGAT+/GAD65+/GAD67+ bouton vGAT protein levels between diagnostic groups.....	125
Figure E.6. Effects of potential comorbid factors on the density and levels of GAD67 from CR+/vGAT+/GAD67+ boutons in schizophrenia	126
Figure E.7. Effects of potential comorbid factors on the density and levels of GAD67 from CR+/vGAT+/GAD65+/GAD67+ boutons in schizophrenia	127
Figure F.1. vGAT+/GAD65+ and vGAT+/GAD65+/GAD67+ bouton GAD65 protein levels between diagnostic groups and effects of schizoaffective diagnosis.....	128
Figure F.2. CB bouton and CR bouton GAD65 protein levels between diagnostic groups	129

PREFACE

I would like to express my gratitude to my committee members, colleagues, family, and friends who provided invaluable guidance and support throughout my graduate studies. Also, I would like to thank the families who gave consent for tissue donation; without their generosity this research would not be possible.

ABBREVIATIONS

AIS: axon initial segment

ANCOVA: analyses of covariance

ATOD: at time of death

CB: calbindin

CR: calretinin

GABA: gamma-aminobutyric acid

GAT1: GABA transporter 1

GAD: glutamic acid decarboxylase

GAD65: 65 kilodalton isoform of glutamic acid decarboxylase

GAD67: 67 kilodalton isoform of glutamic acid decarboxylase

IR: immunoreactive

PV: parvalbumin

PB: phosphate buffer

PBS: phosphate buffered saline

PMI: postmortem interval

PFC: prefrontal cortex

RT: room temperature

SST: somatostatin

vGAT: vesicular GABA transporter

VIP: vasoactive intestinal peptide

1.0 INTRODUCTION

Schizophrenia is a devastating psychiatric illness with a worldwide prevalence of 0.5-1% (Lewis and Lieberman, 2000). Individuals with the illness typically come to clinical attention around late adolescence or early adulthood, and many suffer a lifetime of disability and emotional distress. Comorbid depression is commonly associated with the illness as well as nicotine, alcohol, and illicit drug use. Individuals with schizophrenia are overrepresented among the homeless, un- and under-employed, unmarried, and socially isolated, and many are on public assistance or are chronically hospitalized (Carpenter and Koenig, 2008). The lifespan of individuals with the illness are reduced by 1-2 decades, and 5-10% commit suicide (Auquier et al., 2007). As a result, schizophrenia can be a considerable financial and emotional burden for family members who are often the primary caretakers of individuals affected by the illness (Gibbons et al., 1984). In addition, schizophrenia incurs a substantial economic cost to society in terms of medical expenditures and lost productivity (Knapp et al., 2004; Wu et al., 2005).

Schizophrenia manifests as a broad spectrum of dysfunctions in motor, perceptual, emotional, and cognitive processes that are classified into three symptom domains (Tandon et al., 2009). The first domain is characterized by positive symptoms, which is generally described by the presence of extra perceptions and behaviors. These symptoms are the features of the illness commonly known as the “psychotic symptoms”, such as delusional ideation, the general belief that something exists in the absence of evidence for its existence; hallucinations, which may occur

in any sensory modality but are most commonly auditory (i.e. hearing voices that are distinct from one's own); and abnormal psychomotor activity, such as disorganized behavior and abnormal posturing and/or rigid movements. The second symptom domain is negative symptoms or the absence of behaviors or emotions that are usually present. These arise from a lack of normal brain function and include social withdrawal and isolation, including from loved ones; avolition (lack of motivation and decision-making); alogia (deficiency in the amount and content of speech), and anhedonia (reduced capacity to experience pleasure). The third symptom domain encompasses cognitive deficits, which span multiple modalities including selective and sustained attention, working and episodic memory, executive and social function, and processing speed, suggesting an overall alteration in cognitive control (Green et al., 2004; Lesh et al., 2011).

Although positive symptoms are frequently the most striking feature of schizophrenia and bring individuals to clinical attention, cognitive impairments are recognized as the core feature of dysfunction (Kahn and Keefe, 2013). Cognitive performance, as measured by IQ tests or scholastic achievement, in youth aged 16 years or younger is inversely related to the risk of developing schizophrenia later in life (Dickson et al., 2012; MacCabe et al., 2008). Scholastic performance appears to significantly decline, with the most pronounced deficits in language skills, between 13 and 16 years of age in individuals who develop schizophrenia compared to their peers (Fuller et al., 2002); however poor cognitive performance may be evident as early as 7 years of age and continue to lag throughout adolescence (Reichenberg et al., 2010). Moreover, a comparison of cognitive functioning in twins discordant for schizophrenia found evidence of impaired cognitive performance in the twin who developed the illness at 12 years of age, and these deficits preceded the first psychotic episode by many years (van Oel et al., 2002).

Cognitive impairments occur throughout the lifespan of schizophrenia patients (Hedman et al., 2013), and may continue to decline after the onset of psychosis (Kahn and Keefe, 2013). The degree of cognitive dysfunction is the best predictor of long-term functional outcome and quality of life (Bowie et al., 2006; Green, 2006). Despite being the core feature of dysfunction, cognitive deficits in schizophrenia are relatively unaffected by current pharmacotherapy, which is almost entirely based on the administration of antipsychotic medication (Dold and Leucht, 2014). While these medications ameliorate positive symptoms associated with schizophrenia, they are no more effective than placebo or practice effects at improving cognitive impairments (Keefe et al., 2008). The development of new treatments to improve cognition in schizophrenia subjects requires the identification of molecular targets based on their role in the pathophysiology of the illness (Insel and Scolnick, 2006).

The prefrontal cortex (PFC) is a brain region critically involved in cognitive processes (Miller and Cohen, 2001). Proper functioning of the PFC requires an intricate balance of excitation and inhibition that is provided by glutamate-releasing (glutamatergic) pyramidal neurons and gamma-aminobutyric acid (GABA)-releasing (GABAergic) neurons, respectively, both of which are altered in the PFC of schizophrenia subjects. This thesis directly assesses the extent of molecular alterations in specific subtypes of GABA neurons, which may be a consequence of glutamatergic deficits. In the following sections I will discuss the role of the PFC during cognitive processes and provide evidence for functional abnormalities in the PFC of schizophrenia subjects. I will then discuss the neuronal circuitry of the PFC and what is known about cellular and molecular deficits in schizophrenia, which will be used to guide hypotheses on alterations of specific GABA neuron subtypes in the illness.

1.1 COGNITIVE CONTROL DEFICITS IN SCHIZOPHRENIA: ROLE OF ALTERED PREFRONTAL CORTEX ACTIVITY

1.1.1 Prefrontal cortex and cognitive control

Cognitive control depends on the coordinated activity of several brain regions including the PFC (Braver et al., 1997; Cohen et al., 1997). The PFC receives afferent inputs from numerous brain regions and based on this connectivity pattern the PFC is thought to be critically important for the integration, active maintenance, and filtering of neural signals across several cognitive, sensory, and motor modalities (Miller and Cohen, 2001). Through the integration of widespread extrinsic and intrinsic neural signals from other brain regions the PFC selects information in order to guide appropriate cognitive responses based on these inputs (Asaad et al., 1998; Rainer et al., 1998; Watanabe, 1990). For example, performance on cognitive control tasks requiring working memory, which is the ability to integrate, temporarily maintain, and manipulate a limited amount of information in order to guide future thought or behavior, is critically dependent on PFC activity (Goldman-Rakic, 1995). Therefore, proper functioning of the PFC is integral for exerting top-down control over a wide variety of behaviors that require cognitive control.

1.1.2 Reduced prefrontal cortex activity in schizophrenia

Functional imaging studies have established altered activity in the PFC of schizophrenia subjects. For example, studies measuring regional cerebral blood flow, which is thought to be positively correlated with neuronal activity, found reduced activity in the PFC of medication-naïve (Weinberger et al., 1988; Weinberger et al., 1986) and antipsychotic-treated (Berman et al., 1986)

subjects with schizophrenia while at rest and when performing tasks requiring working memory. Similarly, multiple studies measuring blood oxygen level dependent signal, an additional quantitative measure thought to reflect neuronal activity, show reduced activity in the PFC during cognitive control tasks (Glahn et al., 2005; Minzenberg et al., 2009; Perlstein et al., 2003). Moreover, cortical gamma-frequency oscillations are a signature of local neural processing thought to underlie higher order cognitive processes in humans (Fries, 2009). The power of gamma-frequency oscillations increases proportionally to the degree of difficulty of cognitive tasks (Howard et al., 2003; Roux et al., 2012). Subjects with schizophrenia exhibit impaired gamma-band power in the PFC and poor cognitive performance compared to non-psychiatric subjects (Cho et al., 2006; Minzenberg et al., 2010).

The integration and processing of neural signals required to generate strong activity within the PFC for proper cognitive functioning is critically dependent on the strong and synchronous firing of pyramidal cells (Goldman-Rakic, 1995) by GABA neurons (Constantinidis et al., 2002; Rao et al., 2000), which constitute ~75% and ~25%, respectively, of all neurons in monkey neocortex (Hendry et al., 1987). In schizophrenia, alterations in pyramidal cells and GABA neurons may contribute to reduced activity of the PFC and cognitive impairments.

1.2 EXCITATORY SIGNALING IN THE PREFRONTAL CORTEX: MARKED DEFICITS OF LAYER DEEP 3-4 PYRAMIDAL CELLS IN SCHIZOPHRENIA

1.2.1 Extrinsic excitatory afferent projections

Excitatory afferent projections between the PFC and other cortical regions are relayed predominantly via pyramidal cells in cortical layer 3, which principally target dendritic spines of pyramidal cells in layers 3-4 (Barbas and Rempel-Clower, 1997; Felleman and Van Essen, 1991). ~80-90% of excitatory projections from pyramidal cells innervate dendritic spines of other pyramidal cells in distant brain regions and nearby, but distinct (e.g. projections from PFC area 46 to PFC area 9), cortical areas (Medalla and Barbas, 2009; Melchitzky et al., 2001). Subcortical excitatory projections from the mediodorsal thalamic nuclei, which provide thalamic afferents to the PFC (Erickson and Lewis, 2004; Giguere and Goldman-Rakic, 1988; Goldman-Rakic and Porrino, 1985; Tobias, 1975), also predominantly target spines of pyramidal cells in layers 3-4 (Giguere and Goldman-Rakic, 1988; Jones and Hendry, 1989). Thalamic projections constitute ~10% of excitatory inputs to dendritic spines within these layer (Ahmed et al., 1994).

1.2.2 Extrinsic excitatory afferent projections to GABA neurons

Although layers deep 3-4 pyramidal cells are the recipients of the vast majority of thalamo-cortical and cortico-cortical excitatory afferent projections, different brain regions preferentially innervate distinct subtypes of GABA neurons (**Figure 1.1**). Nearly all GABA neurons in primate PFC can be separated into non-overlapping subtypes by the expression of the calcium-binding proteins parvalbumin (PV), calbindin (CB), and calretinin (CR). Specifically, ~25%, ~20%, and

~45% of all GABA neurons express PV, CB, and CR, respectively (Conde et al., 1994; del Rio and DeFelipe, 1996; Gabbott and Bacon, 1996). In rat, thalamic afferents predominantly target PV neurons, and to a lesser extent CB and CR neurons (Rotaru et al., 2005). In monkey PFC, CB neurons are the predominant GABAergic subtype that receives projections from the anterior cingulate cortex (ACC) (Medalla and Barbas, 2009; Medalla and Barbas, 2010), suggesting that CB neurons in the PFC receive projections from brain regions responsible for distinct cognitive behaviors. For example, when performing a cognitive control task PFC area 9 shows greater activity during delay periods when subjects are maintaining information prior to making a response, which is consistent with the role of top-down control of the PFC (MacDonald et al., 2000). By contrast, the ACC is more active during the response phase, suggesting that it has a strong role in performance monitoring. In monkey PFC, CR neurons are the predominant GABAergic subtype that receives projections from pyramidal cells in nearby brain areas, such as projections from area 46 to area 9 (Medalla and Barbas, 2009), which perform similar functions during working memory tasks (Levy and Goldman-Rakic, 1999; Petrides, 2000; Petrides et al., 1993; Tanila et al., 1992; Tanji and Hoshi, 2008).

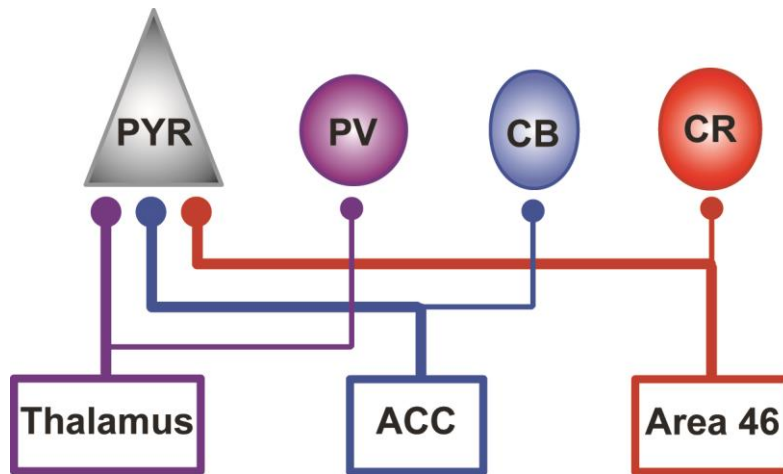


Figure 1.1. Schematic diagram of extrinsic excitatory projections from different brain regions to distinct neurons within PFC area 9. The thicker lines depict a greater percentage of innervations from the thalamus, anterior cingulate cortex (ACC), and PFC area 46 to the pyramidal cell (PYR) than to PV, CB, and CR neurons.

1.2.3 Local excitatory afferent inputs

Ultrastructural analyses in monkey PFC found that ~50% of local axon collaterals from supragranular pyramidal cells innervate the dendritic spines of local pyramidal cells, whereas the majority of the remaining inputs contact local PV neurons (Melchitzky et al., 2001; Melchitzky and Lewis, 2003). However, studies using transgenic mice to identify specific GABA neurons and glutamate uncaging to activate pyramidal cells across different layers of somatosensory cortex suggest that all GABA neurons receive local excitatory inputs but the laminar location of pyramidal cells providing those inputs differs for distinct GABA neurons (Xu and Callaway,

2009). For example, PV neurons in layers 2-3 receive stronger excitatory inputs from pyramidal cells around cortical layer 4 (**Figure 1.2**). By contrast CR-containing neurons in layers 2-3 receive stronger excitatory inputs from pyramidal cells in layers 2-3. Moreover, in monkey PFC, > 80% of CR neurons express vasoactive intestinal peptide (VIP; ~80% of VIP neurons contain CR) (Gabbott and Bacon, 1997), and VIP-containing neurons in layers 2-3 of mouse somatosensory cortex receive the greatest strength of excitatory inputs from pyramidal cells in layers 2-3. CB neurons were not directly assessed; however, > 50% of CB neurons express somatostatin (SST), and ~85% of SST neurons contain CB (Gonchar and Burkhalter, 1997; Kubota et al., 1994; Rogers, 1992). Similar to PV cells, SST neurons generally receive greater excitatory drive from pyramidal cells around layer 4.

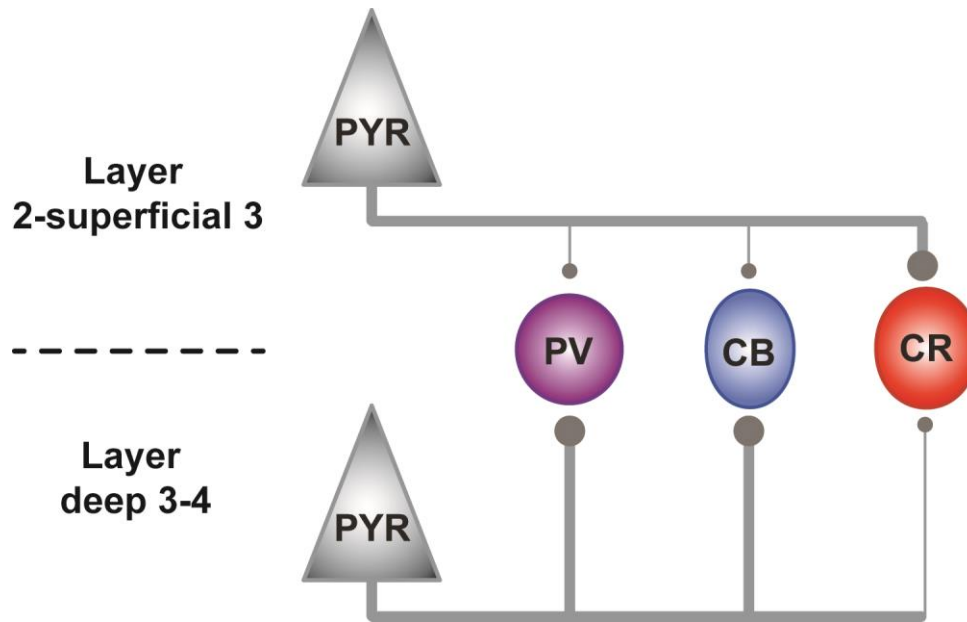


Figure 1.2. Schematic diagram of relative strength of excitatory drive from local pyramidal cells in different cortical layers to GABA neuron subtypes. The thicker lines from the pyramidal cells (PYR) depict greater strength of excitatory drive to PV, CB, and CR neurons.

1.2.4 Deficits in layers deep 3-4 pyramidal cells

Because cortico-cortical and thalamo-cortical afferent projections almost exclusively innervate dendritic spines of layer 3-4 pyramidal cells, spine density presumably reflects the amount of excitatory drive to these neurons and in general the PFC. Therefore, proper integration and processing of incoming neural signals critically depends on the integrity of layer 3-4 pyramidal cells. Several morphological alterations of pyramidal cells in PFC layers deep 3-4 are reported in

schizophrenia. These alterations include a lower density of dendritic spines (Glantz and Lewis, 2000; Konopaske et al., 2014), reduction in the number and length of dendrites (Broadbelt et al., 2002; Glantz and Lewis, 2000; Kalus et al., 2000), and smaller somal size (Pierri et al., 2001; Pierri et al., 2003; Rajkowska et al., 1998), which correlates with the extent of dendritic and axonal arborization in certain neuronal populations (Gilbert and Kelly, 1975; Hayes and Lewis, 1993; Jacobs et al., 1997; Lund et al., 1975). Similar morphological alterations for deep layer 3 pyramidal cells are also observed in other brain regions (Garey et al., 1998; Sweet et al., 2004; Sweet et al., 2009; Sweet et al., 2003) including the ACC (Broadbelt et al., 2002). By contrast, pyramidal cells located in other layers of the PFC do not appear to be as greatly affected by these alterations (Kolluri et al., 2005), suggesting that the deficits are specific to, or are at least more pronounced in, layers deep 3-4 pyramidal cells. The consistency that these morphological alterations are reported in the PFC and other brain regions suggest that they are a conserved feature of the illness.

Multiple factors may contribute to the morphological deficits in deep layer 3 pyramidal cells in schizophrenia. For example, activity-dependent glutamate signaling can modify the structure and formation of dendrites and spines (Maletic-Savatic et al., 1999; McKinney et al., 1999; Xie et al., 2005; Xie et al., 2007), and significant genome-wide variations in several loci associated with glutamate signaling are reported in schizophrenia (Schizophrenia Working Group of the Psychiatric Genomics, 2014). Total neuron number and volume of the mediodorsal thalamic nuclei and the number of putative thalamic projections to the PFC are lower in schizophrenia (Byne et al., 2001; Byne et al., 2002; Gilbert et al., 2001; Lewis et al., 2001; Pakkenberg, 1990; Popken et al., 2000; Young et al., 2000), which presumably results in reduced PFC activity; however, thalamic projections only account for a small proportion of glutamatergic

inputs to the cortex (Ahmed et al., 1994). Other sources of excitatory inputs to deep layer 3 pyramidal cells such as intrinsic collaterals from other pyramidal cells or projections from other cortical regions, such as the ACC, may also contribute to lower PFC activity. Morphological deficits in layer 3 pyramidal cells of the ACC are reported in schizophrenia, and numerous functional imaging studies suggest that the activity of both the PFC and ACC is altered in schizophrenia patients during cognitive control tasks (Allen et al., 2007; Cho et al., 2006; Ikuta et al., 2012; Kerns et al., 2005; Minzenberg et al., 2010; Quintana et al., 2004; Schultz et al., 2012; Yucel et al., 2007). Alternatively, alterations for gene products that regulate cellular morphology, such as reduced expression for mRNAs that facilitate the formation and maintenance of spines, may reflect intrinsic deficits in spine structure (Hill et al., 2006; Ide and Lewis, 2010; Konopaske et al., 2015). Altered expression of proteins that regulate and maintain neuronal structure are also reported in the PFC of schizophrenia (Jones et al., 2002; Somenarain and Jones, 2010). Taken together, reduced number of excitatory inputs, reductions in the strength of glutamatergic signaling, intrinsic alterations in the transcription/translation of structural proteins, or a combination of these possibilities may contribute to reduced activity of layer deep 3-4 pyramidal cells in schizophrenia.

Considering that local excitatory afferents from layers deep 3-4 pyramidal cells preferentially innervate specific GABA neuron subtypes (**Figure 1.2**), it may be predicted that GABA neurons receiving the greatest strength of inputs from layers deep 3-4 pyramidal cells (i.e. PV and CB neurons) are also preferentially altered in schizophrenia. By contrast, GABA neurons that receive the greatest strength of inputs from pyramidal cells in other layers (i.e. CR neurons) may not be as greatly affected.

1.3 GABA NEURONS: REDUCED GAD67 EXPRESSION WITHIN A SUBSET OF NEURONS IN THE PREFRONTAL CORTEX OF SCHIZOPHRENIA

1.3.1 Unique functional roles of GABA neuron subtypes in cortical networks

1.3.1.a PV neurons

PV neurons can be subdivided into basket and chandelier cells. PV basket cells principally target the perisomatic region and proximal dendrites of pyramidal cells (Melchitzky et al., 1999), whereas chandelier cells exclusively innervate the axon initial segment (AIS) of pyramidal cells (Szentagothai and Arbib, 1974). By targeting the perisomatic region of pyramidal cells PV neurons exert strong control over their output (Glickfeld et al., 2009; Kato et al., 2013; Woodruff et al., 2011). Moreover, in vivo studies using optogenetic techniques to increase PV cell activity induce gamma-frequency oscillations in cortex (Cardin et al., 2009; Sohal et al., 2009), whereas genetic manipulations that decrease PV cell activity reduce hippocampal gamma synchrony in vitro and impair working memory performance (Fuchs et al., 2007).

1.3.1.b CB neurons

CB is expressed in diverse subtypes of cortical GABA neurons and also pyramidal cells (DeFelipe et al., 1989; Freund et al., 1990; Gonzalez-Albo et al., 2001; Hayes and Lewis, 1992; Hof and Morrison, 1991). Much of what is known about the structure and function of GABAergic CB neurons comes from studying SST neurons, which is exclusively expressed by GABA neurons (Gonchar and Burkhalter, 2003; Gonzalez-Albo et al., 2001; Kubota et al., 1994; Sugino et al., 2006). SST neurons mainly target dendritic shafts and spines of pyramidal cells (Melchitzky and Lewis, 2008), whereby they regulate the integration of excitatory inputs within

local cortical circuits (Kapfer et al., 2007; Lovett-Barron et al., 2012) and from thalamic afferents (Xu et al., 2013), and provide feedback inhibition in and between cortical layers (Wang et al., 2004). Moreover, SST neurons provide a layer of tonic inhibition over the cortical network (Gentet et al., 2012), and suppressing the activity of SST neurons increases the overall excitability (i.e. gain) of pyramidal cells (Urban-Ciecko et al., 2015).

1.3.1.c CR neurons

CR neurons mainly contact the dendrites and soma of GABA neurons (Melchitzky et al., 2005; Melchitzky and Lewis, 2008), whereby they mediate disinhibitory control of pyramidal cells. Much of what is known about the specific functions of CR neurons comes from studying VIP neurons using transgenic mouse models. These studies have strongly established that VIP neurons almost exclusively innervate other GABA neurons, many of which are SST and to a lesser extent PV neurons, and that this innervation pattern occurs across cortical and hippocampal regions (Donato et al., 2013; Fu et al., 2014; Kawaguchi Y, 1996; Lee et al., 2013; Neske et al., 2015; Pfeffer et al., 2013; Rogers, 1992; Staiger et al., 2004; Tyan et al., 2014). By mainly contacting GABA neurons CR/VIP neurons mediate selective amplification of local signal processing of pyramidal cells, which has been shown to be important for a number of sensory and cognitive processes (Donato et al., 2013; Fu et al., 2014; Lee et al., 2013; Pi et al., 2013).

1.3.2 Differential expression of the 65 kDa and 67 kDa isoforms of glutamic acid decarboxylase in GABA neuron subtypes

The strength of signaling from GABA neurons is partially dependent on the amount of GABA available for synaptic release, which is synthesized within axonal boutons by the 65 kDa and 67 kDa isoforms of the enzyme glutamic acid decarboxylase (GAD65 and GAD67, respectively). The majority of GABA neurons appear to express both GAD65 and GAD67 mRNAs, but a small proportion only expresses GAD67 mRNA. Specifically, ~20% of GABA neurons in monkey visual cortex are detectable by only GAD67 mRNA (Hendrickson et al., 1994), and GAD67-only mRNA expressing neurons are also evident in monkey PFC (Rocco et al., 2015). Moreover, 5-10% of GABA neurons in CA1 and CA3 of rat hippocampus are detectable by mRNA for only GAD67 (Stone et al., 1999), suggesting that GAD67-only expressing neurons are present across brain regions and in different species. By contrast, no study to date has found evidence for GABA neurons that only express GAD65 mRNA.

Neuronal differences in GAD65 and GAD67 mRNA expression are also evident at the protein level within axonal boutons. Out of all GABAergic boutons in monkey PFC, ~50% contain protein levels for both GAD65 and GAD67 (GAD65+/GAD67+), ~20% contain only GAD67 (GAD67+), and ~30% contain only GAD65 (GAD65+) (Rocco et al., 2015), which together with the mRNA findings suggests that GAD65+/GAD67+ and GAD65+ boutons arise from neurons expressing mRNAs for both GADs, whereas GAD67+ boutons arise from neurons expressing only GAD67 mRNA. Differences in the biophysical properties between the enzymes may explain why some boutons are GAD65+. For example, the half-life of GAD65 is > 24 hours, while that of GAD67 is ~2 hours (Battaglioli et al., 2003).

At the cell-type specific level all PV basket cell boutons appear to be GAD65+/GAD67+ and those from PV chandelier cells appear to all be GAD67+ (Fish et al., 2011; Glausier et al., 2014). These findings appear to be recapitulated at the transcript level because two distinct subtypes of PV neurons are distinguishable by expressing mRNAs for both GADs and only GAD67, which are presumably basket and chandelier cells, respectively (**Appendix A Figure A.1**). CB and CR neurons give rise to GAD65+/GAD67+, GAD67+, and GAD65+ boutons. Consistent with the mRNA findings, the majority of CB and CR neurons express mRNAs for both GADs and a small proportion contain mRNA for only GAD67 (Rocco et al., 2015). Similar to CB and CR neurons, boutons from SST and VIP neurons give rise to GAD65+/GAD67+, GAD67+, and GAD65+ boutons (Rocco et al., 2015).

1.3.3 GAD67 protein levels report on network activity

Although GAD65 and GAD67 perform the same general function, they are products of separate genes (Erlander et al., 1991). Chronic reductions in network activity in rat cortical cultures lower GAD67 mRNA and protein levels, whereas GAD65 mRNA expression is less strongly associated with decreased GAD65 protein levels (Patz et al., 2003). Other studies have also shown that protein levels for both GAD65 and GAD67 are reduced under conditions of chronic network inactivity (Hartman et al., 2006; Lau and Murthy, 2012). By contrast, GAD67, but not GAD65, protein levels are reduced in response to acute increases in GABA levels (Rimvall and Martin, 1994; Sheikh and Martin, 1998), suggesting that GAD67 is more strongly coupled to decreases in network activity. Differences in the half-life of the enzymes (i.e. > 24 hours and ~2 hours for GAD65 and GAD67, respectively) may explain why GAD67 is more transcriptionally regulated and more responsive to acute reductions in network activity compared to GAD65 (Huang, 2009).

1.3.4 Lower GAD67 expression in a subset of prefrontal cortex neurons in schizophrenia

Perhaps the most widely and consistently reported finding in postmortem studies of subjects with schizophrenia is lower mRNA expression for GAD67 (Akbarian et al., 1995; Curley et al., 2011; Duncan et al., 2010; Guidotti et al., 2000; Hashimoto et al., 2003; Volk et al., 2000), which is accompanied by lower total GAD67 protein levels (Curley et al., 2011; Guidotti et al., 2000; Impagnatiello et al., 1998). Only ~30% of GABAergic neurons in schizophrenia PFC lack detectable levels of GAD67 mRNA, whereas the others express GAD67 mRNA at normal levels (Akbarian et al., 1995; Volk et al., 2000). The subset of GABAergic neurons with markedly lower GAD67 mRNA expression is prominent across PFC layers 2-5 (Akbarian et al., 1995; Volk et al., 2000). This deficit occurs without a loss in total neuron density (Akbarian et al., 1995) or number (Thune et al., 2001), suggesting that all GABA neurons are present but that a subset have a markedly reduced capacity to synthesize GABA. A more recent study found that the density of neurons detectable by GAD67 mRNA was unchanged in schizophrenia (Guillozet-Bongaarts et al., 2014), supporting the idea that all GABA neurons are present but some have markedly low levels of GAD67 expression. By contrast, expression of other gene products involved in GABAergic neurotransmission is reported to be unaffected or only modestly altered in the PFC of schizophrenia subjects. For example, mRNA and protein levels for GAD65 are unchanged (Guidotti et al., 2000; Hashimoto et al., 2008; Impagnatiello et al., 1998), as well as the density of GAD65-immunoreactive (IR) puncta (Benes et al., 2000); however, GAD65 mRNA and protein levels may be preferentially lower in the PFC of subjects diagnosed with schizoaffective disorder (Glausier et al., 2015). Moreover, mRNA for the vesicular GABA transporter (vGAT), which packages GABA into synaptic vesicles, was reported to be unchanged or only modestly lower in the PFC of schizophrenia subjects (Fung et al., 2011; Hoftman et al., 2013).

Roughly 1/3 of the ~30% of neurons with markedly reduced GAD67 mRNA expression are comprised of PV neurons. Specifically, ~50% of all PV neurons, which are ~25% of all GABA neurons, lack detectable levels of GAD67 mRNA expression across all PFC layers in schizophrenia subjects (Hashimoto et al., 2003); though, this study did not differentiate between PV basket and chandelier cells. A more recent study that used a small cohort of schizophrenia and matched non-psychiatric comparison subjects to quantify protein levels in PV basket cell boutons found that GAD67 protein levels were ~50% lower in PFC layers 3-4 in the illness (Curley et al., 2011), which suggests that at least some PV basket cells are affected with marked reductions in GAD67 expression. Convergent findings suggest that PV chandelier cells may also be affected by marked reductions in GAD67 expression. For example, the convergence of multiple chandelier cell boutons at the AIS appears as a distinctive structure termed a cartridge (Lewis and Lund, 1990), which can be visualized with multiple markers involved in GABA signaling including PV and the GABA transporter, GAT1 (DeFelipe and del Carmen Gonzalez-Albo, 1998; DeFelipe et al., 1989). In schizophrenia, the density of GAT1-IR cartridges is reduced by 40% across PFC layers 2-6 (Pierri et al., 1999; Woo et al., 1998). By contrast, the density of AISs visualized by immunoreactivity for the $\alpha 2$ subunit of the GABA A receptor is 2-fold greater in PFC layers 2-superficial 3 (Volk et al., 2002). These pre- and post-synaptic alterations are speculated to be compensatory for deficits in GABA signaling that may result from reduced GAD67 protein levels in PV chandelier cell boutons because lower GAT1 levels would presumably increase the latency of post-synaptic responses upon GABA release (Overstreet and Westbrook, 2003), and the up-regulation of GABA A receptors at the AIS would increase the efficacy of GABA binding. However, GAD67 levels have not been assessed in PV chandelier cell boutons in schizophrenia.

Therefore, whether PV basket and chandelier cells are similarly affected by marked reductions in GAD67 expression or if one subtype is preferentially affected is unknown.

Considering that PV neurons only constitute ~1/3 of the neurons that lack detectable GAD67 mRNA expression in schizophrenia, CB and/or CR neurons must have lower GAD67 expression levels; however, these subtypes may be differentially affected in the illness. For example, > 50% of CB neurons express somatostatin (SST), and ~85% of SST neurons contain CB (Gonchar and Burkhalter, 1997; Kubota et al., 1994; Rogers, 1992). Deficits in SST mRNA expression are widely reported in the PFC of schizophrenia subjects (Fung et al., 2010; Gabriel et al., 1996; Hashimoto et al., 2008; Hashimoto et al., 2008; Mellios et al., 2009; Morris et al., 2008). Both the density of SST mRNA-positive neurons and levels of SST mRNA per neuron are lower across PFC layers 2-superficial 6 (Morris et al., 2008). Moreover, lower SST mRNA expression correlates with lower GAD67 mRNA expression at both the tissue and cellular levels (Hashimoto et al., 2008; Morris et al., 2008), which suggests that at least some CB neurons give rise to boutons with reduced GAD67 protein levels. By contrast, CR mRNA and total protein expression, as well as the density of CR-IR boutons are unaltered (Fung et al., 2010; Hashimoto et al., 2008; Hashimoto et al., 2003; Woo et al., 1998). CR mRNA levels do not correlate with lower GAD67 mRNA levels in the illness (Hashimoto et al., 2008), suggesting that CR neurons are relatively unaltered. Since CB neurons constitute ~20% of all GABA neurons, the ~30% of GABA neurons with markedly reduced GAD67 mRNA levels may be comprised of PV and CB neurons, which are the subtypes that receive high levels of excitatory inputs from pyramidal cells exhibiting the greatest signaling deficits in schizophrenia (i.e. pyramidal cells in layers deep 3-4).

1.3.5 Potential mechanisms for lower GAD67 expression in schizophrenia

The cause(s) of lower GAD67 expression in the PFC of schizophrenia is unclear because the deficit occurs across multiple layers and it is unknown if only specific subtypes of GABA neurons are affected or if a proportion of several different neurons are affected. The previous convergent findings suggesting that PV and SST neurons, but not CR neurons, have marked deficits in GAD67 expression is consistent with our prediction that the GABA neuron subtypes that receive the greatest strength of excitatory drive from layers deep 3-4 pyramidal cells (**Figure 1.2**) exhibit the greatest activity-dependent alterations (i.e. lower GAD67 expression) in schizophrenia. Therefore, we hypothesize that GAD67 levels are markedly reduced in PV and CB, but not CR, neurons (**Figure 1.3**).

Alternatively, multiple other mechanisms may contribute to lower GAD67 expression. For example, allelic variants in the gene encoding GAD67, *GADI*, are associated with lower GAD67 expression levels and an increased risk of schizophrenia (Addington et al., 2005; Straub et al., 2007). Dysregulated epigenetic mechanisms, such as altered chromatin-associated histone modifications and higher-order chromatin structure at the *GADI* promoter region are also associated with lower GAD67 expression in the illness (Bharadwaj et al., 2013; Huang et al., 2007; Tang et al., 2011). Reduced mRNA expression for upstream regulatory factors of the *GADI* gene have been reported in schizophrenia and correlate with reduced levels of GAD67 mRNA (Kimoto et al., 2014). However, along with previous findings, our findings suggest that the subset of GABA neurons with markedly lower GAD67 expression is comprised of a proportion of several subtypes of GABA neurons, and none of these alternative factors provide an obvious mechanism that could account for lower GAD67 expression in just a subset of neurons.

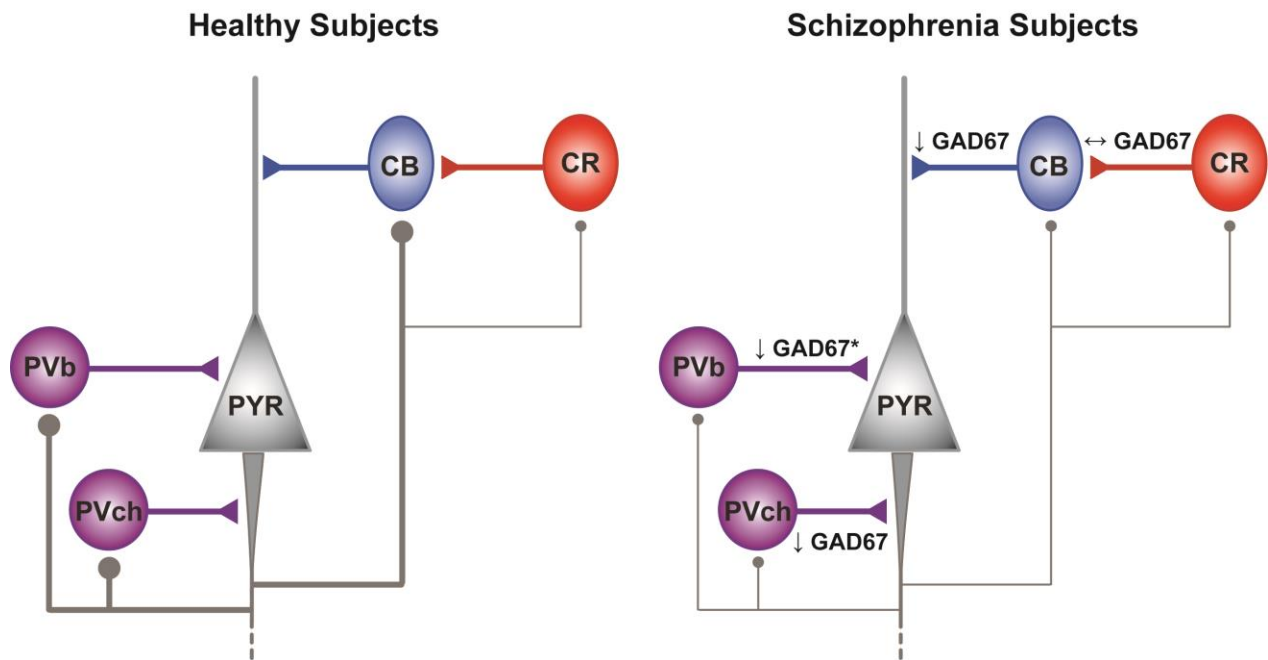


Figure 1.3. Schematic diagram of predicted GAD67 expression alterations in GABA neuron subtypes in response to reduced excitatory drive from layer deep 3-4 pyramidal cells. The asterisk indicates GAD67 protein level findings in boutons from PV basket cells (PVb) in PFC layers 3-4 of schizophrenia (Curley et al., 2011). GAD67 expression levels have not been directly assessed in PV chandelier (PVch), CB, and CR neurons in the illness. The thicker lines from the pyramidal cell (PYR) depict greater strength of excitatory drive to PV, CB, and CR neurons.

1.4 GOALS OF THIS DISSERTATION

Cognitive impairments are a core feature of schizophrenia and are, in part, a result of glutamatergic and GABAergic deficits in the PFC. Only ~30% of neurons in the PFC lack detectable GAD67 mRNA expression. The overall goal of this dissertation is to determine if chandelier cells, CB neurons, or CR neurons are preferentially affected by markedly reduced GAD67 expression or if a proportion of each subtype is affected. Development of novel methods to unbiasedly detect protein level changes in human postmortem tissue using quantitative multi-label fluorescence confocal microscopy techniques (2.0) was required to first ask how well the prior reported deficits in GAD67 mRNA levels in schizophrenia translate to GAD67 protein levels within axonal boutons, the site of vesicular GABA release (3.0). Consistent with the mRNA findings, we found that only a subset of boutons had markedly reduced GAD67 protein levels, which led us to assess GAD67 protein levels in boutons from chandelier cells (4.0), and CB and CR neurons (5.0) in the PFC of schizophrenia subjects. Gaining insight into which of these subtypes is affected is important for understanding potential causal effects of a GAD67 deficit in schizophrenia.

2.0 QUANTITATIVE METHODS TO ASSESS PROTEIN LEVELS IN AXONAL BOUTONS IN POSTMORTEM HUMAN TISSUE USING FLUORESCENCE CONFOCAL MICROSCOPY TECHNIQUES

2.1 INTRODUCTION

A quantitative method to unbiasedly assess the colocalization of multiple synaptic proteins within axonal boutons in postmortem human tissue using fluorescence confocal microscopy techniques is described in the following section. These methods are a detailed description of the human subjects cohort and the procedures used to assess bouton protein levels between matched pairs of schizophrenia and comparison subjects in **3.0**, **4.0**, and **5.0**.

2.2 HUMAN SUBJECTS COHORT

2.2.1 Brain collection

Brain specimens were recovered during autopsies conducted at the Allegheny County Medical Examiner's Office (Pittsburgh, PA, USA) after obtaining consent from the next of kin. The left hemisphere of each brain was blocked coronally at 1-2 cm intervals, immersed in ice cold 4% paraformaldehyde for 48 hours and then washed in a series of graded sucrose solutions and

cryoprotected in a 30% glycerol/ 30% ethylene glycol solution at -30°C until sectioned. Tissue blocks containing PFC area 9 were sectioned coronally at 40 µm on a cryostat and stored in cryoprotectant solution at -30°C until processed for immunohistochemistry. The University of Pittsburgh's Committee for the Oversight of Research Involving the Dead and Institutional Review Board for Biomedical Research approved all procedures.

2.2.2 Subject pairing

An independent committee of experienced research clinicians made consensus DSM-IV diagnoses for each subject using the results of structured interviews conducted with family members and/or review of medical records (Hashimoto et al., 2008). To reduce biological variance between diagnostic groups, and to control for experimental variance, each schizophrenia subject was matched to one comparison subject with no known history of neurological or psychiatric disorder (N= 20 pairs) perfectly for sex, and as closely as possible for PMI, age, and time stored in cryoprotectant solution at -30°C (**Table 2.1**). The rate of protein degradation, which begins at death, varies between different proteins (Beneyto et al., 2008; Curley et al., 2011). In contrast to RNA studies using postmortem human tissue, in which the RNA integrity number (i.e. RIN) can be used as a quantitative measure of RNA degradation, there is currently no equivalent quantitative measure for protein degradation. Also, aging can differentially affect gene expression (Hoftman et al., 2013). To reduce the effects of these confounding variables we selected all available schizophrenia subjects from the Brain Tissue Donation Program at the University of Pittsburgh with PMI < 16 hours and age ≤ 55 years (**Appendix B Table B.1**). Importantly, an independent samples t-test found that there were no diagnostic group differences in PMI, age, or freezer storage time.

Table 2.1. Summary of demographic and postmortem characteristics of human subjects. There were no diagnostic group differences in age ($t_{38} = 0.276$, $p = 0.784$), postmortem interval ($t_{38} = 0.327$, $p = 0.745$), or freezer storage time ($t_{38} = 0.268$, $p = 0.790$).

	Comparison Group (N=20)		Schizophrenia Group (N=20)	
	N	%	N	%
Male	14	70	14	70
White	17	85	18	90
Black	3	15	2	10
	Mean	SD	Mean	SD
Age (years)	45.8	8.7	45.1	7.3
Postmortem interval (hours)	9.9	4.0	9.5	3.4
Freezer storage time (years)	13.8	5.3	13.3	5.1

2.3 EXPERIMENTAL METHODS

2.3.1 Experimental design

For each subject (N=40), four sections containing PFC area 9 spaced ~500 μm apart were used. To minimize experimental variance within and across subject pairs, two separate

immunohistochemistry runs consisting of two sections per subject (80 sections total per run) were performed with all sections within a run processed simultaneously. The only difference between runs was that antibodies against CB and CR were used in Run #1 and Run #2, respectively, all other antibodies were the same (**Table 2.2**).

Table 2.2. Experimental design and list of primary antibodies.

	Species	Antigen	Dilution	Source	Chapter
Run #1	Rabbit	CB	1:1000	Swant # CB-38a Lot: 9.03	5
	Mouse	vGAT	1:500	Synaptic Systems # 131011 Lot: 131011/41	3, 4, 5
	Guinea pig	GAD65	1:500	Synaptic Systems # 198104 Lot: 198104/3	4, 5
	Goat	GAD67	1:100	R&D Systems # AF2086 Lot: KRD0110031	3, 4, 5
Run #2	Rabbit	CR	1:1000	Swant # 7699/4 Lot: 18_3_13	5
	Mouse	vGAT	1:500	Synaptic Systems # 131011 Lot: 131011/42	3, 4, 5
	Guinea pig	GAD65	1:500	Synaptic Systems # 198104 Lot: 198104/4	4, 5
	Goat	GAD67	1:100	R&D Systems # AF2086 Lot: KRD0110031	3, 4, 5

2.3.2 Immunohistochemistry

The antigenicity of some synaptic proteins is reduced in postmortem human tissue. For example, the detection of vGAT immunoreactivity in postmortem human tissue requires antigen retrieval procedures, which is a method that improves antigenicity (Jiao et al., 1999) (**Figure 2.1**). Importantly, the detection of GAD65, GAD67, CB, and CR are not affected by the antigen retrieval method used here. Accordingly, before the sections were immunolabeled they were incubated in 0.01M sodium citrate in distilled H₂O at 80°C for 75 minutes (Jiao et al., 1999), cooled to room temperature (RT), and then rinsed with 0.1M phosphate buffer (PB).

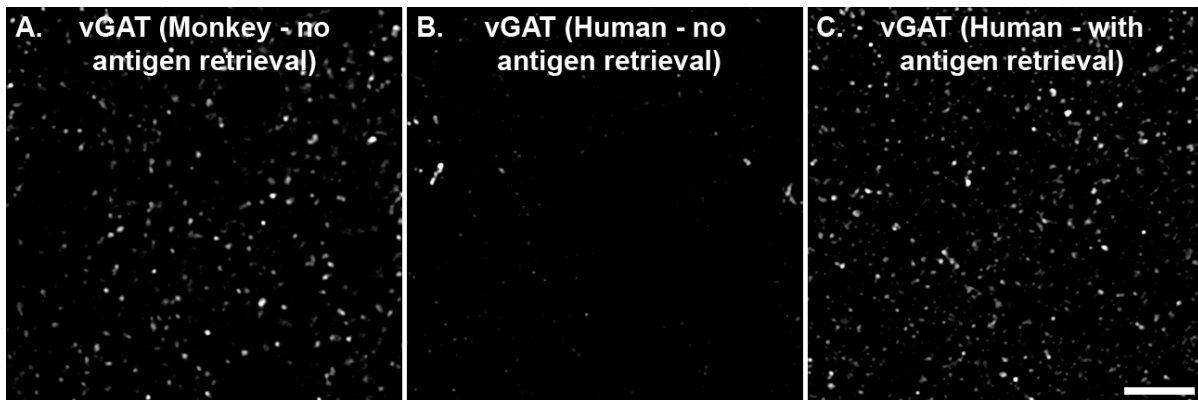


Figure 2.1. Antigen retrieval and vGAT detection in postmortem human tissue. Single plane images from a perfusion-fixed monkey PFC tissue section (A) and immersion-fixed human PFC tissue sections from the same human subject that were immunolabeled for vGAT (B and C). No antigen retrieval was performed on A and B, but C did receive antigen retrieval. The tissue section in B and C were immunolabeled simultaneously, imaged using the same exposure setting, and the histogram settings for the images are identical. Bar = 10 μ m.

Next, the sections were incubated in 1% sodium borohydride in PB for 30 minutes at RT to reduce autofluorescence due to aldehyde fixation and then rinsed in 0.1M phosphate buffered saline (PBS). The sections were permeabilized with 0.3% Triton X-100 in PBS for 30 minutes at RT, incubated in 20% donkey serum in PBS for 2 hours at RT, and then incubated for ~72 hours at 4°C in PBS containing 2% donkey serum and primary antibodies (**Table 2.2**). Antibody specificity was verified in our laboratory or other laboratories (vGAT (Guo et al., 2009); GAD65 and GAD67 (Fish et al., 2011)). Sections were then rinsed for 2 hours in PBS and incubated for 24 hours in PBS containing 2% donkey serum and secondary antibodies (donkey host) conjugated to Alexa Fluor 405 (CB or CR), Alexa Fluor 488 (vGAT), Cy 3 (GAD65) or Alexa Fluor 647 (GAD67) at 4°C. All Alexa Fluor dyes were from Invitrogen (Grand Island, NY, USA; 1:500 for all) and Cy 3 was from Fitzgerald (Acton, MA, USA; 1:500). After washing, sections were mounted (ProLong Gold antifade reagent, Invitrogen) on slides, which were coded to blind diagnosis and subject number, and stored at 4°C until imaged. Secondary antibody specificity was verified by omitting the primary antibody in control experiments. Multiple pilot studies were performed to determine if any primary/secondary combinations influenced the outcome; results from these studies indicated that the ability to detect each antigen was not dependent on the secondary antibody spectra.

2.4 DATA COLLECTION

2.4.1 Microscopy equipment

Data were collected on an Olympus (Center Valley, PA) IX81 inverted microscope equipped with an Olympus spinning disk confocal unit, Hamamatsu EM-CCD digital camera (Bridgewater, NJ), and high precision BioPrecision2 XYZ motorized stage with linear XYZ encoders (Ludl Electronic Products Ltd., Hawthorne NJ) using a 60X 1.40 N.A. SC oil immersion objective. The equipment was controlled by SlideBook 5.0 (Intelligent Imaging Innovations, Inc., Denver, CO, USA), which was the same software used for post-image processing.

2.4.2 Image acquisition

3D image stacks (2D images successively captured at intervals separated by 0.25 μm in the z-dimension) that were 512 x 512 pixels (~137 x 137 μm) were acquired over 50% of the total thickness of the tissue section starting at the coverslip. Importantly, imaging the same percentage of the tissue section thickness rather than a constant depth controls for the potential confound of storage and/or mounting related volume differences (e.g. z-axis shrinkage).

Over- or under-exposing fluorescently labeled images can greatly influence the quality of the acquired data as well as confound the results. For example, over-exposing tissue sections may result in images with saturated pixels, which create a ceiling effect for intensity measurements. Alternatively, under-exposing tissue sections may yield images where only the brightest objects are detectable, which may bias the number of IR objects assessed. The latter scenario is particularly important when measuring protein levels that may be reduced in disease states.

Examples of things in brain tissue that can greatly influence exposure settings include artifacts introduced during experimental procedures, variability of protein content in distinct IR neuronal structures, a high density of unlabeled cell bodies, blood vessels, and autofluorescence from lipofuscin, which is a lipoprotein byproduct of lysosomal degradation that accumulates with senescence and is prominent in postmortem human brain tissue (Brody, 1960).

Over- or under-exposing fluorescently labeled images occur at a higher frequency when using constant exposure settings rather than optimal exposure settings (i.e., those that yield the greatest dynamic range with no saturated pixels). Therefore, to reduce the effects of confounds caused by exposure settings each image stack was collected using optimal exposure settings for each immunofluorescent channel, with differences in exposures normalized during image processing. TetraSpeck microspheres (fluorescent blue/green/orange/dark red; Invitrogen) were used to confirm the absence of alignment issues between wavelengths of each channel.

2.4.3 Novel method for detecting lipofuscin autofluorescence

Lipofuscin autofluorescence can greatly influence exposure settings during image acquisition, but it is also a potential confound for quantitative measures, such as fluorescence intensity and object density analyses. Because of its broad spectral properties lipofuscin autofluorescence may be detected across all of the fluorescent wavelengths used to detect our immunolabeled antigens. In general, signal from lipofuscin autofluorescence is most robust when the signal of the immunolabeled antigens is relatively low. By contrast, lipofuscin autofluorescence may be undetectable when the signal of the immunolabeled antigens is relatively high. Previous immunofluorescent experiments in postmortem human tissue detected lipofuscin autofluorescence by immunolabeling fewer antigens and using a standard excitation/emission filter setting (i.e. the

filter setting used to detect Alexa Fluor 405 immunolabeled antigens) to detect lipofuscin (Curley et al., 2011; Glausier et al., 2014). However, we took advantage of lipofuscin's broad spectral properties, and were able to detect lipofuscin autofluorescence via stokes shift using the excitation and emission filter settings that are typically used for detecting Alexa Fluor 405 and 647, respectively (**Figure 2.2**). These specific filter settings were used because they yielded robust lipofuscin autofluorescence signal without detecting any signal from immunolabeled antigens across all secondary antibody spectra. This approach yielded an additional channel, which was used to detect lipofuscin autofluorescence, without sacrificing a fluorescent channel that was used to detect our immunolabeled antigens (**Figure 2.3**). Since lipofuscin autofluorescence is relatively consistent within and across subjects compared to immunoreactive fluorescence signal, and because its fluorescence intensity levels and volume do not differ between pairs of schizophrenia and age-matched comparison subjects (Curley et al., 2011; Glausier et al., 2015), we used a constant exposure setting to detect lipofuscin autofluorescence.

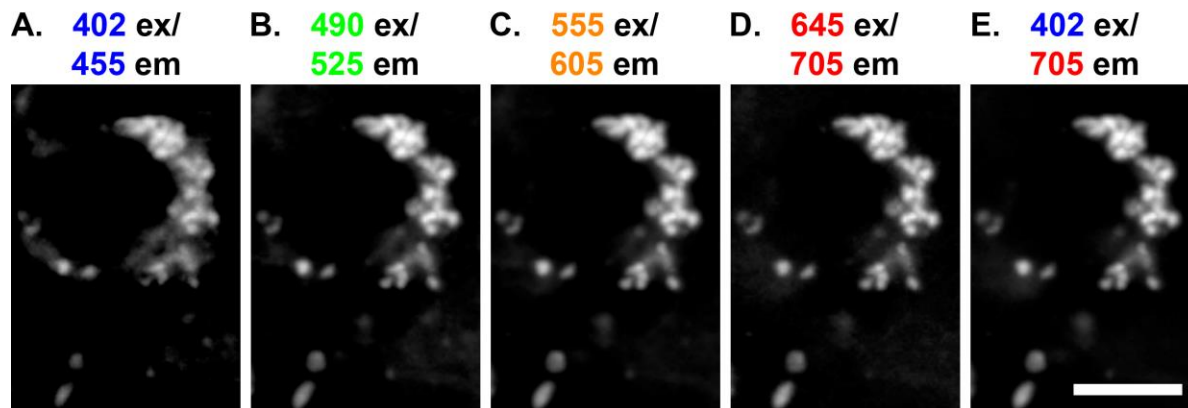


Figure 2.2. Custom filter setting to detect lipofuscin. (A-E) Projection image (5 z-planes taken 0.25 μm) of an unlabeled human tissue section showing the excitation (ex) and emission (em) wavelengths obtained using the Sedat Quad 89000 filter set (Chroma Technology; Bellow Falls, VT, USA) that were used to detect lipofuscin autofluorescence. (A-D) Standard filter settings used to detect (A) Alexa Fluor 405, (B) Alexa Fluor 488, (C) Cy 3, and (D) Alexa Fluor 647. (E) Excitation and emission filter settings from A and D, respectively. Bar = 10 μm .

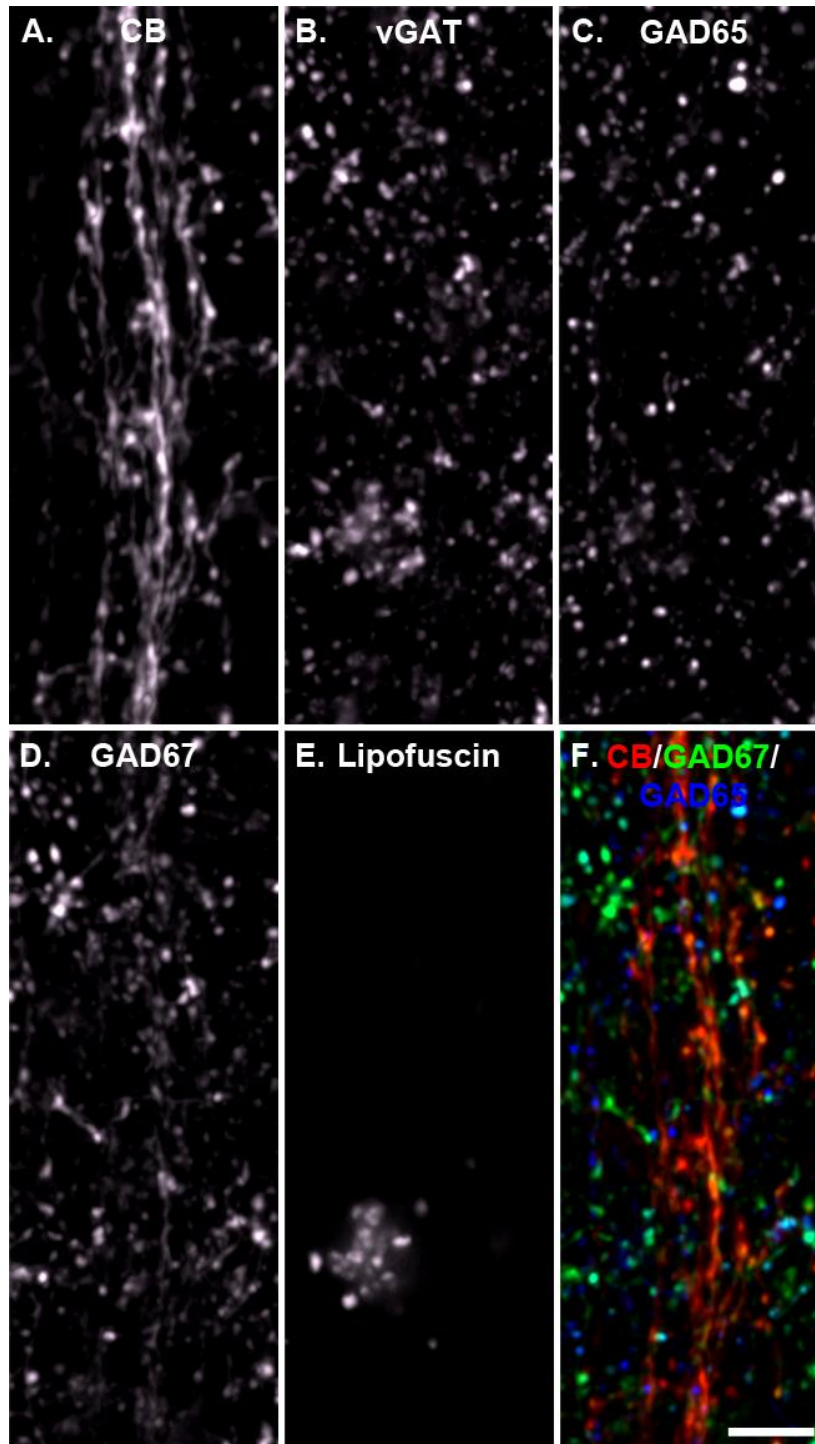


Figure 2.3. Lipofuscin detection in immunolabeled tissue. (A-F) Projection image (10 z-planes taken 0.25 μm) of a human PFC tissue section immunolabeled for CB, vGAT, GAD65, and GAD67. Detection of the single channel

images for (A) CB, (B) vGAT, (C) GAD65, (D) GAD67, and (E) Lipofuscin were performed using the filter settings specified in Figure 2.2 panels A, B, C, D, and E, respectively. (F) Merged image of A, C, and D. Bar = 10 μm .

2.4.4 Sampling

As determined by measurements made in Nissl stained sections of human PFC (Pierri et al., 1999), the boundaries of the six cortical layers, defined by cytoarchitectonic criteria, in area 9 can be precisely estimated based on the distance from the pial surface to the gray/white matter border. For sampling the total gray matter of the PFC, we divided the cortical mantle into layers as follows: layer 1 (pia-10%), layer 2-superficial 3 (10-35%), layer deep 3/ 4 (35-60%), layer 5 (60-80%), and layer 6 (80%-gray/white matter border) (**Figure 2.4**). Ten, systematic randomly sampled image stacks were taken within each of these subdivisions using a sampling grid of 180 x 180 μm^2 . Running means using pilot data indicated that 10 sites per subdivision were sufficient to limit intra-subject variability for intensity and density measures. The same investigator (BRR), who was blind to subject and diagnosis, collected a total of 8,000 image stacks (1,600 stacks per layer). Importantly, subjects within a pair were imaged on the same day.

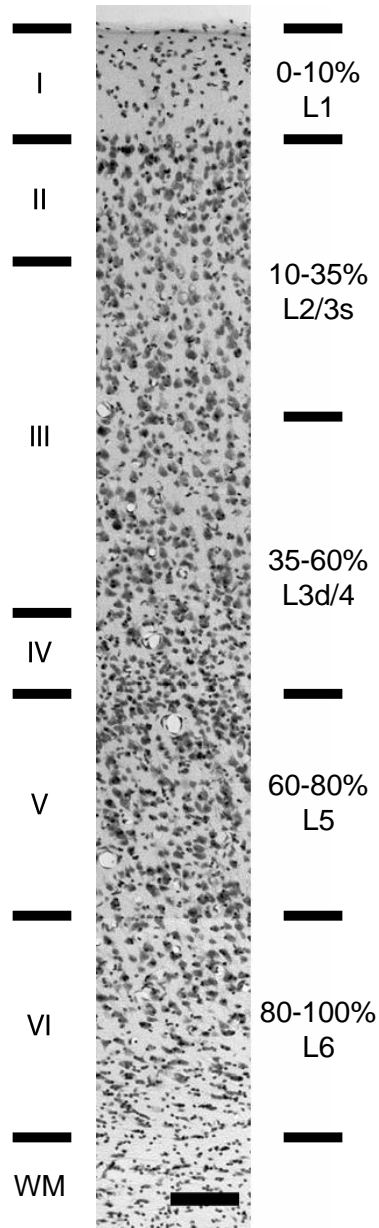


Figure 2.4. Layer delineation for sampling within total PFC gray matter. Nissl stained monkey PFC tissue section showing layer delineation by cytoarchitectonic criteria (Roman numerals) and by layer 1 (L1), layer 2/superficial 3 (L2/3s), layer deep 3/4 (L3d/4), layer 5 (L5), and layer 6 (L6), which correspond to 0-10%, 10-35%, 35-60%, 60-80%, and 80-100%, respectively, of the total gray matter area spanning from pia to the gray/white matter border. Bar = 250 μ m.

2.5 DATA SEGMENTATION

2.5.1 Image processing

Each channel used to detect immunoreactivity was deconvolved using AutoQuant's Blind Deconvolution algorithm (MediaCybernetics; Rockville, MD, USA). No processing was performed on the channel used to detect lipofuscin autofluorescence.

For data segmentation, a Gaussian channel was made for each fluorescent channel by calculating a difference of Gaussians using sigma values of 0.7 and 2. This was done to improve the ability to discriminate between non-overlapping immunoreactive puncta (**Figure 2.5**). Importantly, the Gaussian channel was used for data segmentation only.

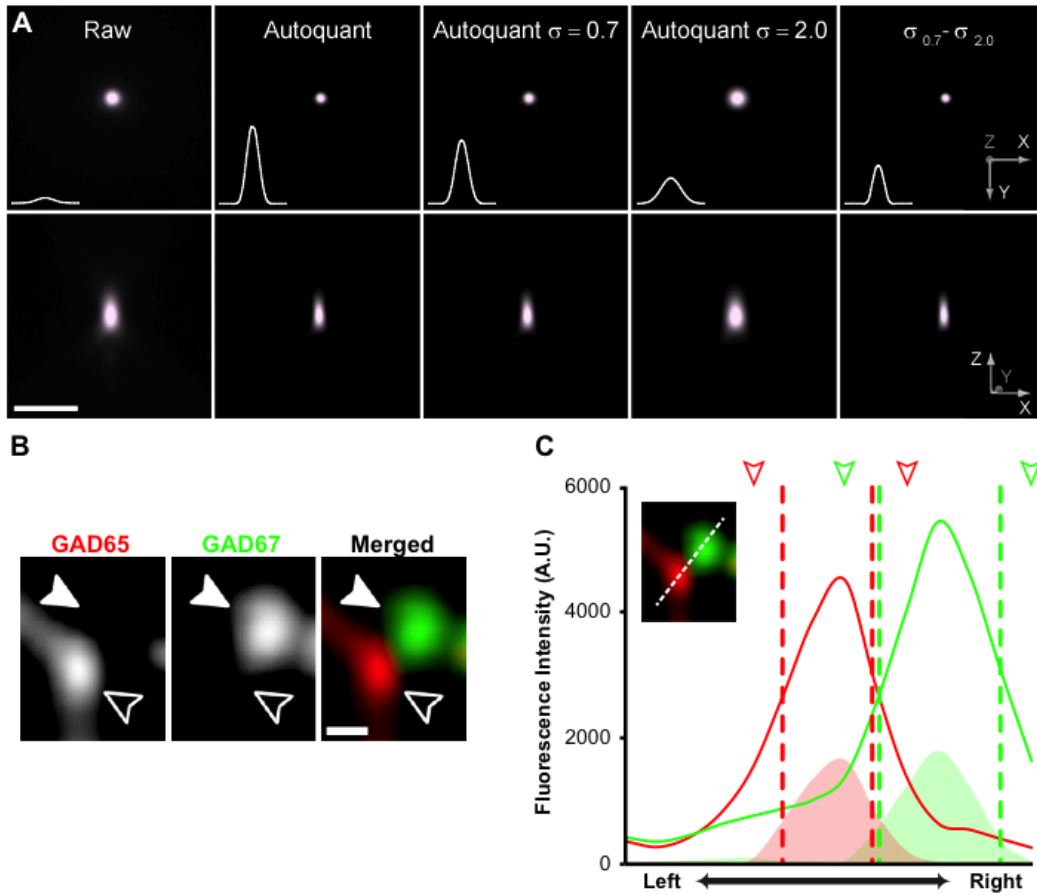


Figure 2.5. Method to improve discrimination of non-overlapping puncta. To improve data segmentation, a Gaussian channel was made for each deconvolved channel by calculating a difference of Gaussians using sigma values of 0.7 and 2, which improves the ability to discriminate puncta. (A) Image of a 100 nm diameter fluorescent microsphere processed as labeled and shown in x,y-axis (top) and x,z-axis (bottom). Autoquant = deconvolved images; σ = Gaussian blur radius; line plots = intensity profile of a line drawn through the center of the microsphere; Bar = 2 μm . Note: after subtracting the Gaussian channels, negative pixel values were converted to zero. (B) Projection image (3 z-planes separated by 0.20 μm) of a GAD65-IR puncta (open arrowhead) and a GAD67-IR puncta (solid arrowhead). Bar = 0.5 μm . (C) Line intensity plots (dotted line within the inset image) of GAD65 (red line) and GAD67 (green line) fluorescent intensity levels in the apposed GAD65-IR and GAD67-IR puncta from B. Shaded plots represent the line intensities after Gaussian subtraction. The dashed lines show the boundaries of GAD65 (red) and GAD67 (green) object masks made using the Autoquant deconvolved Gaussian subtracted channel

and the iterative approach described in **2.5.2**. Red and green arrowheads show the boundaries of the GAD65 and GAD67 masks, respectively, made using the Autoquant channel prior to Gaussian subtraction. Importantly, the Gaussian subtracted channel is used for data segmentation only; fluorescence intensity levels are calculated from the Autoquant deconvolved channels.

2.5.2 Masking immunoreactive objects

Data segmentation was performed as described (Fish et al., 2008), with a few exceptions. A single optimal threshold value, which incorporated the Ridler-Calvard iterative thresholding algorithm (Ridler and Calvard, 1978) and also accounted for variance in fluorescence intensity between sites was used to obtain an initial value for iterative segmentation for each channel within each image stack. Multiple iterations with subsequent threshold settings increasing by 25 gray levels were performed in MATLAB R2012 (MathWorks; Natick, MA, USA). After each iteration, the object masks were size-gated within a range of 0.03-0.5 μm^3 .

The lipofuscin channel was masked using a single optimal threshold value for each image stack, and each lipofuscin mask was size-gated so that all were $\geq 0.03 \mu\text{m}^3$. Any CB, CR, vGAT, GAD65, and GAD67 object masks that overlapped a lipofuscin mask were eliminated from analyses. A paired analysis of covariance (ANCOVA) model, which included the sum fluorescence intensity of lipofuscin as the dependent measure, diagnostic group as the main effect, subject pair as the blocking factor, and tissue storage time as a covariate, and an unpaired ANCOVA which included age, PMI, and storage time as covariates found no differences in

lipofuscin fluorescence intensity between schizophrenia (648 ± 140 a.u.) and comparison (656 ± 147 a.u.) subjects (paired $F_{1,19} = 0.08$, $p = 0.79$; unpaired $F_{1,36} = 0.03$, $p = 0.86$).

2.6 DATA ANALYSES

2.6.1 Virtual cropping

For analyses, the image stacks were virtually cropped in the x-, y-, and z-dimensions. This was done using the center x-, y-, and z-coordinates of the IR puncta object masks. In the x- and y-dimensions the center of each object mask had to be contained in the central 490 x 490 pixels of the image. To select the z-dimension used for analyses, the z-position of each object mask was normalized by the following equation:

$$Z_{\text{coordinate}} (\# \text{ of z-planes for image stack} / 40)$$

Next, each object mask was placed in one of 40 z-bins based on its normalized z-position. The mean object mask density and mean fluorescence intensity for CB, CR, vGAT, GAD65, and GAD67 were determined within each z-bin, and used for an analysis of variance with post-hoc comparison via Tukey's honestly significant difference test. The maximum number of adjacent z-bins that were not significantly different for both intensity and object mask number across all channels were used for analyses ($n = 17$ bins, which corresponded to $8.5 \mu\text{m}$ of the cut tissue thickness). By taking this approach we controlled for possible edge effects (i.e. all puncta assessed were fully represented in the virtual space), differences in antibody penetration, and differences in fluorochromes. The final object masks were then used to collect information on the deconvolved channels.

2.6.2 Method for defining colocalization

All vGAT-IR puncta were considered to be boutons (vGAT+ boutons)(Chaudhry et al., 1998; McIntire et al., 1997). vGAT+ boutons that contained GAD immunoreactivity were classified as containing detectable levels of GAD65 and low to no GAD67 levels (vGAT+/GAD65+ boutons), low to no GAD65 levels and detectable levels of GAD67 (vGAT+/GAD67+ boutons), and detectable levels of both GADs (vGAT+/GAD65+/GAD67+ boutons). Initially to obtain the vGAT+/GAD+ bouton subpopulations, mask operations, which assess the degree of overlap between voxels of distinct object masks, were used to identify GAD65 and vGAT object masks that overlapped each other's centers and did not overlap a GAD67 object mask (vGAT+/GAD65+ boutons). vGAT+/GAD67+ boutons were similarly defined. vGAT object masks that overlapped the center of both a GAD65 and GAD67 object mask were defined as vGAT+/GAD65+/GAD67+. **Figure 2.6** illustrates the accuracy of defining boutons as GAD65-IR, GAD67-IR, or GAD65-IR/GAD67-IR using only mask operations.

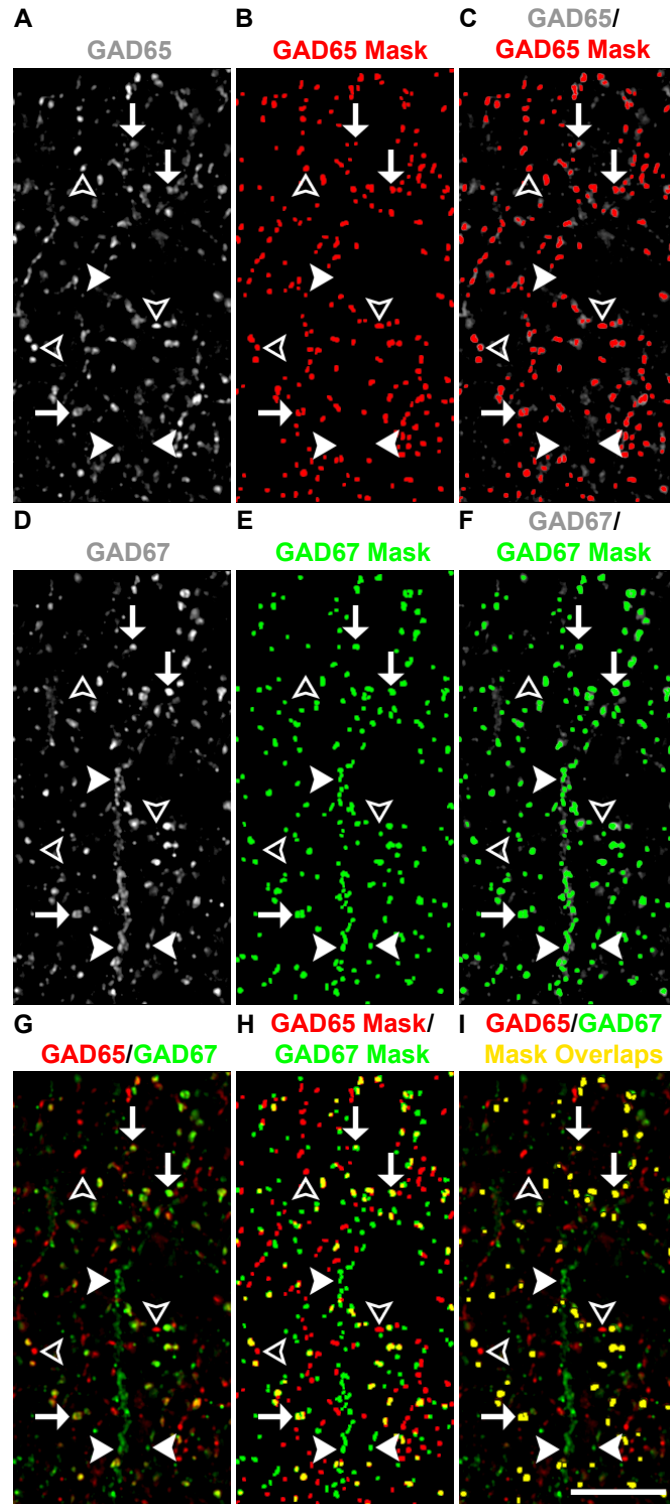


Figure 2.6. GAD content in boutons that were defined using only mask operations. Example showing the use of mask operations to assess colocalization of GAD65-IR and GAD67-IR puncta. (A-I) Projection images (3 z-planes

taken 0.20 μm apart) of a monkey PFC tissue section immunolabeled for GAD65 and GAD67. Single GAD65 (A) and GAD67 (D) channels. Corresponding GAD65 (B) and GAD67 (E) object masks. Overlay of GAD65 and GAD67 channels with their corresponding object masks (C and F, respectively). (G) Merged GAD65 and GAD67 channels. (H) Merged GAD65 and GAD67 object masks. (I) The image in G overlaid with those object masks in H that are colocalized (yellow), which designate GAD65+/GAD67+ boutons. Arrows depict putative GAD65+ boutons (open arrowheads), GAD67+ boutons (solid arrowheads), and GAD65+/GAD67+ boutons (arrows). Bar = 10 μm .

Next, intensity information from the boutons defined by using mask operations was used to define the remaining vGAT+ boutons. Specifically, the mean fluorescence intensity of GAD65 for all vGAT+/GAD65+ and vGAT+/GAD65+/GAD67+ boutons and the mean fluorescence intensity of GAD67 for all vGAT+/GAD67+ and vGAT+/GAD65+/GAD67+ boutons that were classified using mask operations criteria were used as seeds in a K-means cluster analysis to classify all boutons per each image stack. **Figure 2.7** shows scatterplots from a single randomly chosen stack for each step of the method used to classify boutons as vGAT+/GAD65+, vGAT+/GAD67+, and vGAT+/GAD65+/GAD67+.

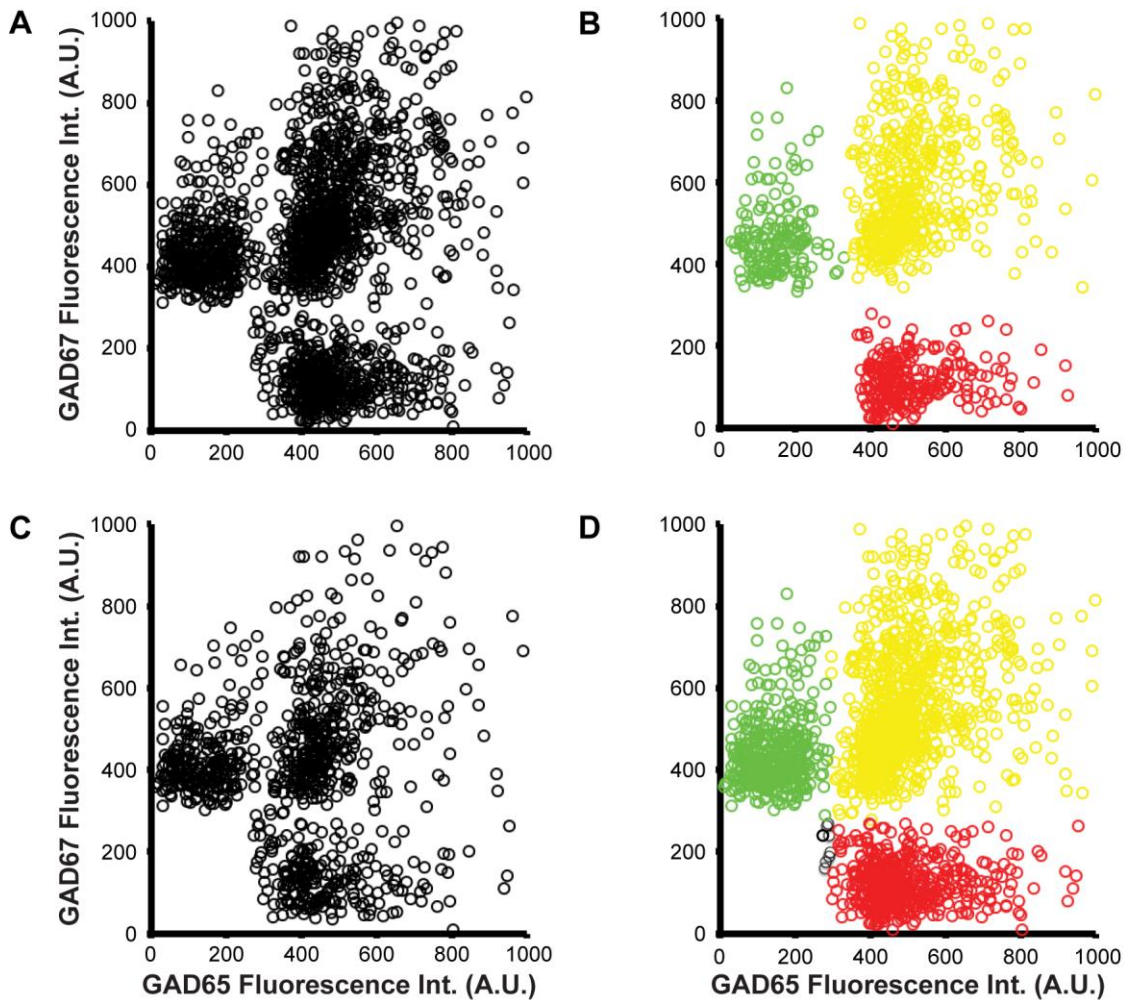


Figure 2.7. Classification of GAD content in vGAT+ boutons. (A-D) Mean GAD65 and GAD67 fluorescence intensities from individual vGAT+ boutons from a randomly selected image stack of monkey PFC immunolabeled for vGAT, GAD65, and GAD67. Each vGAT+ bouton was classified as vGAT+/GAD65+, vGAT+/GAD67+, or vGAT+/GAD65+/GAD67+ using mask operations and K-means cluster analysis. (A) Scatterplot of mean GAD65 and GAD67 fluorescence intensities of all vGAT object masks that overlapped a GAD65 and/or GAD67 object mask. (B) Mask operations was used to select vGAT object masks in A that overlapped the center of a GAD65 object mask and did not overlap a GAD67 object mask (red; vGAT+/GAD65+ boutons), that overlapped the center of a GAD67 object mask and did not overlap a GAD65 object mask (green; vGAT+/GAD67+ boutons), or that overlapped the center of a single GAD65 and a single GAD67 object mask (yellow; vGAT+/GAD65+/GAD67+ boutons).

vGAT+/GAD+ boutons classified by only mask operations accounted for ~70% of all vGAT+ boutons that were GAD-IR. (C) vGAT object masks in A that did not meet the mask operations classification criteria used in B. (D) All vGAT object masks in A classified using the mean GAD65 and GAD67 fluorescence intensity values calculated from the three vGAT+/GAD+ bouton subpopulations in B as seeds in a K-means cluster analysis. Black data points were vGAT object masks that did not meet criteria to be classified as vGAT+/GAD65+, vGAT+/GAD67+, or vGAT+/GAD65+/GAD67+ boutons using these criteria.

2.7 CONCLUSION

The methodology used here is an unbiased quantitative approach to assess bouton protein levels via the colocalization of multiple pre-synaptic proteins in postmortem human tissue. Every step of the method was meant to reduce the effects of confounding variables inherent in human tissue and in studies using fluorescence confocal microscopy. This Chapter is a detailed description of the methods that were used to quantify bouton density and bouton protein levels in **3.0**, **4.0**, and **5.0** between matched pairs of schizophrenia and comparison subjects.

3.0 MARKEDLY LOWER GAD67 PROTEIN LEVELS IN A SUBSET OF BOUTONS IN THE PREFRONTAL CORTEX OF SCHIZOPHRENIA

Adapted from: Rocco BR, Lewis DA, Fish KN. Markedly lower glutamic acid decarboxylase 67 protein levels in a subset of boutons in schizophrenia. Submitted April 22, 2015 to Biological Psychiatry

3.1 INTRODUCTION

Cognitive deficits, such as impairments in working memory, are recognized as core clinical features in schizophrenia (Kahn and Keefe, 2013), and these impairments are thought to reflect, at least in part, disturbances in GABA neurons within the PFC (Lewis, 2014). Perhaps the most widely and consistently reported finding in postmortem studies of schizophrenia subjects is lower levels of mRNA for GAD67 (Akbarian et al., 1995; Curley et al., 2011; Duncan et al., 2010; Guidotti et al., 2000; Hashimoto et al., 2003; Volk et al., 2000). Although less well-studied, the deficit in GAD67 mRNA has been reported to be accompanied by lower GAD67 protein levels (Curley et al., 2011; Guidotti et al., 2000; Impagnatiello et al., 1998). The consistency of these findings suggests that lower GAD67 expression in schizophrenia is a common feature of the illness. Other findings indicate that it is not a consequence of illness chronicity or other factors frequently associated with the illness, such as use of antipsychotic medications (Curley et al.,

2011; Hoftman et al., 2013).

However, not all GABA neurons exhibit lower GAD67 mRNA expression in schizophrenia. Specifically, ~30% of GABA neurons in schizophrenia PFC lack detectable levels of GAD67 mRNA, whereas the others express GAD67 mRNA at normal levels (Akbarian et al., 1995; Volk et al., 2000). The subset of GABA neurons with markedly lower GAD67 mRNA expression is prominent in PFC layers 2-5 (Akbarian et al., 1995; Volk et al., 2000). This deficit occurs in the absence of a change in total neuron density (Akbarian et al., 1995) or number (Thune et al., 2001), suggesting that all GABA neurons are present but that a subset have a markedly reduced capacity to synthesize GABA. Moreover, expression of some other gene products that can affect GABAergic neurotransmission are reported to be unaffected or only slightly altered in schizophrenia. For example, mRNA for vGAT is reported to be unchanged or only modestly lower in the PFC of schizophrenia subjects (Fung et al., 2011; Hoftman et al., 2013), suggesting that the ability to load GABA into vesicles is preserved in the illness.

Although the timing of onset of the GAD67 mRNA deficit is unknown, dysfunction of the PFC in schizophrenia appears to be a late developmental event. For example, in children who are later diagnosed with schizophrenia, working memory performance appears to be intact until about 9 years of age and then subsequently declines (Reichenberg et al., 2010). Because working memory relies on the coordinated firing of PFC pyramidal neurons (Goldman-Rakic, 1995) by GABA neurons (Constantinidis et al., 2002; Rao et al., 2000), these findings suggest that the GAD67 deficit may arise during childhood. Knowing if structural alterations in GABAergic axonal boutons occur in schizophrenia could inform on the timing of the GAD67 deficit in the illness. For example, genetic reduction of GAD67 expression in PV basket cells during early stages of development results in fewer boutons, whereas the same reduction later does not alter

axonal architecture (Chattopadhyaya et al., 2007). Thus, it would be expected that a reduction in GAD67 expression during the pre- or peri-natal periods in individuals who are later diagnosed with schizophrenia would be accompanied by fewer GABAergic boutons.

In concert, these findings suggest the following testable hypotheses: 1) The density of all GABAergic boutons is unaltered in the PFC of subjects with schizophrenia; 2) GAD67 protein levels are markedly lower in a subset of these boutons.

3.2 MATERIALS AND METHODS

3.2.1 Experimental procedures

Specific procedures for tissue procurement, subject pairing, immunohistochemistry, and data collection and segmentation are described in **2.0**. Briefly, PFC tissue sections from 20 pairs of schizophrenia and matched comparison subjects (**Table 2.1**) were immunolabeled for vGAT and GAD67 (**Table 2.2**). Bouton density and relative fluorescence intensity levels of vGAT and GAD67 within boutons were assessed within total gray matter using quantitative confocal microscopy techniques.

3.2.2 Definitions of vGAT+ and vGAT+/GAD67-IR boutons

All vGAT- IR puncta were considered to be GABAergic boutons (vGAT+ boutons)(Chaudhry et al., 1998; McIntire et al., 1997). vGAT+ boutons were classified as being IR for GAD67 (vGAT+/GAD67-IR boutons) as follows: initially, mask operations were used to identify vGAT

and GAD67 object masks that overlapped each other's centers as described in 2.6.2. Next, for each site the mean fluorescence intensity of GAD67 for all boutons identified in the first step were used as seeds in a K-means cluster analysis to classify vGAT+ boutons as being GAD67-IR. An example of boutons classified as vGAT+ and vGAT+/GAD67-IR is shown in **Figure 3.1**.

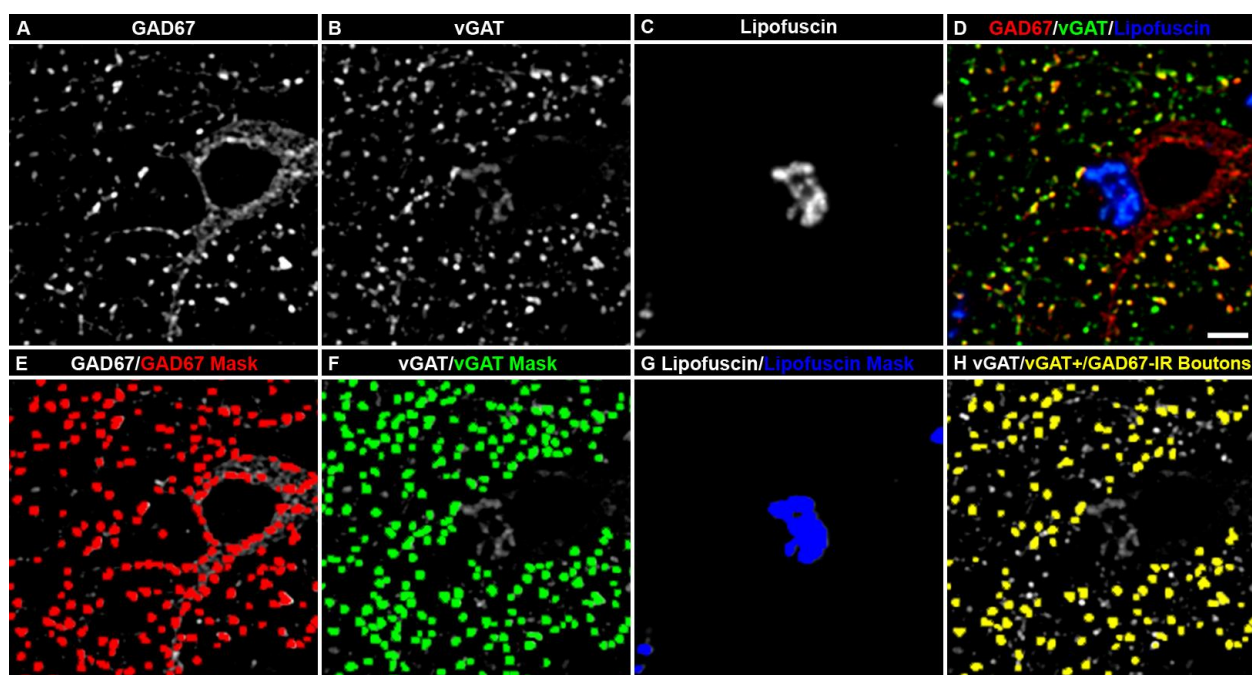


Figure 3.1. vGAT and GAD67 colocalization in human postmortem tissue. (A-H) Projection image (5 z-planes separated by 0.25 μm) of a human PFC tissue section immunolabeled for vGAT and GAD67. Single GAD67 (A) and vGAT (B) IR channels, and single channel of lipofuscin (C) autofluorescence. (D) Merged GAD67, vGAT, and lipofuscin channels. Single GAD67, vGAT, and lipofuscin channels overlaid with their corresponding object masks (E, F, and G, respectively). Importantly, the object masks in F define the vGAT+ boutons (green object masks). (H) Single vGAT channel overlaid with vGAT object masks from F that were defined as vGAT+/GAD67-IR boutons (yellow object masks). Bar = 5 μm .

3.2.3 Statistics

Data are presented as mean bouton density (\pm standard deviation; SD) and mean sum fluorescence intensity (\pm SD). Two analyses of covariance (ANCOVA) models were used to analyze the bouton density and protein level data. Because subjects were selected and processed as pairs, the first paired ANCOVA model included bouton density or protein level as the dependent variable, diagnostic group as the main effect, subject pair as a blocking factor, and tissue storage time as a covariate. Subject pairing is an attempt to balance diagnostic groups for sex, age, and PMI, and to account for the parallel processing of tissue samples, and thus is not a true statistical paired design. Consequently, a second unpaired ANCOVA model was performed that included age, PMI, and storage time as covariates. All statistical tests were conducted with α -level= 0.05.

We also assessed the potential influence of other factors that are frequently comorbid with the diagnosis of schizophrenia using ANCOVA models. For these analyses, we compared subjects with schizophrenia using each variable (sex; diagnosis of schizoaffective disorder; use of nicotine at the time of death (ATOD), antipsychotics ATOD, antidepressants ATOD, or benzodiazepines and/or sodium valproate ATOD) as the main effect and age, tissue storage time, and PMI as covariates. A Bonferroni-adjusted α -level of $0.05/6 = 0.008$ was used to assess significance.

Reported ANCOVA statistics include only those covariates that were statistically significant. As a result, the reported degrees of freedom vary across analyses.

3.3 RESULTS

3.3.1 vGAT+ bouton density and vGAT protein levels are unchanged in schizophrenia

A total of $968,186 \pm 82,032$ and $948,895 \pm 95,695$ vGAT+ boutons for each schizophrenia and comparison subject, respectively, were analyzed. The density of vGAT+ boutons did not differ (paired $F_{1, 19} = 0.69$, $p = 0.417$; unpaired $F_{1, 38} = 0.47$, $p = 0.497$) between diagnostic groups (schizophrenia: 0.033 ± 0.003 boutons/ μm^3 ; comparison: 0.032 ± 0.003 boutons/ μm^3 ; **Figure 3.2A**). Also, bouton levels of vGAT protein did not differ (paired $F_{1, 19} = 3.34$, $p = 0.083$; unpaired $F_{1, 38} = 3.64$, $p = 0.064$) between diagnostic groups (schizophrenia: 564 ± 72 a.u.; 611 ± 83 a.u.; **Figure 3.2B**).

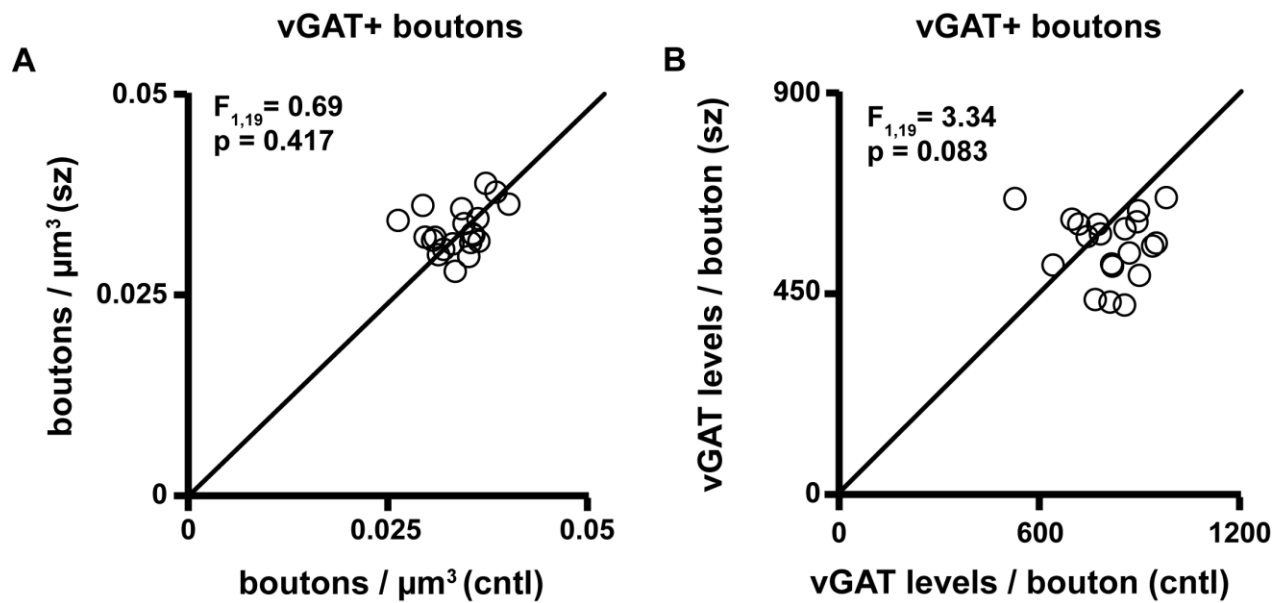


Figure 3.2. vGAT+ bouton densities and vGAT protein levels. Mean vGAT+ bouton density (A) and bouton vGAT protein levels (B) in total gray matter. The data points in each scatterplot represent a matched pair of schizophrenia (sz) and comparison (cntl) subject. Points below the unity line reflect pairs in which the measures are lower for the schizophrenia relative to the comparison subject.

3.3.2 vGAT+/GAD67-IR bouton density is lower in schizophrenia

The density of vGAT+/GAD67-IR boutons was 16% lower (paired $F_{1, 19} = 10.39$, $p = 0.004$; unpaired $F_{1, 38} = 12.44$, $p = 0.001$) in schizophrenia (0.015 ± 0.003 boutons/ μm^3) relative to comparison (0.018 ± 0.002 boutons/ μm^3) subjects (**Figure 3.3A**). These findings suggest that a subset of vGAT+ boutons lack detectable GAD67 protein levels.

3.3.3 vGAT+/GAD67-IR bouton GAD67 protein levels are lower in schizophrenia

vGAT protein levels in vGAT+/GAD67-IR boutons did not differ (paired $F_{1, 18} = 0.16$, $p = 0.69$; unpaired $F_{1, 37} = 0.06$, $p = 0.81$) between diagnostic groups (schizophrenia: 822 ± 134 a.u.; comparison: 817 ± 122 a.u.; **Appendix C Figure C.1**). By contrast, GAD67 protein levels in vGAT+/GAD67-IR boutons were 14% lower (paired $F_{1, 19} = 9.57$, $p = 0.006$; unpaired $F_{1, 38} = 8.33$, $p = 0.006$) in schizophrenia (808 ± 120 a.u.) relative to comparison (942 ± 172 a.u.) subjects (**Figure 3.3B**). To assess if lower GAD67 levels were present in all vGAT+/GAD67-IR boutons in subjects with schizophrenia, GAD67 levels per bouton in the comparison group were divided into 10 equally spaced bins and each bouton from both subject groups was placed into a bin based on its GAD67 level (**Figure 3.3C**). The presence of boutons in the bin corresponding to the upper 10th percentile suggests that some boutons do not have a reduction in GAD67 levels.

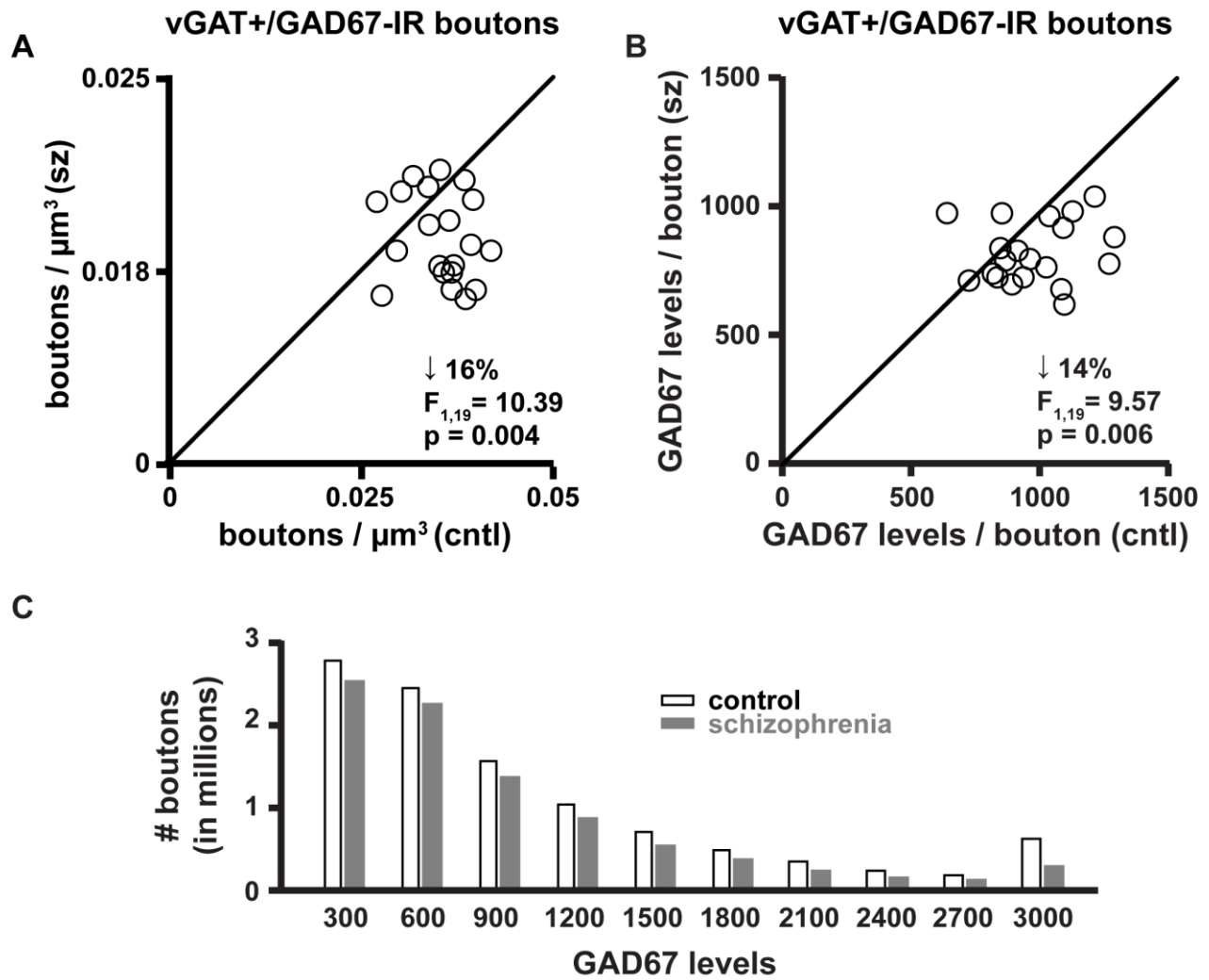


Figure 3.3. vGAT+/GAD67-IR bouton densities and GAD67 protein levels. Mean bouton density (A) and GAD67 protein levels per vGAT+/GAD67-IR bouton (B) in total gray matter. (C) To assess if GAD67 levels were 14% lower across all boutons in schizophrenia, the range of GAD67 levels in the comparison group was used to make 10 equally separated bins and each bouton from both diagnostic groups was placed into a bin based on its GAD67 level.

3.3.4 Lower vGAT+/GAD67-IR bouton density and GAD67 protein levels are not attributable to comorbid factors

GAD67 protein levels in vGAT+/GAD67-IR boutons, and the density of vGAT+/GAD67-IR boutons did not differ as a function of sex, nicotine use ATOD, benzodiazepines and/or sodium valproate ATOD, antidepressants ATOD, antipsychotics ATOD, or diagnosis of schizoaffective disorder (**Figure 3.4**).

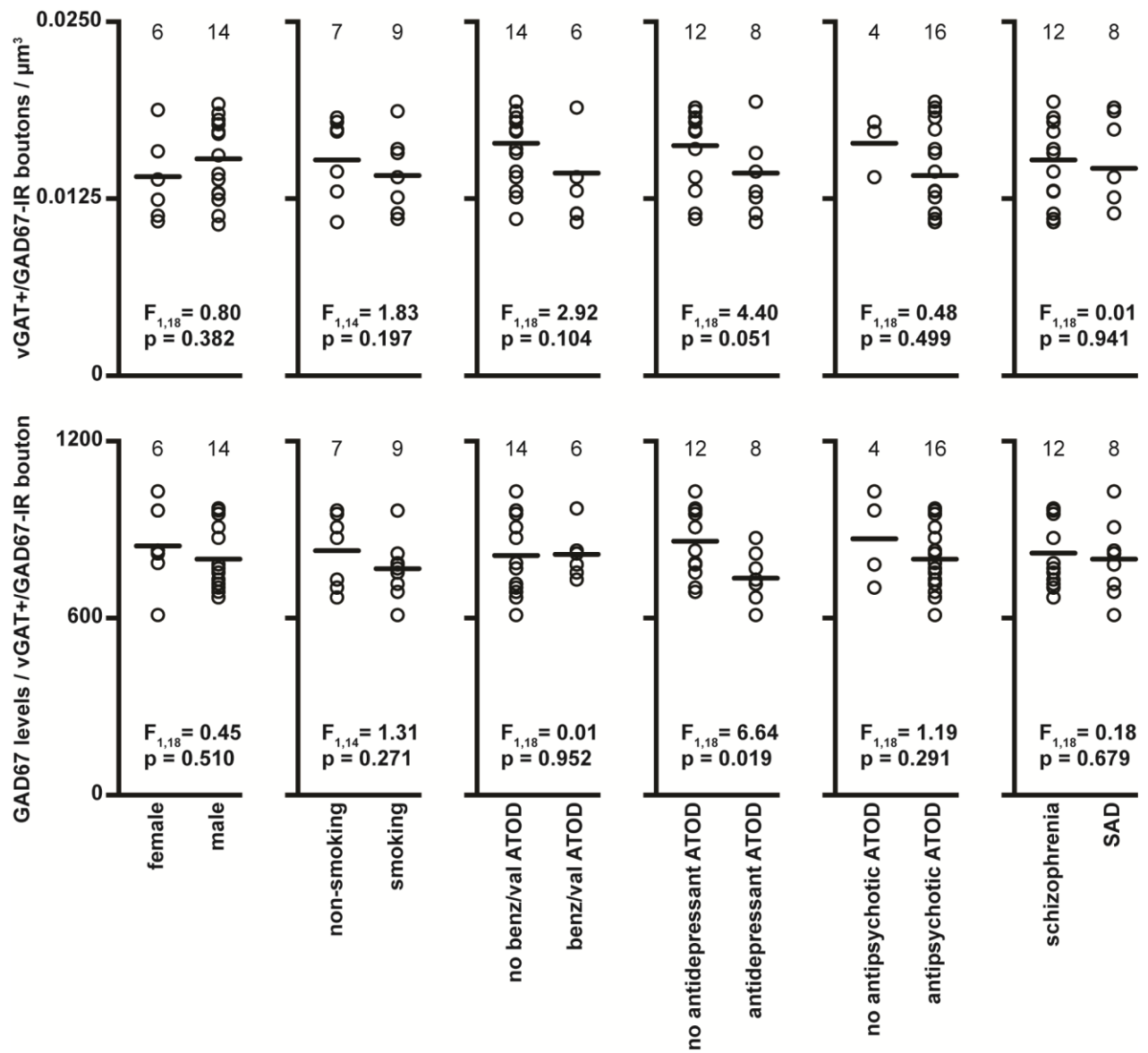


Figure 3.4. Effects of comorbid factors on vGAT+/GAD67-IR bouton density and levels of GAD67 in subjects with schizophrenia. ATOD, at time of death; benz/val; benzodiazepines/valproic acid; SAD, schizoaffective disorder.

3.4 DISCUSSION

In schizophrenia neither neuronal density (Akbarian et al., 1995) nor total neuron number (Thune et al., 2001) are altered in the PFC, suggesting that all GABA neurons are present. In support of this interpretation, others have found no difference in the density of GAD65-IR puncta in the PFC of subjects with schizophrenia relative to comparison subjects (Benes et al., 2000). However, in primate PFC not all boutons contain detectable levels of GAD65 (Fish et al., 2011; Glausier et al., 2014; Rocco et al., 2015). Here, the presence of vGAT, which is required to package GABA for vesicular release (Chaudhry et al., 1998), and therefore is a marker of all GABAergic terminals, was used to quantify GABAergic bouton density. Importantly, vGAT mRNA levels (Fung et al., 2011; Hoftman et al., 2015) are not altered in schizophrenia. We found no differences in the density of vGAT+ boutons between schizophrenia and comparison subjects in the PFC. In concert, these findings support the hypothesis that the density of GABAergic axonal boutons is unaltered in the PFC of subjects with schizophrenia.

Convergent findings suggest that in addition to its role as the primary inhibitory neurotransmitter in the adult brain, GABA signaling is crucial for the maturation of inhibitory synapses (Huang, 2009). For example, genetic knockdown of GAD67 in developing GABA neurons results in a cell-autonomous reduction in bouton formation (Chattopadhyaya et al., 2007). By contrast, reduced GAD67 expression in mature GABA neurons does not alter bouton number or morphology. Thus, the observations made here of markedly lower bouton GAD67 levels but a normal complement of vGAT boutons suggests that the GAD67 deficit in schizophrenia occurs after the maturation of the affected GABA neurons. Interestingly, in monkey PFC mature levels of vGAT and GAD67 mRNA are not achieved until the peripubertal period (Hoftman et al., 2013). This interpretation is supported by the finding that in schizophrenia working memory

performance appears to be intact prior to 9 years of age, but slowly declines afterwards (Reichenberg et al., 2010), suggesting that GAD67 levels within PFC GABA neurons involved in working memory are reduced later in development.

At the cellular level, the density of GABA neurons with detectable levels of GAD67 mRNA is ~30% lower across cortical layers 2-5 in the PFC of subjects with schizophrenia, whereas the levels of GAD67 mRNA within the other neurons do not differ from healthy comparison subjects (Akbarian et al., 1995; Volk et al., 2000). These findings led us to hypothesize that GAD67 protein levels are markedly lower in a subset of boutons. Our finding that GAD67 protein levels are markedly lower in 16% of GABAergic boutons such that they are no longer detectable by GAD67 immunoreactivity supports this hypothesis. However, considering that ~30% of GABA neurons are affected by marked deficits in GAD67 mRNA expression it was surprising that GAD67 levels were not markedly lower in more boutons. We did find that mean GAD67 levels were 14% lower in the remaining vGAT+/GAD67-IR boutons. This finding could reflect a general 14% reduction in vGAT+/GAD67-IR bouton GAD67 levels, but some boutons appear to have normal levels of GAD67 protein (**Figure 3.3C**), suggesting that a subset of boutons have lower, but still detectable GAD67 levels. The idea that the capacity to synthesize GABA is impaired in a subset of GABAergic boutons is in accordance with evidence that GAD67 mRNA is lower only in a subset of GABA neurons. PV neurons appear to be affected by markedly reduced GAD67 mRNA expression (Hashimoto et al., 2003), and GAD67 levels have been reported to be lower in boutons of PV basket cells (Curley et al., 2011).

The cause(s) of lower PFC GAD67 levels in schizophrenia is unclear but multiple mechanisms may contribute to the deficit. For example, allelic variants in the gene encoding GAD67, GAD1, are associated with lower GAD67 expression and an increased risk of

schizophrenia (Addington et al., 2005; Straub et al., 2007). Dysregulated epigenetic mechanisms, such as altered chromatin-associated histone modifications and higher-order chromatin structure at the GAD1 promoter region are also associated with lower GAD67 expression in the illness (Bharadwaj et al., 2013; Huang et al., 2007; Tang et al., 2011). Reduced mRNA expression for upstream regulatory factors of the GAD1 gene have been reported in schizophrenia and correlate with reduced levels of GAD67 mRNA (Kimoto et al., 2014). However, none of these factors provide an obvious mechanism to account for lower GAD67 mRNA in just a subset of GABA neurons and lower GAD67 protein in just a subset of boutons. Alternatively, lower GAD67 expression may be a compensatory response to lower activity in cortical pyramidal neurons (Lewis et al., 2012) in which case those GABA neurons that receive high levels of excitatory drive from pyramidal neurons, such as PV neurons (Melchitzky and Lewis, 2003), might be predicted to be preferentially affected. The fact that the number of excitatory inputs to the affected pyramidal neurons is reduced during late childhood and adolescence (Petanjek et al., 2011) might account for the late developmental reduction in GAD67 predicted by the results of the present study.

4.0 GAD67 PROTEIN LEVELS ARE UNCHANGED IN CHANDELIER CELL BOUTONS IN THE PREFRONTAL CORTEX OF SCHIZOPHRENIA

4.1 INTRODUCTION

~30% of neurons in the PFC of schizophrenia subjects lack detectable GAD67 mRNA expression (Akbarian et al., 1995; Volk et al., 2000), which is associated with a lack of detectable GAD67 protein levels in 16% of vGAT+ boutons, and a 14% reduction in GAD67 levels in boutons with detectable GAD67 immunoreactivity (**3.0**). These deficits occur without a change in neuronal density or number (Akbarian et al., 1995; Thune et al., 2001) and bouton density (**3.0**). Several findings suggest that reduced GAD67 expression affects multiple subtypes of GABA neurons (Curley et al., 2011; Fung et al., 2010; Morris et al., 2008; Woo et al., 1998), and therefore identifying which GABA neuron subtypes are affected by lower GAD67 levels is important for understanding the potential causes of a GAD67 deficit in schizophrenia.

PV neurons contribute to the subset of GABA neurons with marked reductions in GAD67 expression. Specifically, roughly half of all PV neurons lack detectable levels of GAD67 mRNA in the PFC of schizophrenia (Hashimoto et al., 2003). PV neurons can be subdivided into basket cells and chandelier cells based on morphological and molecular properties. For example, PV basket cells principally target the perisomatic region and proximal dendrites of pyramidal cells (Melchitzky et al., 1999), whereas chandelier cells exclusively innervate the AIS of pyramidal

cells (Szentagothai and Arbib, 1974). Moreover, boutons from PV basket cells are GAD65+/GAD67+, whereas those from chandelier cells are GAD67+ (Fish et al., 2011; Glausier et al., 2014). In schizophrenia, GAD67 protein levels are ~50% lower in PV basket cell boutons in PFC layers 3-4 (Curley et al., 2011), suggesting that at least some PV basket cells have reductions in GAD67 expression.

GAD67 levels have not been assessed in PV chandelier cells in schizophrenia; however convergent findings suggest that GAD67 levels may be lower in their boutons. The convergence of multiple chandelier cell boutons at the AIS appears as a distinctive structure termed a cartridge (Lewis and Lund, 1990), which can be visualized with multiple markers involved in GABA signaling including PV, vGAT, and the GABA transporter, GAT1 (DeFelipe and del Carmen Gonzalez-Albo, 1998; DeFelipe et al., 1989; Fish et al., 2013). In schizophrenia, the density of GAT1-IR cartridges is reduced by 40% across PFC layers 2-6 (Pierri et al., 1999; Woo et al., 1998). By contrast, the density of AISs visualized by immunoreactivity for the $\alpha 2$ subunit of the GABA A receptor is 2-fold greater in PFC layers 2-superficial 3 (Volk et al., 2002). These pre- and post-synaptic alterations are hypothesized to be compensatory for deficits in GABA signaling that may result from reduced GAD67 protein levels in PV chandelier cell boutons (Lewis, 2011) because lower GAT1 levels would presumably increase the latency of post-synaptic responses upon GABA release (Overstreet and Westbrook, 2003), and the up-regulation of GABA A receptors at the AIS would increase the efficacy of GABA binding. Together, these findings led us to hypothesize that GAD67 protein levels are markedly lower in chandelier cell boutons in the PFC of schizophrenia subjects

4.2 MATERIALS AND METHODS

4.2.1 Experimental Procedures

Specific procedures for tissue procurement, subject pairing, immunohistochemistry, and data collection and segmentation are described in 2.0. Briefly, PFC tissue sections from 20 pairs of schizophrenia and matched comparison subjects (**Table 2.1**) were immunolabeled for vGAT, GAD65, and GAD67 (**Table 2.2**). Sections immunolabeled in Run #1 were used to assess measures of cartridge density and relative vGAT and GAD67 fluorescence intensity levels within cartridge boutons across PFC layers 2-6 using quantitative confocal microscopy techniques. Secondary measures of bouton density and relative vGAT and GAD67 fluorescence intensity levels within boutons were assessed in PFC total gray matter using Run #1 and #2.

4.2.2 Definition of cartridges and vGAT+ cartridge boutons

Cartridges were identified in layers 2/3s, 3d/4, 5, and 6 by their distinctive structure using vGAT immunoreactivity (**Figure 4.1**). Within each field, an unbiased counting frame ($\sim 68 \times 68 \mu\text{m}^2$) consisting of two exclusion lines and two inclusion lines placed over the image stack was used to identify potential vGAT-IR cartridges for analysis. vGAT-IR cartridges were included for analysis and manually traced only if they were considered to be completely visualized as indicated by (1) continuity across z-planes; (2) the entire cartridge was contained within a virtual sampling box. The sampling box started and ended one z-plane from the top and bottom of the image stack, respectively, and had x-y start/end coordinates that were located 20 pixels from any edge. The entire structure of every vGAT-IR cartridge that met these criteria was manually

masked (**Figure 4.1G**). vGAT object masks that overlapped a cartridge mask were considered to be vGAT+ cartridge boutons (**Figure 4.1H**).

Secondary analyses were performed using vGAT+ boutons that were IR for GAD67 only (vGAT+/GAD67+) or GAD65 and GAD67 (vGAT+/GAD65+/GAD67+), which were classified using a multistep process. Initially, mask operations were used to identify vGAT and GAD65 or GAD67 object masks that overlapped each other's centers. vGAT+/GAD67+, and vGAT+/GAD65+/GAD67+ boutons that did not meet the mask operations criteria were classified by GAD65 and GAD67 fluorescence intensity as described in **2.6.2**. Examples of boutons classified as vGAT+/GAD67+ and vGAT+/GAD65+/GAD67+ are shown in **Appendix D Figure D.1**.

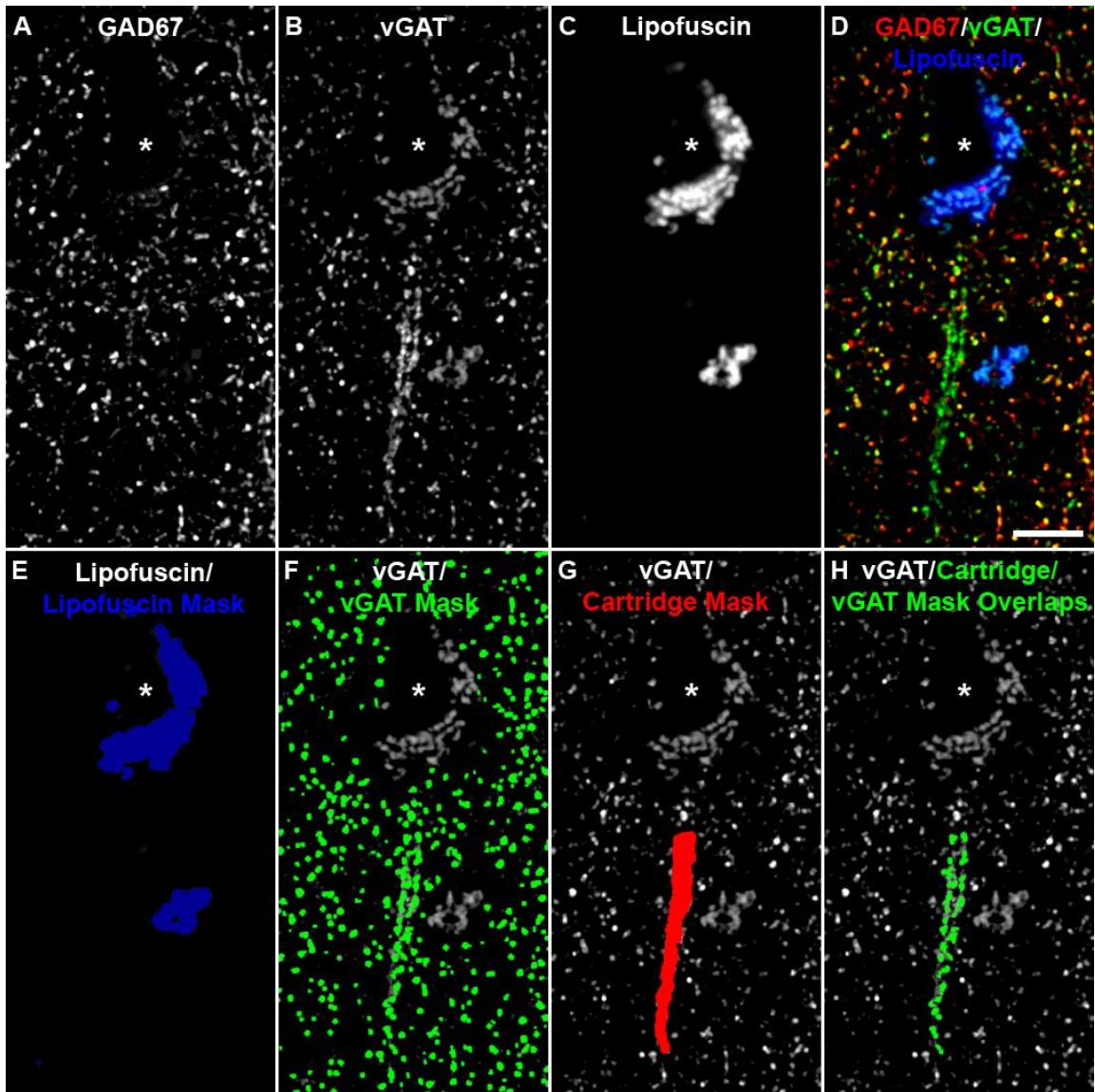


Figure 4.1. Identification of vGAT-IR cartridges and vGAT+ cartridge boutons. Projection image (5 z-planes taken 0.25 μm apart) of a human PFC tissue section immunolabeled for vGAT and GAD67. Single channel images of (A) GAD67, (B) vGAT, and (C) lipofuscin autofluorescence. (D) Merged image of A, B, and C. (E) Image from C overlaid with its corresponding object mask. (F-H) Image from B overlaid with its corresponding object masks (F), manually traced cartridge mask (G), and object masks from F that overlapped the cartridge mask from G (H). The cartridge mask was used to assess the density of cartridges between diagnostic groups, whereas the vGAT masks that overlapped the cartridge mask were used to assess relative fluorescence intensity levels in cartridge boutons. The asterisks designate an unlabeled soma. Bar = 10 μm .

4.2.3 Statistics

Data are presented as mean cartridge density (\pm SD), mean bouton density (\pm SD), and mean sum fluorescence intensity (\pm SD). For measurements assessing cartridge density the cartridge masks were used (**Figure 4.1G**) and for measurements of vGAT+ cartridge bouton fluorescence intensity the vGAT object masks that overlapped a cartridge mask were used (**Figure 4.1H**). Because PV-IR cartridge boutons are GAD67+ (Fish et al., 2011; Glausier et al., 2014), vGAT object masks that overlapped a cartridge mask and a GAD65 object mask were excluded from analyses assessing GAD67 fluorescence intensity in vGAT+ cartridge boutons.

Two ANCOVA models were used to analyze cartridge number, bouton density, and bouton fluorescence intensity level data. Because subjects were selected and processed as pairs, the first paired ANCOVA model included cartridge density, bouton density, bouton vGAT levels, or bouton GAD67 levels as the dependent variable, diagnostic group as the main effect, subject pair as a blocking factor, and tissue storage time as a covariate. Subject pairing is an attempt to balance diagnostic groups for sex, age, and PMI, and to account for the parallel processing of tissue samples, and thus is not a true statistical paired design. Consequently, a second unpaired ANCOVA model was performed that included age, PMI, and tissue storage time as covariates. All statistical tests were conducted with α -level= 0.05.

We also assessed the potential influence of other factors that are frequently comorbid with the diagnosis of schizophrenia using ANCOVA models. For these analyses, we compared subjects with schizophrenia using each variable (sex; diagnosis of schizoaffective disorder; use of nicotine ATOD, antipsychotics ATOD, antidepressants ATOD, or benzodiazepines and/or sodium valproate ATOD) as the main effect and sex, age, tissue storage time, and PMI as covariates. A Bonferroni-adjusted α -level of $0.05/6 = 0.008$ was used to assess significance.

Reported ANCOVA statistics include only those covariates that were statistically significant. As a result, the reported degrees of freedom vary across analyses.

4.3 RESULTS

4.3.1 Cartridge density and vGAT+ boutons per cartridge are unchanged in schizophrenia

The density of cartridges was not statistically different between diagnostic groups (paired $F_{1, 19} = 2.73$, $p = 0.115$; unpaired $F_{1, 38} = 2.72$, $p = 0.107$); however, cartridge density was non-significantly 12% greater in schizophrenia (1.01 ± 0.23 cartridges/counting frame) than comparison (0.90 ± 0.22 cartridges/counting frame) subjects (**Figure 4.2A**). Similarly, the number of vGAT+ boutons per cartridge did not differ (paired $F_{1, 19} = 3.96$, $p = 0.061$; unpaired $F_{1, 38} = 2.54$, $p = 0.119$) between diagnostic groups, but were non-significantly 6% increased in the illness (schizophrenia: 16.45 ± 1.71 boutons/cartridge; comparison: 15.50 ± 2.04 boutons/cartridge; **Figure 4.2B**).

4.3.2 Cartridge bouton GAD67 protein levels are unchanged in schizophrenia

GAD67 protein levels in vGAT+ cartridge boutons were not statistically different between diagnostic groups (paired $F_{1, 19} = 2.35$, $p = 0.142$; unpaired $F_{1, 38} = 2.46$, $p = 0.125$), but were non-significantly 12% lower in schizophrenia (638 ± 163 a.u.) than comparison (725 ± 186 a.u.) subjects (**Figure 4.2C**). Also, vGAT protein levels in vGAT+ cartridge boutons were unaltered (paired $F_{1, 19} = 0.18$, $p = 0.676$; unpaired $F_{1, 38} = 0.15$, $p = 0.699$) between diagnostic groups

(schizophrenia: 1498 ± 313 a.u.; comparison: 1463 ± 242 a.u.; **Figure 4.2D**). Because GAD67 levels were only trending lower in chandelier cell boutons, these findings suggest that significant reductions in GAD67 protein levels may only affect GAD65+/GAD67+ boutons (e.g. PV basket cell boutons). Other subtypes of GABA neurons in primate PFC give rise to GAD67+ boutons (Rocco et al., 2015); therefore, we assessed the density and GAD67 protein levels in vGAT+/GAD65+/GAD67+ and vGAT+/GAD67+ boutons.

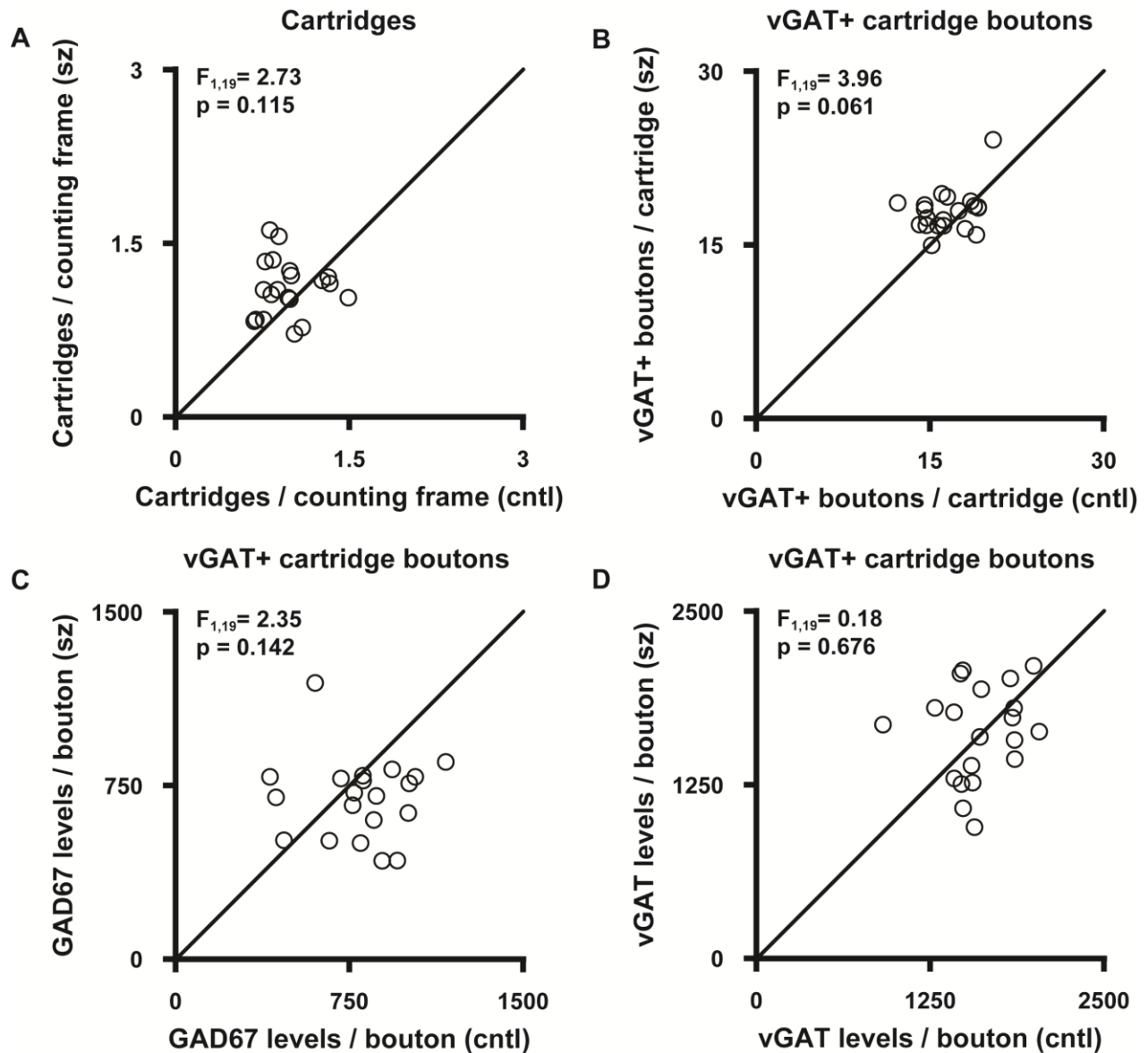


Figure 4.2. Cartridge density, vGAT+ boutons per cartridge, and cartridge bouton GAD67 and vGAT protein levels between diagnostic groups. Mean cartridge density (A), vGAT+ boutons per cartridge (B), GAD67 protein levels in vGAT+ cartridge boutons (C), and vGAT protein levels in vGAT+ cartridge boutons (D) across layers 2-6. Each data point represents a schizophrenia (sz) and matched comparison (cntl) subject pair. Points below the unity line reflect pairs in which the measure is lower for the schizophrenia subject.

4.3.3 vGAT+/GAD65+/GAD67+ bouton density is lower in schizophrenia

vGAT+/GAD65+/GAD67+ bouton density was 11% lower (paired $F_{1, 19} = 5.80$; unpaired $p = 0.026$; $F_{1, 38} = 6.62$, $p = 0.014$) in schizophrenia (0.0097 ± 0.0017 boutons/ μm^3) relative to comparison (0.0109 ± 0.0014 boutons/ μm^3) subjects (**Figure 4.3A**). An analysis of all vGAT+ boutons that contained GAD65 immunoreactivity regardless of the presence of GAD67 immunoreactivity (vGAT+/GAD65-IR boutons) found that the density of these boutons did not differ (paired $F_{1, 19} = 0.03$, $p = 0.856$; unpaired $F_{1, 37} = 0.004$, $p = 0.948$;) between diagnostic groups (schizophrenia: 0.0168 ± 0.0014 boutons/ μm^3 ; comparison: 0.0168 ± 0.0020 boutons/ μm^3 ; **Figure 4.3B**), which is similar to previous reports of no change in the density of GAD65-IR puncta in the PFC (Benes et al., 2000). These findings suggest that a proportion of vGAT+/GAD65+/GAD67+ boutons lack detectable GAD67 protein levels in schizophrenia.

4.3.4 vGAT+/GAD65+/GAD67+ bouton GAD67 protein levels are lower in schizophrenia

GAD67 protein levels were 17% lower (paired $F_{1, 19} = 12.91$, $p = 0.002$; unpaired $F_{1, 38} = 12.55$, $p = 0.001$;) in vGAT+/GAD65+/GAD67+ boutons in schizophrenia (927 ± 139 a.u.) relative to comparison (1115 ± 193 a.u.) subjects (**Figure 4.3C**). By contrast, vGAT protein levels in these boutons did not differ (paired $F_{1, 19} = 0.13$, $p = 0.722$; unpaired $F_{1, 38} = 0.14$, $p = 0.713$) between diagnostic groups (schizophrenia: 915 ± 140 a.u.; comparison: 931 ± 133 a.u.; **Figure 4.3D**).

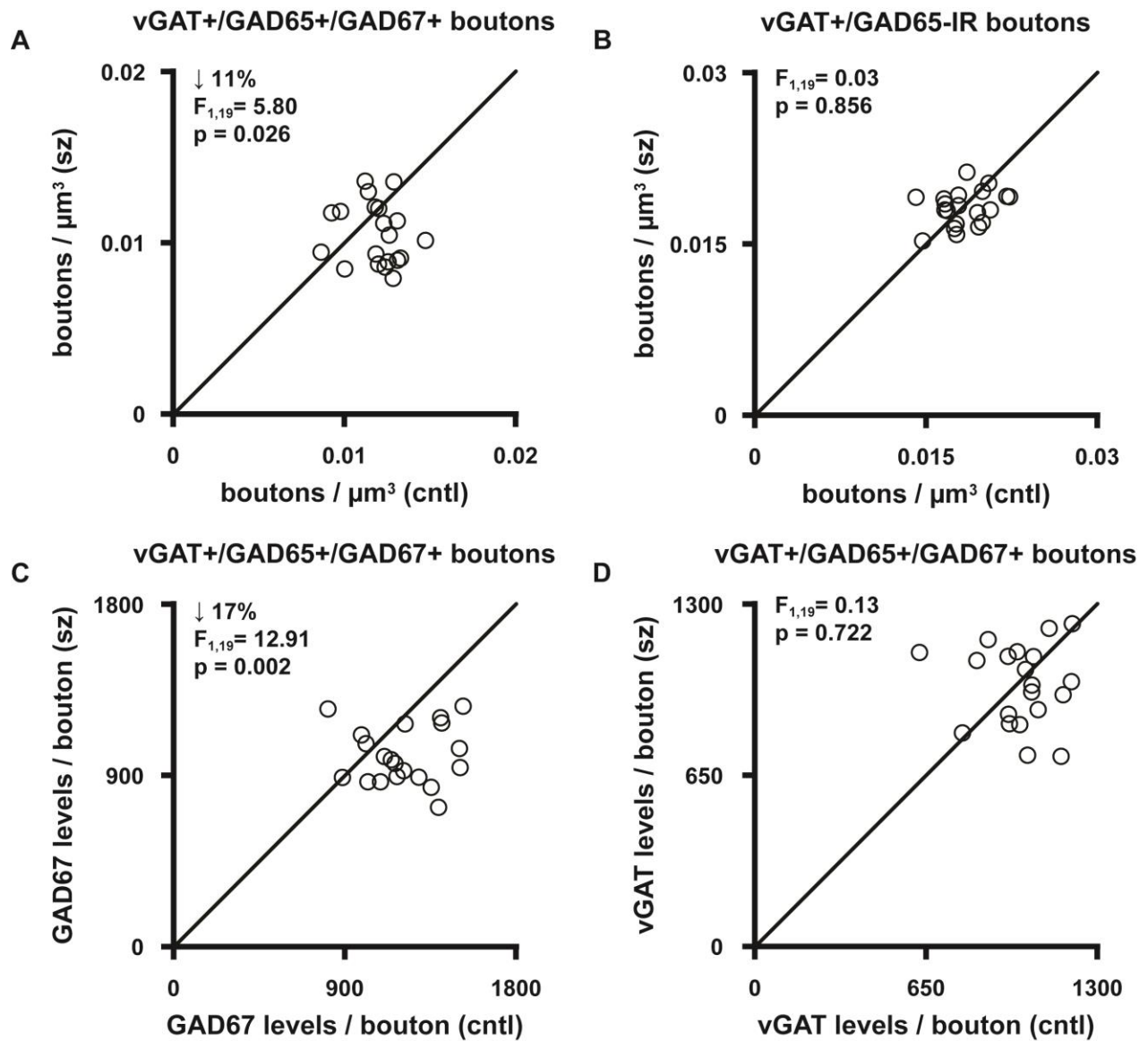


Figure 4.3. vGAT+/GAD65+/GAD67+ bouton density, and GAD67 and vGAT protein levels between diagnostic groups. Mean vGAT+/GAD65+/GAD67+ bouton density (A), vGAT+/GAD65-IR bouton density (B), and GAD67 protein levels (C), and vGAT protein levels (D) in vGAT+/GAD65+/GAD67+ boutons in total gray matter.

4.3.5 vGAT+/GAD67+ bouton density is lower in schizophrenia

The density of vGAT+/GAD67+ boutons was 24% lower (paired $F_{1, 19} = 14.83$, $p = 0.001$; unpaired $F_{1, 38} = 15.10$, $p < 0.0005$) in schizophrenia (0.0051 ± 0.0014 boutons/ μm^3) than comparison (0.0067 ± 0.0012 boutons/ μm^3) subjects (**Figure 4.4A**). This deficit was associated with a 26% increase (paired $F_{1, 19} = 10.82$, $p = 0.004$; unpaired $F_{1, 38} = 7.57$, $p = 0.009$) in the density of vGAT+ boutons without detectable GAD65 and/or GAD67 immunoreactivity (vGAT+/GAD- boutons) in the illness (schizophrenia: 0.0112 ± 0.0028 boutons/ μm^3 ; comparison 0.0089 ± 0.0026 boutons/ μm^3 ; **Figure 4.4B**). Therefore, a proportion vGAT+/GAD67+ boutons lack detectable GAD67 protein levels in schizophrenia.

4.3.6 vGAT+/GAD67+ bouton GAD67 protein levels are lower in schizophrenia

GAD67 protein levels in vGAT+/GAD67+ boutons were 13% lower (paired $F_{1, 18} = 14.74$, $p = 0.001$; unpaired $F_{1, 36} = 5.61$, $p = 0.023$) in schizophrenia (537 ± 94 a.u.) relative to comparison (617 ± 124 a.u.) subjects (**Figure 4.4C**). By contrast, vGAT protein levels in vGAT+/GAD67+ boutons did not differ (paired $F_{1, 19} = 0.06$, $p = 0.817$; unpaired $F_{1, 37} = 0.13$, $p = 0.723$) between diagnostic groups (schizophrenia: 617 ± 115 a.u.; comparison: 610 ± 95 a.u.; **Figure 4.4D**).

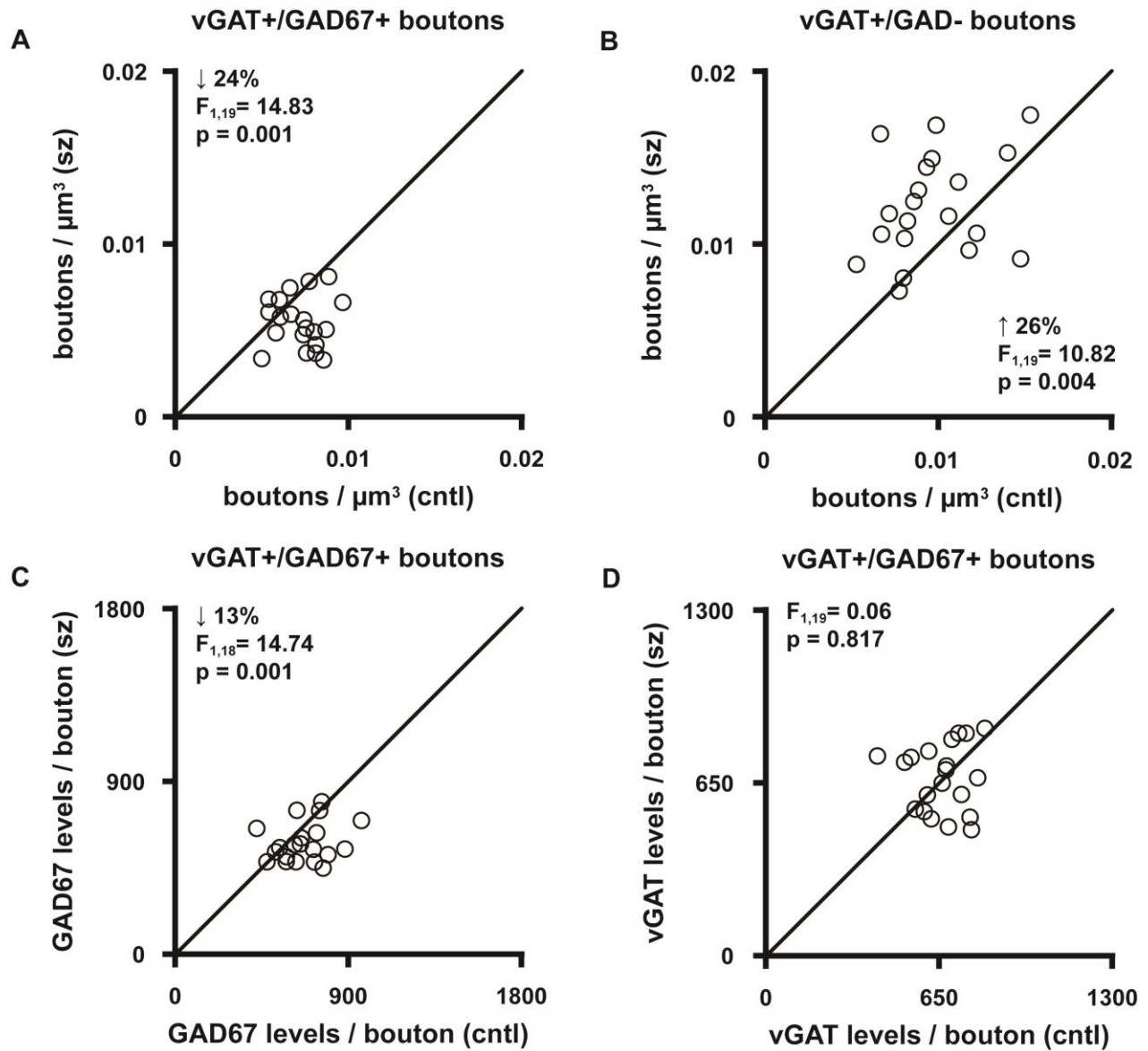


Figure 4.4. vGAT+/GAD67+ bouton density and GAD67 and vGAT protein levels between diagnostic groups.

Mean vGAT+/GAD67+ bouton density (A), vGAT+ boutons without detectable GAD65 and/or GAD67 immunoreactivity (vGAT+/GAD- boutons) density (B), and GAD67 protein levels (C) and GAD65 protein levels (D) in vGAT+/GAD67+ boutons in total gray matter.

4.3.7 Lower vGAT+/GAD67+ and vGAT+/GAD65+/GAD67+ bouton density and GAD67 protein level measures are not attributable to comorbid factors

In schizophrenia subjects, the density of vGAT+/GAD67+ and vGAT+/GAD65+/GAD67+ boutons, and GAD67 protein levels in vGAT+/GAD67+ boutons did not differ as a function of sex, diagnosis of schizoaffective disorder, or use of nicotine ATOD, benzodiazepine and/or sodium valproate ATOD, antidepressant ATOD, or antipsychotic ATOD (**Appendix D Figures D.2 and D.3**). By contrast, schizophrenia subjects on antidepressants ATOD had 16% lower levels of GAD67 in vGAT+/GAD65+/GAD67+ boutons (unpaired $F_{1, 18} = 9.20$, $p = 0.007$; **Appendix D Figure D.3**). To confirm that there was a disease effect on these measures, we reassessed each measure using the two analyses of covariance models described in **4.2.3** with antidepressants ATOD included as a covariate. GAD67 levels in vGAT+/GAD65+/GAD67+ boutons were still significantly lower in schizophrenia relative to comparison subjects for the paired analysis (paired $F_{1, 19} = 12.91$, $p = 0.002$; unpaired $F_{1, 37} = 0.11$, $p = 0.748$.) when antidepressant ATOD was included as a covariate.

4.4 DISCUSSION

About half of all PV neurons in the PFC of schizophrenia subjects lack detectable GAD67 mRNA expression (Hashimoto et al., 2003). Pre- and postsynaptic alterations at the site of PV chandelier cell inputs (Volk et al., 2002; Woo et al., 1998) are thought to compensate for reduced GABA signaling from these cells (Lewis, 2011), which led us to hypothesize that GAD67 protein levels are significantly reduced in boutons from chandelier cells. We found that the density of

cartridges, which are distinctive structures formed by the convergence of multiple chandelier cell boutons at the AIS (Lewis and Lund, 1990), and boutons per cartridge were not significantly different between diagnostic groups but were trending higher in schizophrenia, and that GAD67 protein levels in chandelier cell boutons were not significantly different between diagnostic groups but were trending lower in schizophrenia.

Our finding of a trending increase in the density of cartridges and boutons per cartridge across PFC layers 2-6 is consistent with a significantly greater density of AISs IR for the $\alpha 2$ subunit of the GABA A receptor in PFC layers 2-superficial 3 in schizophrenia (Volk et al., 2002). Although we do not report on density differences in specific layers, the $\alpha 2$ -IR AIS findings suggest that the difference in cartridge density would be greatest in the superficial layers. In monkey PFC layers 2-4, the number of chandelier cell boutons per AIS decreases between 3 months and adulthood (Fish et al., 2013). As a result, there is a reduction in the densities of cartridges IR for PV and GAT1, and $\alpha 2$ -IR AISs (Anderson et al., 1995; Cruz et al., 2003). Together, these findings suggest that higher vGAT-IR cartridge and GABA A $\alpha 2$ -IR AIS densities are the result of fewer chandelier cell boutons being pruned over development (Hoftman et al., 2013; Hyde et al., 2011).

By contrast, our finding of a trending increase in the density of vGAT-IR cartridges is not consistent with a significantly lower density of GAT1-IR cartridges across PFC layers 2-6 in schizophrenia (Woo et al., 1998). In the same study the overall density of GAT1-IR boutons was unchanged in the illness, suggesting that undetectable GAT1 immunoreactivity is specific to chandelier cells. Consistent with this idea, GAT1 mRNA expression is unchanged at the tissue level in schizophrenia (Hoftman et al., 2013), but is lower in PV neurons (Bitanhirwe and Woo, 2014). Together with our results, these findings suggest that the lower density of GAT1-IR

cartridges in schizophrenia reflects a marked reduction in GAT1 protein levels in chandelier cell boutons. Pharmacological blockade of GAT1 increases the latency of postsynaptic responses upon GABA release at rat hippocampal synapses (Overstreet and Westbrook, 2003). Considering that GAD67 protein levels are only trending lower, vGAT protein levels are unaltered, and GAT1 levels are significantly reduced at some chandelier cell inputs, similar effects may occur at chandelier cell synapses in the illness. Therefore, rather than compensating for lower GABA production from chandelier cells in schizophrenia, reductions in GAT1 may enhance their signaling effects.

The postsynaptic responses from chandelier cells are dynamic and highly responsive to network activity. By exclusively targeting the AIS, the site of action potential generation (Kole et al., 2008; Meeks and Mennerick, 2007; Palmer and Stuart, 2006), chandelier cells are thought to strongly regulate the output of pyramidal cells. While the synaptic effects of chandelier cells appear to be mainly inhibitory under physiological conditions (Woodruff et al., 2011), multiple studies have reported that they can also depolarize cortical and hippocampal pyramidal cells (Molnar et al., 2008; Sauer et al., 2012; Szabadics et al., 2006; Woodruff et al., 2011). These different effects are partially due to activity-dependent network fluctuations. For example, the effects from chandelier cell inputs are hyperpolarizing when the state of the network is highly active and depolarizing when the network is relatively quiescent (Woodruff et al., 2011). Reduced activity within the PFC of schizophrenia (Minzenberg et al., 2009) may favor more depolarizing responses from chandelier cells (Lewis, 2011).

These findings also suggest that reductions in GAD67 levels in schizophrenia affect PV basket cells to a greater degree than PV chandelier cells, which may result from a greater magnitude reduction in GAD67 mRNA expression in basket cells or a greater proportion of

basket cells being affected. In mouse somatosensory cortex, chandelier cells receive a greater percentage of excitatory afferent inputs from near layers 2-3 compared to basket cells, which receive most of their inputs from around layer 4 (Xu and Callaway, 2009). This is consistent with findings in mice suggesting that chandelier cells are enriched in layer 2 compared to deeper layers (Taniguchi et al., 2013). Therefore, GAD67 levels may be lower in PV basket cells because they receive a greater number of inputs from the middle PFC layers, which may have the greatest deficits in excitatory signaling in schizophrenia (Glausier and Lewis, 2013).

Since GAD67 protein levels are lower to a greater degree in PV basket cell boutons compared to chandelier cell boutons, and PV basket and chandelier cells give rise to GAD65+/GAD67+ and GAD67+ boutons, respectively (Fish et al., 2011; Glausier et al., 2014), we assessed if GAD67 levels were significantly lower in only GAD65+/GAD67+ boutons. We found that 11% of vGAT+/GAD65+/GAD67+ boutons lacked detectable GAD67 protein levels in schizophrenia, and that GAD67 protein levels were overall 17% lower in vGAT+/GAD65+/GAD67+ boutons. Similarly, GAD67 protein levels were undetectable in 24% of vGAT+/GAD67+ boutons, and GAD67 levels were overall 13% lower in these boutons.

Lower bouton GAD67 levels appear to be a consequence of schizophrenia pathology, and not of comorbid factors commonly associated with the illness. However, GAD67 levels in vGAT+/GAD65+/GAD67+ boutons were lower to a greater degree in subjects with schizophrenia taking antidepressants ATOD. Antidepressant use alone is unlikely to account for these effects since taking antidepressants was previously shown to not account for lower GAD67 mRNA and total protein expression in the PFC of schizophrenia subjects (Curley et al., 2011; Guidotti et al., 2000). In this cohort, all schizophrenia subjects on antidepressants were also taking antipsychotics ATOD. Interestingly, chronic co-administration of fluvoxamine and haloperidol was shown to

reduce GAD67 protein levels in rat frontal cortex (Chertkow et al., 2006). By contrast, haloperidol alone resulted in a significant increase in both GAD67 mRNA and protein levels. Co-administration of antidepressants and antipsychotics can improve negative symptoms (Silver, 2003; Silver et al., 2000; Silver and Nassar, 1992), suggesting that the reduction of GAD67 within boutons might be beneficial in some subjects with schizophrenia. Future studies designed to directly assess the molecular and behavioral outcome of concomitantly taking these medications will be important for developing future pharmacotherapy strategies.

In concert, these findings suggest that lower GAD67 protein levels similarly affect neurons giving rise to GAD65+/GAD67+ and GAD67+ boutons in schizophrenia. However, it is unknown if significant reductions in GAD67 protein levels only affect GAD65+/GAD67+ boutons from PV basket cells. Moreover, non-statistically significant but trending reductions in GAD67 protein levels are unique to chandelier cells, and therefore it is unknown what GABA neuron subtype(s) give rise to GAD67+ boutons with significant reductions in GAD67 protein levels. A vast majority of GABA neurons in primate PFC can be grouped into non-overlapping subtypes by expressing PV, CB, or CR (Conde et al., 1994; del Rio and DeFelipe, 1996; Gabbott and Bacon, 1996). Both CB and CR neurons give rise to GAD65+/GAD67+ and GAD67+ boutons (Rocco et al., 2015), suggesting that they may be affected by significant reductions in GAD67 protein levels in schizophrenia; however, CB and CR neurons are thought to be differentially affected in the illness. For example, > 50% of CB neurons express SST (~85% of SST neurons contain CB) (Gonchar and Burkhalter, 1997; Kubota et al., 1994; Rogers, 1992). In schizophrenia, both the density of SST mRNA-positive neurons and levels of SST mRNA per neuron are lower in the PFC (Morris et al., 2008). Lower SST mRNA levels are correlated with lower GAD67 mRNA levels at both the tissue and cellular levels (Hashimoto et al., 2008; Morris

et al., 2008), suggesting that at least some boutons from CB neurons have significantly reduced GAD67 protein levels. By contrast, CR mRNA levels are unaltered and do not correlate with lower GAD67 mRNA levels in schizophrenia (Hashimoto et al., 2008), which is interpreted as CR neurons are unaffected (Hashimoto et al., 2008; Hashimoto et al., 2008; Hashimoto et al., 2003; Lewis et al., 2005; Volk et al., 2012). Importantly, CB and CR neurons play unique functional roles in the neuronal network and identifying if lower bouton GAD67 levels differentially affect these subtypes will be important for understanding the pathophysiological changes in schizophrenia.

5.0 GAD67 PROTEIN LEVELS ARE LOWER IN AXONAL BOUTONS FROM CALBINDIN AND CALRETININ NEURONS IN SCHIZOPHRENIA

5.1 INTRODUCTION

GAD67 protein levels are undetectable in 16% of axonal boutons in the PFC of schizophrenia subjects (**3.0**), which presumably arise from the ~30% of neurons that lack detectable GAD67 mRNA expression (Akbarian et al., 1995; Volk et al., 2000). Marked reductions in GAD67 expression affects neurons that give rise to GAD65+/GAD67+ and GAD67+ boutons. Specifically, 11% of GAD65+/GAD67+ boutons and 24% of GAD67+ boutons lack detectable GAD67 protein levels (**4.0**). ~50% of all PV neurons in the PFC of schizophrenia subjects lack detectable GAD67 mRNA expression (Hashimoto et al., 2003). All boutons from PV basket cells are GAD65+/GAD67+ (Fish et al., 2011; Glausier et al., 2014), and it was found that in PFC layers 3-4 of schizophrenia subjects GAD67 levels were ~50% lower in PV basket cell boutons, which were defined as the colocalization of PV-IR and GAD65-IR puncta with or without detectable GAD67 immunoreactivity (Curley et al., 2011). Along with the mRNA findings, these findings suggest that at least some PV basket cell boutons may lack detectable GAD67 protein levels. By contrast, PV chandelier cells give rise to GAD67+ boutons (Fish et al., 2011; Glausier et al., 2014), and in schizophrenia GAD67 protein levels are non-statistically significant 12% lower in boutons from chandelier cells (**4.0**). Therefore, it is unknown what subtypes of GABA

neurons give rise to GAD67+ boutons with markedly reduced GAD67 protein levels, and if GAD65+/GAD67+ boutons from neuronal subtypes other than PV basket cells have marked reductions in GAD67 levels.

Neurons that express PV, CB, and CR constitute ~25%, ~20%, and ~45%, respectively, of all GABA neurons in primate PFC (Conde et al., 1994; del Rio and DeFelipe, 1996; Gabbott and Bacon, 1996). At the transcript level, the majority of CB and CR neurons express mRNA for both GAD65 and GAD67 but a proportion of these neurons expresses mRNA for only GAD67 (Rocco et al., 2015). The finding that CB and CR neurons give rise to GAD67+ and GAD65+/GAD67+ boutons suggests that GAD67+ boutons arise from CB and CR neurons expressing only GAD67 mRNA and GAD65+/GAD67+ boutons are from those neurons that express mRNAs for both GADs. Similarly, neurons that express SST, which includes > 50% of CB neurons (~85% of SST neurons contain CB) (Gonchar and Burkhalter, 1997; Kubota et al., 1994; Rogers, 1992), give rise to GAD67+ and GAD65+/GAD67+ boutons.

GAD67 expression has not been assessed in CB and CR neurons in schizophrenia; however, correlative findings suggest that GAD67 levels are lower in CB, but not CR, neurons. For example, deficits in SST mRNA expression are widely reported in the PFC of schizophrenia subjects (Fung et al., 2010; Gabriel et al., 1996; Hashimoto et al., 2008; Hashimoto et al., 2008; Mellios et al., 2009; Morris et al., 2008). The density of SST mRNA-positive neurons and levels of SST mRNA per neuron are lower (Morris et al., 2008), and lower SST mRNA expression correlates with lower GAD67 mRNA expression at both the tissue and cellular levels (Hashimoto et al., 2008; Morris et al., 2008). By contrast, CR mRNA and total protein expression, as well as the density of CR-IR boutons are unaltered (Fung et al., 2010; Hashimoto et al., 2008; Hashimoto et al., 2003; Woo et al., 1998). CR mRNA levels do not correlate with lower GAD67 mRNA

levels in the illness (Hashimoto et al., 2008), suggesting that CR neurons are relatively unaltered.

Considering that PV neurons constitute ~25% of all GABA neurons and only half of all PV neurons have a marked deficit in GAD67 mRNA expression, they only account for ~12% out of the ~30% of GABA neurons that lack detectable GAD67 levels. Therefore, the remaining GABA neurons with markedly lower GAD67 expression may be comprised of SST neurons. Since CB/SST neurons give rise to GAD67+ and GAD65+/GAD67+ boutons, we hypothesize that in the PFC of schizophrenia subjects GAD67 protein levels are markedly lower in GAD67+ and GAD65+/GAD67+ boutons from CB neurons. By contrast, GAD67 levels in boutons arising from CR neurons are unaltered.

5.2 MATERIALS AND METHODS

5.2.1 Experimental procedures

Specific procedures for tissue procurement, subject pairing, immunohistochemistry, and data collection and segmentation are described in 2.0. Briefly, PFC tissue sections from 20 pairs of schizophrenia and matched comparison subjects (**Table 2.1**) were immunolabeled for vGAT, GAD65, GAD67, and CB or CR (**Table 2.2**). Quantitative confocal microscopy techniques were used to assess bouton density and relative fluorescence intensity levels within total gray matter.

5.2.2 Definitions of CB and CR boutons

vGAT+/GAD67+ and vGAT+/GAD65+/GAD67+ boutons were classified as containing

immunoreactivity for CB (CB+/vGAT+/GAD67+ and CB+/vGAT+/GAD65+/GAD67+) or CR (CR+/vGAT+/GAD67+ and CR+/vGAT+/GAD65+/GAD67+) using a multistep process. Initially, vGAT+/GAD67+ and vGAT+/GAD65+/GAD67+ boutons were defined as described in **2.6.2**. Mask operations were then used to identify vGAT object masks from these distinct bouton subpopulations and CB or CR object masks that overlapped each other's centers. Next, for each site the mean fluorescence intensity of CB or CR for all CB+/vGAT+/GAD+ and CR+/vGAT+/GAD+ boutons classified using mask operations criteria were used as seeds in a K-means cluster analysis to classify the remaining vGAT+/GAD+ boutons as CB+ or CR+. **Figure 5.1** shows examples of CB+ boutons and **Figure 5.2** shows examples of CR+ boutons classified as vGAT+/GAD67+ and vGAT+/GAD65+/GAD67+.

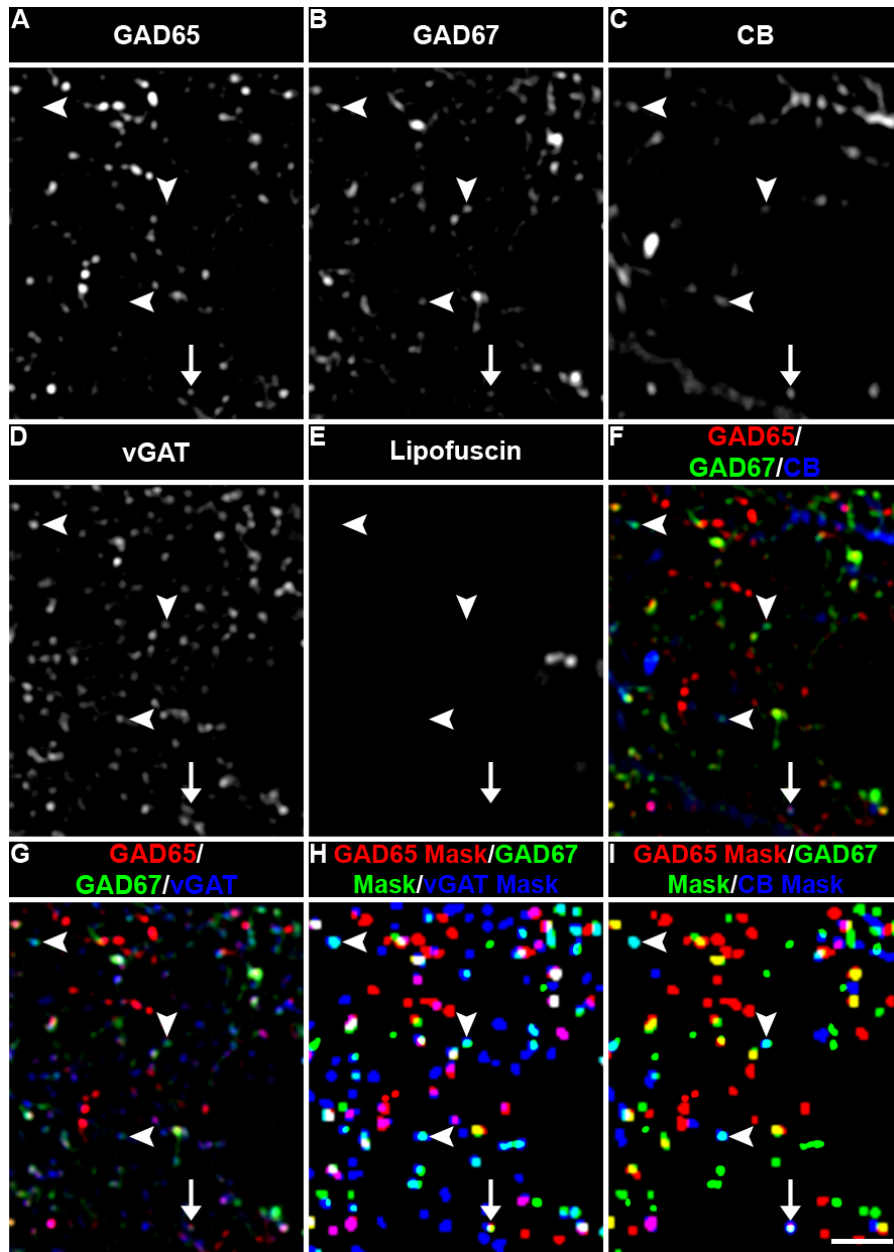


Figure 5.1. Examples of CB+/vGAT+/GAD67+ and CB+/vGAT+/GAD65+/GAD67+ boutons. Projection image (3 z-planes taken 0.25 μm apart) of a human PFC tissue section immunolabeled for CB, vGAT, GAD65, and GAD67. Single channel images of (A) GAD65, (B) GAD67, (C) CB, (D) vGAT, and (E) lipofuscin autofluorescence. (F) Merged image of A, B, and C. (G) Merged image of A, B, D. (H) Object masks corresponding to A, B, and D. (I) Object masks corresponding to A, B, and C. Arrows indicate CB+/vGAT+/GAD67+ (arrowheads) and CB+/vGAT+/GAD65+/GAD67+ (arrow) boutons. Bar = 5 μm .

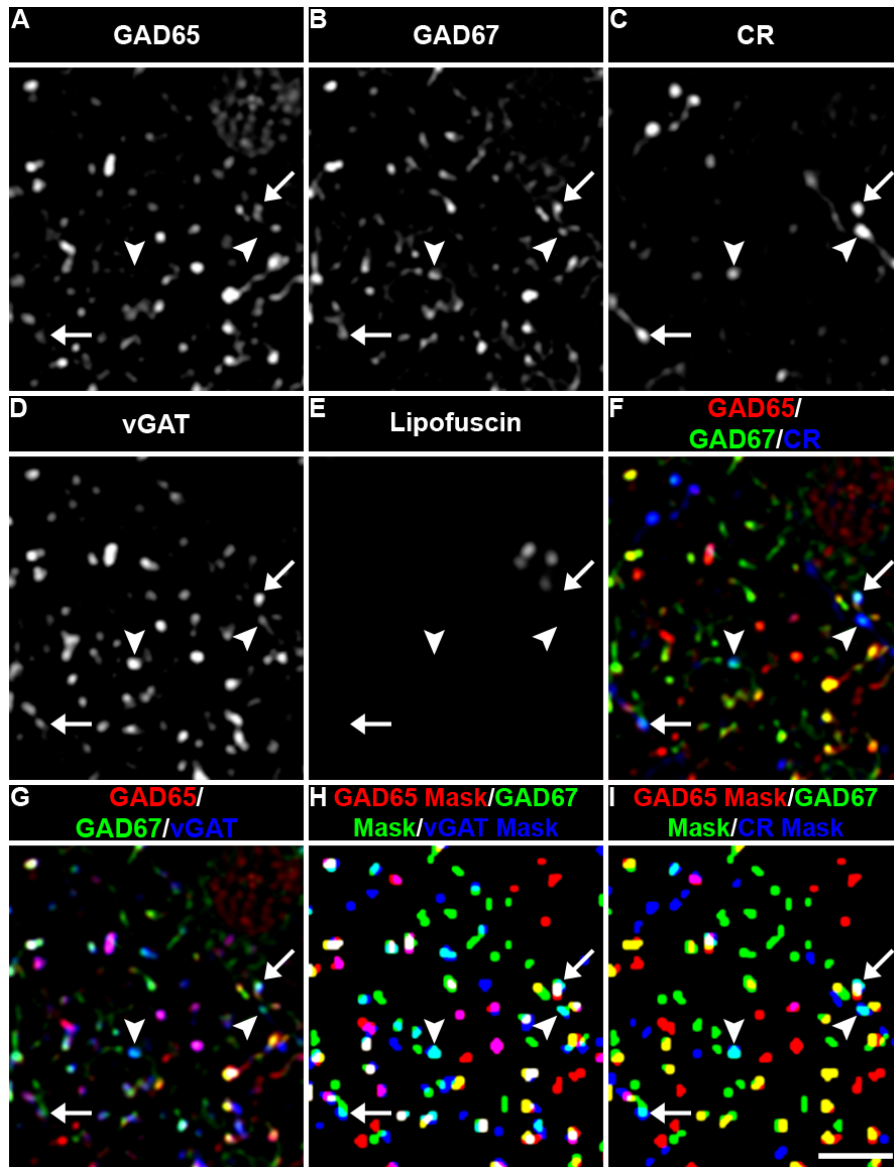


Figure 5.2. Examples of CR+/vGAT+/GAD67+ and CR+/vGAT+/GAD65+/GAD67+ boutons. Projection image (3 z-planes taken 0.25 μm apart) of a human PFC tissue section immunolabeled for CR, vGAT, GAD65, and GAD67. Single channel images of (A) GAD65, (B) GAD67, (C) CR, (D) vGAT, and (E) lipofuscin autofluorescence. (F) Merged image of A, B, and C. (G) Merged image of A, B, D. (H) Object masks corresponding to A, B, and D. (I) Object masks corresponding to A, B, and C. Arrows indicate CR+/vGAT+/GAD67+ (arrowheads) and CR+/vGAT+/GAD65+/GAD67+ (arrows) boutons. Bar = 5 μm .

5.2.3 Statistics

Data are presented as mean bouton density (\pm SD), and mean sum fluorescence intensity (\pm SD). Two ANCOVA models were used to analyze bouton density and bouton protein level data. Because subjects were selected and processed as pairs, the first paired ANCOVA model included bouton density, bouton GAD67 levels, bouton CB levels, bouton CR levels, and bouton vGAT levels as the dependent variable, diagnostic group as the main effect, subject pair as a blocking factor, and tissue storage time as a covariate. Subject pairing is an attempt to balance diagnostic groups for sex, age, and PMI, and to account for the parallel processing of tissue samples, and thus is not a true statistical paired design. Consequently, a second unpaired ANCOVA model was performed that included age, PMI, and tissue storage time as covariates. All statistical tests were conducted with α -level= 0.05.

We also assessed the potential influence of other factors that are frequently comorbid with the diagnosis of schizophrenia using ANCOVA models. For these analyses, we compared subjects with schizophrenia using each variable (sex; diagnosis of schizoaffective disorder; use of nicotine ATOD, antipsychotics ATOD, antidepressants ATOD, or benzodiazepines and/or sodium valproate ATOD) as the main effect and age, PMI, tissue storage time, and sex as covariates. A Bonferroni-adjusted α -level of $0.05/6 = 0.008$ was used to assess significance.

Reported ANCOVA statistics include only those covariates that were statistically significant. As a result, the reported degrees of freedom vary across analyses.

5.3 RESULTS

5.3.1 CB+/vGAT+/GAD67+ and CB+/vGAT+/GAD65+/GAD67+ bouton density is unaltered in schizophrenia

The density of CB+/vGAT+/GAD67+ boutons did not differ (paired $F_{1, 19} = 3.50$, $p = 0.077$; unpaired $F_{1, 38} = 2.37$, $p = 0.132$) between schizophrenia (0.00080 ± 0.00029 boutons/ μm^3) and comparison (0.00092 ± 0.00024 boutons/ μm^3) subjects (**Figure 5.3A**). Similarly, the density of CB+/vGAT+/GAD65+/GAD67+ boutons did not differ (paired $F_{1, 19} = 0.18$, $p = 0.678$; unpaired $F_{1, 38} = 0.13$, $p = 0.719$) between diagnostic groups (schizophrenia: 0.00071 ± 0.00031 boutons/ μm^3 ; comparison: 0.00074 ± 0.00025 boutons/ μm^3 ; **Figure 5.3B**). Thus, GAD67 protein levels were detectable in the vast majority of CB+/vGAT+/GAD67+ and CB+/vGAT+/GAD65+/GAD67+ boutons in schizophrenia.

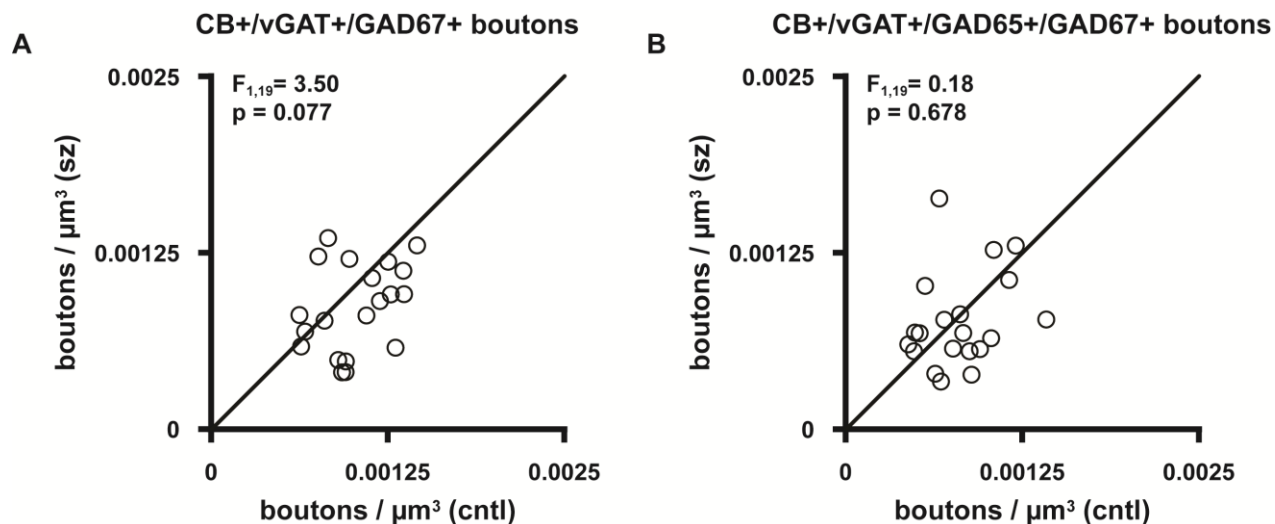


Figure 5.3. CB+/vGAT+/GAD67+ and CB+/vGAT+/GAD65+/GAD67+ bouton density between diagnostic groups. Mean density of CB+/vGAT+/GAD67+ boutons (A) and CB+/vGAT+/GAD65+/GAD67+ boutons (B) in total gray matter. Each data point represents a schizophrenia (sz) and matched comparison (cntl) subject pair. Points below the unity line reflect pairs in which the measure is lower for the schizophrenia subject.

5.3.2 CB+/vGAT+/GAD67+ and CB+/vGAT+/GAD65+/GAD67+ bouton GAD67 protein levels are lower in schizophrenia

GAD67 protein levels were 15% lower (paired $F_{1,18} = 6.70$, $p = 0.019$; unpaired $F_{1,37} = 5.66$, $p = 0.023$) in CB+/vGAT+/GAD67+ boutons in schizophrenia (843 ± 155 a.u.) relative to comparison (994 ± 239 a.u.) subjects (**Figure 5.4A1**). Similarly, GAD67 levels in CB+/vGAT+/GAD65+/GAD67+ boutons were 17% lower (paired $F_{1,19} = 11.21$, $p = 0.003$;

unpaired $F_{1, 37} = 11.39$, $p = 0.002$) in the illness (schizophrenia: 1337 ± 213 a.u.; comparison: 1605 ± 294 a.u.; **Figure 5.4B1**).

5.3.3 CB+/vGAT+/GAD67+ and CB+/vGAT+/GAD65+/GAD67+ bouton CB protein levels are lower in schizophrenia

CB protein levels in CB+/vGAT+/GAD67+ boutons were 14% lower (paired $F_{1, 19} = 4.88$, $p = 0.04$; unpaired $F_{1, 37} = 5.02$, $p = 0.031$) in schizophrenia (458 ± 102 a.u.) relative to comparison (535 ± 125 a.u.) subjects (**Figure 5.4A2**). Similarly, CB levels in CB+/vGAT+/GAD65+/GAD67+ boutons were 13% lower (paired $F_{1, 19} = 5.72$, $p = 0.027$; unpaired $F_{1, 37} = 5.65$, $p = 0.023$) in the illness (schizophrenia: 427 ± 75 a.u.; comparison: 493 ± 103 a.u.; **Figure 5.4B2**).

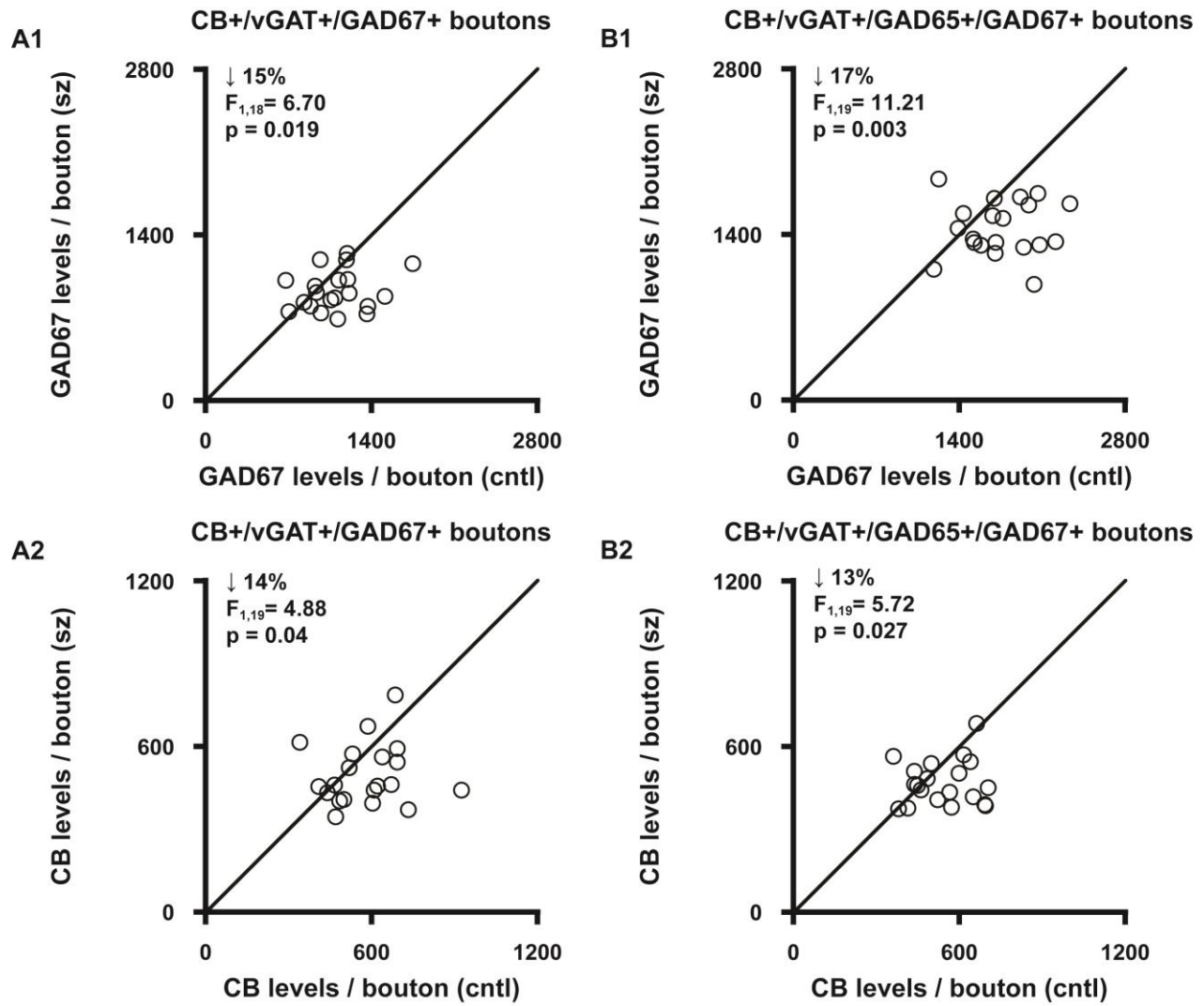


Figure 5.4. CB+/vGAT+/GAD67+ and CB+/vGAT+/GAD65+/GAD67+ bouton GAD67 and CB protein levels between diagnostic groups. Mean GAD67 protein levels (A1 and B1) and CB protein levels (A2 and B2) in CB+/vGAT+/GAD67+ (A) and CB+/vGAT+/GAD65+/GAD67+ (B) boutons in total gray matter.

5.3.4 CB+/vGAT+/GAD67+ and CB+/vGAT+/GAD65+/GAD67+ bouton vGAT protein levels are unaltered in schizophrenia

Levels of vGAT protein did not differ within CB+/vGAT+/GAD67+ boutons (paired $F_{1, 19} = 0.58$, $p = 0.458$; unpaired $F_{1, 38} = 0.53$, $p = 0.47$) and CB+/vGAT+/GAD65+/GAD67+ boutons (paired $F_{1, 19} = 0.02$, $p = 0.886$; unpaired $F_{1, 38} = 0.02$, $p = 0.884$) between schizophrenia (CB+/vGAT+/GAD67+ boutons: 815 ± 175 a.u.; CB+/vGAT+/GAD65+/GAD67+ boutons: 1081 ± 206 a.u.) and comparison (CB+/vGAT+/GAD67+ boutons: 778 ± 143 a.u.; CB+/vGAT+/GAD65+/GAD67+ boutons: 1072 ± 167 a.u.) subjects (**Appendix E Figures E.1**).

5.3.5 Differences in CB+/vGAT+/GAD67+ and CB+/vGAT+/GAD65+/GAD67+ bouton GAD67 and CB protein levels in schizophrenia are not attributable to comorbid factors

In schizophrenia subjects, GAD67 and CB protein levels in CB+/vGAT+/GAD67+ and CB+/vGAT+/GAD65+/GAD67+ boutons did not differ as a function of sex, nicotine use ATOD, benzodiazepine and/or sodium valproate ATOD, antidepressant ATOD, antipsychotic ATOD, or diagnosis of schizoaffective disorder (**Appendix E Figures E.2 and E.3**).

5.3.6 CR+/vGAT+/GAD67+ and CR+/vGAT+/GAD65+/GAD67+ bouton density is lower in schizophrenia

The density of CR+/vGAT+/GAD67+ boutons was 22% lower (paired $F_{1, 19} = 7.78$, $p = 0.012$; unpaired $F_{1, 38} = 7.63$, $p = 0.009$) in schizophrenia (0.00075 ± 0.00024 boutons/ μm^3) than comparison (0.00096 ± 0.00024 boutons/ μm^3) subjects (**Figure 5.5A**). These findings suggest that

a subset of CR+/vGAT+/GAD67+ boutons lack detectable GAD67 protein levels. In support of our interpretation, the density of CR+/vGAT+ boutons that lacked detectable GAD65 and/or GAD67 immunoreactivity was 21% greater (paired $F_{1, 19} = 5.31$, $p = 0.033$; unpaired $F_{1, 38} = 3.80$, $p = 0.059$) in the illness (schizophrenia: 0.00141 ± 0.00035 boutons/ μm^3 ; comparison: 0.00117 ± 0.00041 boutons/ μm^3 ; **Appendix E Figures E.4**).

Similarly, CR+/vGAT+/GAD65+/GAD67+ bouton density was 19% lower (paired $F_{1, 19} = 5.02$, $p = 0.037$; unpaired $F_{1, 38} = 4.03$, $p = 0.052$) in schizophrenia (0.00096 ± 0.00029 boutons/ μm^3) than comparison (0.001184 ± 0.00041 boutons/ μm^3) subjects (**Figure 5.5B**), suggesting that GAD67 protein levels are undetectable in a subset of these boutons. By contrast, the density of CR+/vGAT+/GAD65+ boutons was 23% greater (paired $F_{1, 19} = 5.72$, $p = 0.027$; unpaired $F_{1, 37} = 4.79$, $p = 0.035$) in the illness (schizophrenia: 0.00054 ± 0.00016 boutons/ μm^3 ; comparison: 0.00044 ± 0.00017 boutons/ μm^3 ; **Appendix E Figures E.4**). An analysis of all CR+/vGAT+ boutons containing GAD65 immunoreactivity (i.e. CR+/vGAT+/GAD65+ and CR+/vGAT+/GAD65+/GAD67+ boutons) found that their density did not differ (paired $F_{1, 19} = 1.31$, $p = 0.266$; unpaired $F_{1, 37} = 0.82$, $p = 0.37$) between diagnostic groups (schizophrenia: 0.00149 ± 0.00027 boutons/ μm^3 ; comparison: 0.00162 ± 0.00053 boutons/ μm^3 ; **Appendix E Figures E.4**). These findings support the idea that a subset of CR+/vGAT+/GAD65+/GAD67+ boutons lack detectable GAD67 levels in schizophrenia.

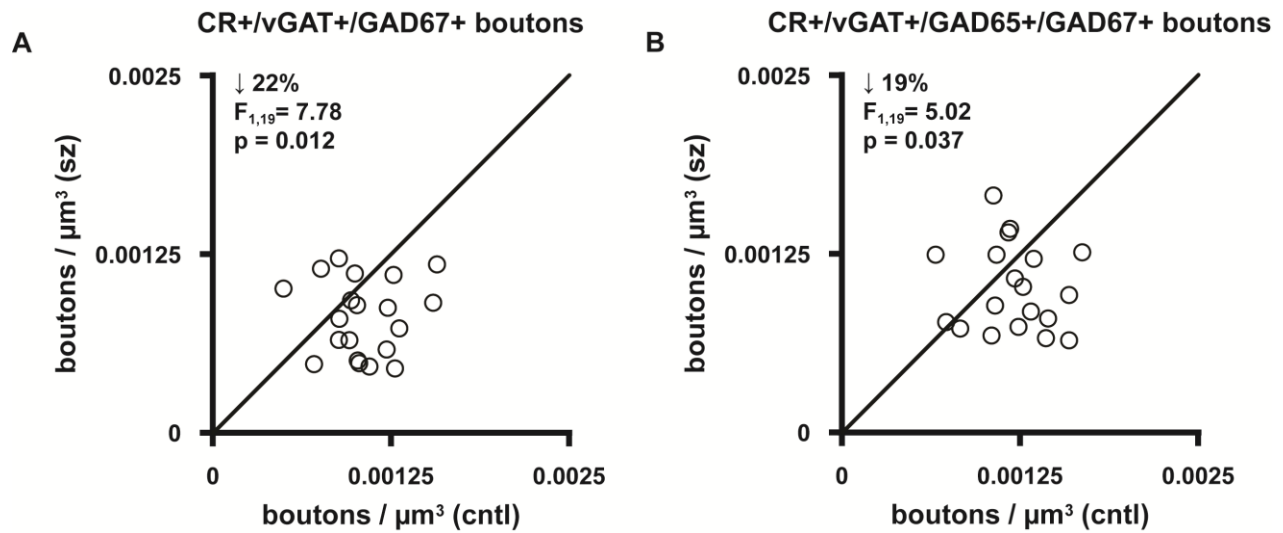


Figure 5.5. CR+/vGAT+/GAD67+ and CR+/vGAT+/GAD65+/GAD67+ bouton density between diagnostic groups. Mean density of CR+/vGAT+/GAD67+ boutons (A) and CR+/vGAT+/GAD65+/GAD67+ boutons (B) in total gray matter.

5.3.7 CR+/vGAT+/GAD67+ and CR+/vGAT+/GAD65+/GAD67+ bouton GAD67 protein levels are lower in schizophrenia

GAD67 protein levels in CR+/vGAT+/GAD67+ boutons were 12% lower (paired $F_{1, 19} = 5.95$, $p = 0.025$; unpaired $F_{1, 37} = 4.30$, $p = 0.045$) in schizophrenia (306 ± 65 a.u.) relative to comparison (351 ± 75 a.u.) subjects (**Figure 5.6A1**). Similarly, GAD67 levels in CR+/vGAT+/GAD65+/GAD67+ boutons were 15% lower (paired $F_{1, 19} = 9.49$, $p = 0.006$;

unpaired $F_{1, 37} = 7.39$, $p = 0.01$) in the illness (schizophrenia: 491 ± 91 a.u.; comparison: 576 ± 113 a.u.; **Figure 5.6B1**).

5.3.8 CR+/vGAT+/GAD67+ and CR+/vGAT+/GAD65+/GAD67+ bouton CR protein levels are unaltered in schizophrenia

CR protein levels in CR+/vGAT+/GAD67+ boutons did not differ (paired $F_{1, 19} = 0.39$, $p = 0.541$, unpaired $F_{1, 37} = 0.13$, $p = 0.723$) between diagnostic groups (schizophrenia: 559 ± 130 a.u.; comparison: 578 ± 126 a.u.; **Figure 5.6A2**). Similarly, CR levels in CR+/vGAT+/GAD65+/GAD67+ boutons did not differ (paired $F_{1, 18} = 3.48$, $p = 0.079$, unpaired $F_{1, 37} = 2.31$, $p = 0.137$; **Figure 5.6B2**) between groups (schizophrenia: 664 ± 147 a.u.; comparison: 740 ± 165 a.u.).

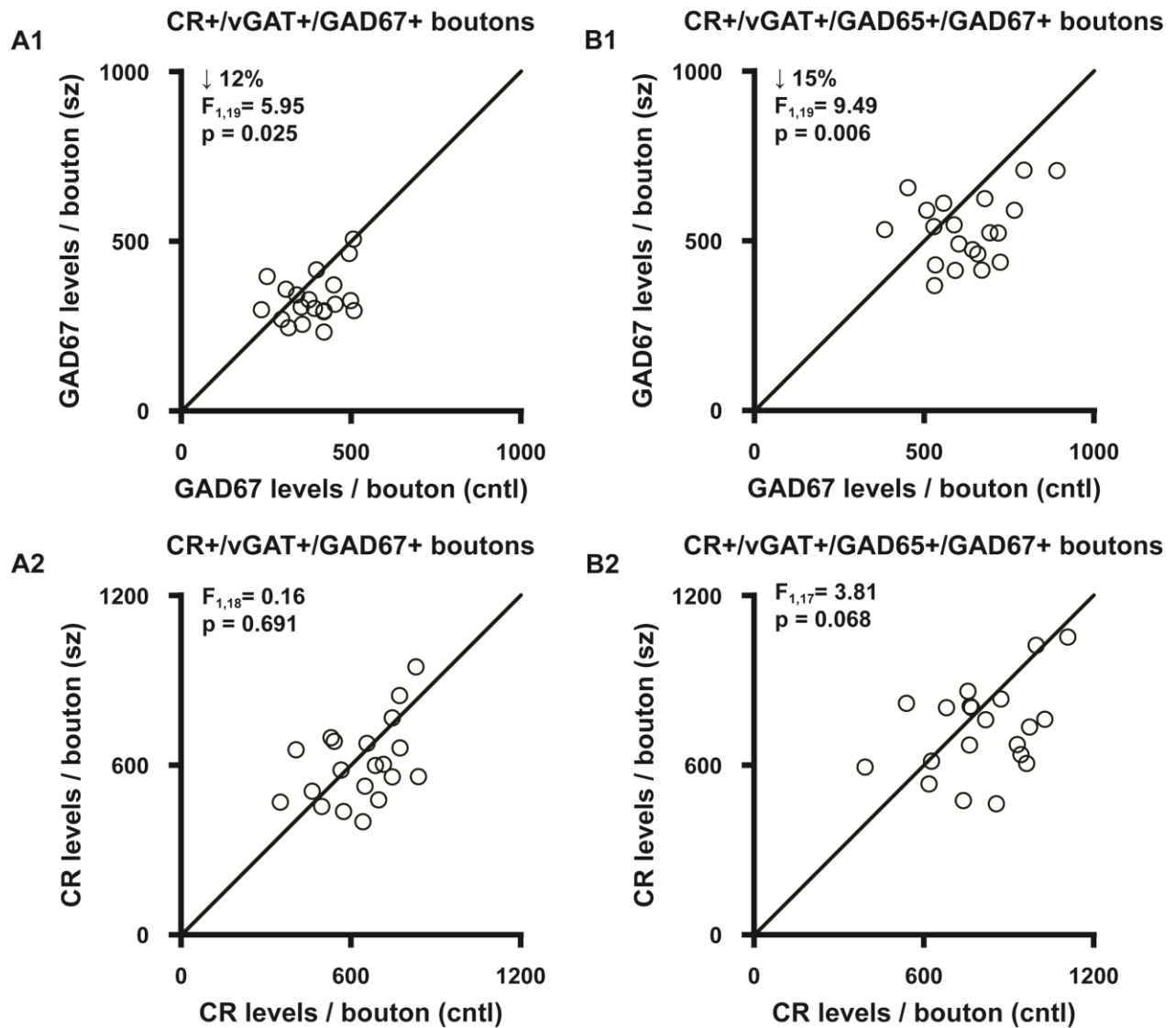


Figure 5.6. CR+/vGAT+/GAD67+ and CR+/vGAT+/GAD65+/GAD67+ bouton GAD67 and CR protein levels between diagnostic groups. Mean GAD67 protein levels (A1 and B1) and CR protein levels (A2 and B2) in CR+/vGAT+/GAD67+ (A) and CR+/vGAT+/GAD65+/GAD67+ (B) boutons in total gray matter.

5.3.9 CR+/vGAT+/GAD67+ and CR+/vGAT+/GAD65+/GAD67+ bouton vGAT protein levels are unaltered in schizophrenia

Levels of vGAT protein were not different in CR+/vGAT+/GAD67+ boutons (paired $F_{1, 18} = 0.0$, $p = 0.99$, unpaired $F_{1, 37} = 0.02$, $p = 0.884$) and CR+/vGAT+/GAD65+/GAD67+ boutons (paired $F_{1, 18} = 0.28$, $p = 0.601$; unpaired $F_{1, 37} = 0.41$, $p = 0.524$) between schizophrenia (CR+/vGAT+/GAD67+ boutons: 622 ± 123 a.u.; CR+/vGAT+/GAD65+/GAD67+ boutons: 935 ± 162 a.u.) and comparison (CR+/vGAT+/GAD67+ boutons: 632 ± 120 a.u.; CR+/vGAT+/GAD65+/GAD67+ boutons: 973 ± 176 a.u.) subjects (**Appendix E Figures E.5**).

5.3.10 Differences in CR+/vGAT+/GAD67+ and CR+/vGAT+/GAD65+/GAD67+ bouton density and GAD67 protein levels in schizophrenia are not attributable to comorbid factors

In schizophrenia subjects, CR+/vGAT+/GAD67+ and CR+/vGAT+/GAD65+/GAD67+ bouton density and GAD67 protein levels did not differ as a function of sex, nicotine use ATOD, benzodiazepine and/or sodium valproate ATOD, antidepressant ATOD, antipsychotic ATOD, or diagnosis of schizoaffective disorder (**Appendix D Figures D.6 and E.7**).

5.4 DISCUSSION

Convergent findings led us to hypothesize that GAD67 protein levels are undetectable in GAD67+ and GAD65+/GAD67+ boutons from CB neurons, but not CR neurons. Our findings rejected these hypotheses. Specifically, we found no statistical difference in the density of

CB+/vGAT+/GAD67+ or CB+/vGAT+/GAD65+/GAD67+ boutons between diagnostic groups, suggesting that GAD67 immunoreactivity was detectable in all GAD67-IR boutons from CB neurons. However, GAD67 levels were 15% lower in CB+/vGAT+/GAD67+ boutons and 17% lower in CB+/vGAT+/GAD65+/GAD67+ boutons in schizophrenia. By contrast, 22% and 19% of CR+/vGAT+/GAD67+ and CR+/vGAT+/GAD65+/GAD67+ boutons, respectively, lacked detectable GAD67 protein levels in the illness. Moreover, GAD67 levels were 12% lower in CR+/vGAT+/GAD67+ boutons and 15% lower in CR+/vGAT+/GAD65+/GAD67+ boutons. In concert, our findings suggest that a significantly greater proportion of CR boutons contribute to the 24% of GAD67+ boutons and the 11% of GAD65+/GAD67+ boutons with markedly reduced GAD67 protein levels, respectively (4.0), compared to CB boutons. Our findings also suggest that CR neurons have a greater magnitude reduction in GAD67 mRNA expression than CB neurons, which may be due to a greater number of CR neurons affected by reduced GAD67 mRNA expression, a greater percentage reduction in GAD67 expression in CR neurons, or both.

CB is expressed in diverse subtypes of cortical GABAergic neurons and glutamatergic pyramidal cells (DeFelipe et al., 1989; Freund et al., 1990; Gonzalez-Albo et al., 2001; Hayes and Lewis, 1992; Hof and Morrison, 1991). Much of what is known about alterations in GABAergic CB neurons in schizophrenia comes from studying neurons that express SST, which is exclusively expressed by GABA neurons (Gonchar and Burkhalter, 1997; Gonchar and Burkhalter, 2003; Gonzalez-Albo et al., 2001; Kubota et al., 1994; Sugino et al., 2006). The detectability of SST immunoreactivity is rapidly degraded postmortem (Hayes et al., 1991) compared to other proteins including CB, which greatly confounds assessments of SST protein levels in human brain tissue. Our findings here report on measurements exclusively from GABAergic CB boutons because only those CB boutons that were IR for vGAT were included.

We found that CB protein levels were 14% and 13% lower in CB+/vGAT+/GAD67+ and CB+/vGAT+/GAD65+/GAD67+ boutons, respectively. Findings in mouse somatosensory cortex suggest that CB neurons receive the greatest strength of excitatory drive from pyramidal cells around layer 4 (Xu and Callaway, 2009). In schizophrenia, pyramidal cells in layers deep 3-4 appear to have the greatest deficits in excitatory drive (reviewed in Glausier and Lewis, 2013). Considering that decreased network activity result in lower CB (Carder et al., 1996; Philpot et al., 1997) and GAD67 (Lau and Murthy, 2012) protein expression, lower bouton CB and GAD67 protein levels in schizophrenia may be a consequence of deficits in excitatory drive from pyramidal cells in PFC layers deep 3-4.

GABAergic CB neurons constitute numerous morphologically diverse neuronal subtypes; however, their synaptic targets and function are generally similar. CB neurons mainly innervate dendritic spines and shafts of pyramidal cells (Melchitzky and Lewis, 2008) and to a lesser extent the dendrites of non-SST expressing GABA neurons (Pfeffer et al., 2013), whereby they regulate the integration of excitatory inputs within local cortical circuits (Lovett-Barron et al., 2012) and from thalamic afferents (Xu et al., 2013), and provide feedback inhibition in and between cortical layers (Wang et al., 2004). Recent in vitro findings suggest that SST neurons in layer 2 of mouse somatosensory cortex are spontaneously and tonically active and thereby provide a blanket of strong inhibition over the cortical network via activation of GABA B receptors (Urban-Ciecko et al., 2015). Suppressing the activity of these neurons using optogenetic techniques increases the overall excitability of local pyramidal cells. Several functional imaging studies have shown reduced activity of the PFC in schizophrenia subjects (Berman et al., 1986; Glahn et al., 2005; Minzenberg et al., 2009; Perlstein et al., 2003; Weinberger et al., 1988; Weinberger et al., 1986). Protein levels for GABA B receptor subunits are reduced in the PFC (Ishikawa et al., 2005) as

well as mRNA expression for $\alpha 5$ -containing GABA A receptors (Beneyto et al., 2011), which are enriched at synapses from SST neurons (Ali and Thomson, 2008; Serwanski et al., 2006). Together with our finding of less GABA production, and presumably release, from CB neurons, these changes may be compensatory responses to less PFC activity in order to achieve greater excitability of pyramidal cells.

Our findings of markedly reduced GAD67 protein levels in boutons from CR neurons in schizophrenia were not due to lack of detectable bouton CR immunoreactivity since CR protein levels were unchanged in these boutons. This finding is consistent with previous reports of no change in CR mRNA expression or total protein levels in the PFC of schizophrenia subjects (Fung et al., 2010; Hashimoto et al., 2008; Hashimoto et al., 2003). Unlike CB and GAD67 protein expression, CR protein levels do not appear to be as responsive to changes in network activity (Carder et al., 1996; Philpot et al., 1997). These properties likely explain why CR mRNA expression did not correlate with lower levels of GAD67 mRNA expression in previous studies of schizophrenia (Hashimoto et al., 2008), which has been interpreted as CR neurons are unaffected in the illness.

In contrast to pyramidal cells in PFC layers deep 3-4 in schizophrenia, pyramidal cells in other PFC layers show less robust alterations in markers of excitatory drive. This may be due to intrinsic deficits in pyramidal cells in layers deep 3-4 and/or deficits in cortico-cortical and thalamo-cortical inputs, which predominantly innervate these cortical layers (Barbas and Rempel-Clower, 1997; Felleman and Van Essen, 1991; Giguere and Goldman-Rakic, 1988; Jones and Hendry, 1989). The majority of local excitatory afferents to CR neurons are from pyramidal cells in layers 2-3 (Xu and Callaway, 2009). However, our finding that GAD67 protein levels are markedly reduced in boutons from CR neurons suggests that excitatory drive from pyramidal cells

in the superficial layers is also reduced in schizophrenia subjects, which may be a consequence of reductions in the strength of excitatory drive from local axon collaterals of pyramidal cells in layers deep 3-4 (Melchitzky et al., 2001; Melchitzky et al., 1998).

Alternatively, > 80% of CR neurons express VIP (Gabbott and Bacon, 1997), and microduplications in the VIP receptor gene, *VIPR2*, confers increased risk for schizophrenia (Levinson et al., 2011; Vacic et al., 2011; Yuan et al., 2014); however, the *VIPR2* microduplication was found to be only present in 0.35% out of > 8,000 schizophrenia subjects (Vacic et al., 2011). Pharmacological-induced overactivation of the VPAC2 receptor, which is encoded by *VIPR2*, in infant mice leads to lower PFC levels of postsynaptic density-95 (PSD-95) and synaptophysin protein, and sensorimotor gating abnormalities (Ago et al., 2015). Schizophrenia subjects are reported to have lower cortical protein levels for PSD-95 and synaptophysin (Glantz and Lewis, 1997; Kristiansen et al., 2006) and lower PSD-95 mRNA expression in the PFC (Ohnuma et al., 2000). Moreover, sensorimotor gating abnormalities are present in the illness (Braff et al., 1999; Swerdlow et al., 2006). Therefore, intrinsic alterations in the overexpression of the *VIPR2* gene in some subjects with schizophrenia may lead to synaptic abnormalities in the PFC. Although it is unknown if any subjects in this cohort carried this microduplication, the low prevalence of this genomic alteration is unlikely to account for our findings.

Similar to CB neurons, CR neurons constitute a morphologically diverse subtype of GABA neuron. CR neurons play a unique disinhibitory role by mainly contacting the dendrites of other GABA neurons and to a much lesser extent the dendrites and perisomatic region of pyramidal cells (Melchitzky et al., 2005; Melchitzky and Lewis, 2008). Studies in mouse suggest that CR/VIP neurons primarily innervate SST and to a lesser extent PV neurons, and that this

innervation pattern occurs across cortical and hippocampal regions (Donato et al., 2013; Fu et al., 2014; Kawaguchi Y, 1996; Lee et al., 2013; Neske et al., 2015; Pfeffer et al., 2013; Rogers, 1992; Staiger et al., 2004; Tyan et al., 2014). By mainly contacting GABA neurons, CR/VIP neurons mediate selective amplification of local signal processing of pyramidal cells (Pi et al., 2013). A reduced capacity for GABA synthesis, and presumably signaling, from CR neurons would decrease the amount of disinhibition of pyramidal cells, which may contribute to lower PFC activity in schizophrenia.

6.0 GENERAL DISCUSSION

6.1 SUMMARY OF FINDINGS

Cognitive impairments are a core feature of schizophrenia and arise, in part, from alterations in glutamatergic and GABAergic signaling in the PFC. ~30% of GABA neurons have marked reductions in GAD67 mRNA expression, and the goal of this dissertation was to determine which GABA neuron subtypes are affected by this deficit. Development of a novel technique to identify lipofuscin (2.0) was required to ask the following specific questions about GABAergic signaling deficits in schizophrenia: 1) How well do bouton GAD67 protein levels reflect the prior findings of markedly lower GAD67 mRNA expression in only a subset of GABA neurons? (3.0); 2) Are GAD67 protein levels lower in chandelier cell boutons? (4.0); 3) Are GAD67 protein levels lower in boutons arising from CB, but not CR, neurons? (5.0). The following discussion reviews the findings of the experimental chapters, and presents a mechanistic hypothesis for the cause of lower GAD67 expression in the affected GABA neuron subtypes. Finally, the implication of this work for altered PFC activity in schizophrenia will be considered.

6.1.1 Lower GAD67 protein levels in a subset of boutons in schizophrenia

Reductions in GAD67 mRNA expression are widely reported in the PFC of schizophrenia subjects but only ~30% of GABA neurons in the PFC lack detectable levels of GAD67 mRNA,

whereas the other neurons contain GAD67 mRNA around normal levels (Akbarian et al., 1995; Volk et al., 2000). We found that the reported marked reduction in GAD67 mRNA levels reflect a marked reduction in GAD67 protein levels in only a subset of GABAergic boutons. Specifically, only 16% of vGAT+ boutons lacked detectable levels of GAD67 protein, and GAD67 levels were 14% lower in boutons that contained GAD67 immunoreactivity (3.0); however, lower GAD67 levels did not affect all boutons similarly. The range of GAD67 levels, including boutons with relatively high levels of GAD67, were similar between diagnostic groups, suggesting that only a subset of boutons has reduced GAD67 protein levels in schizophrenia, which presumably arise from the neurons with marked deficits in GAD67 mRNA expression. By contrast, the density of vGAT+ boutons was unaltered (3.0). Moreover, bouton vGAT protein levels were not different in all GABAergic boutons or in boutons from any of the GABA neuron subtypes assessed (4.0 and 5.0), which corroborates previous vGAT mRNA findings in the illness (Fung et al., 2011; Hoftman et al., 2013), and suggests that the capacity to package GABA into synaptic vesicles is overall intact despite lower GABA production.

6.1.2 GAD67 expression in GABA neuron subtypes in schizophrenia

PV, CB, and CR neurons constitute ~25%, ~20%, and ~45% of all GABA neurons in primate neocortex (Conde et al., 1994; del Rio and DeFelipe, 1996; Gabbott and Bacon, 1996). Since about half of all PV neurons lack detectable GAD67 mRNA expression (Hashimoto et al., 2003), GAD67 protein levels are ~50% reduced in boutons from PV basket cells in PFC layers 3-4 (Curley et al., 2011), and correlative evidence suggest that GAD67 expression is lower in PV chandelier and SST, but not CR neurons (Hashimoto et al., 2008; Morris et al., 2008), it was unknown if the ~30% of neurons with marked reductions in GAD67 mRNA expression were

comprised of only PV and SST neurons. Our findings that GAD67 protein levels were trending lower in chandelier cell boutons (4.0), significantly lower in boutons from CB and CR neurons (5.0) suggest that no single subtype is completely affected by lower GAD67 expression in schizophrenia, but rather a proportion of each subtype contributes to the pool of GABA neurons with marked reductions in GAD67 expression.

6.2 LOWER BOUTON GAD67 PROTEIN LEVELS AS A CONSEQUENCE OF REDUCED ACTIVITY IN SCHIZOPHRENIA

6.2.1 Local excitatory afferent inputs

Studies in mouse somatosensory cortex suggest that PV and CB neurons receive the greatest strength of excitatory drive from pyramidal cells in layers deep 3-4, whereas CR neurons receive the greatest drive from pyramidal cells in layers 2-superficial 3 (Xu and Callaway, 2009). Although this connectivity pattern may be different in other cortical areas and in human PFC, our findings suggest that GAD67 expression may be reduced as a compensatory response to overall lower activity of the PFC and not necessarily predicted by the amount or strength of inputs from layers deep 3-4 pyramidal neurons; however, lower PFC activity may be a consequence of cell-autonomous deficits in layers deep 3-4 pyramidal cells, a reduction in the strength of feedforward afferent inputs to these layers, or a combination of both possibilities (reviewed in Glausier and Lewis, 2013). About half of all local axon collaterals from layers deep 3-4 pyramidal cells and ~90% of afferents from deep 3-4 pyramidal cells in proximal cortical areas innervate dendritic spines, including spines in the superficial layers (Melchitzky et al., 2001; Melchitzky et al., 1998).

Therefore, reductions in the activity of pyramidal cells in the superficial layers may be a consequence of reduced strength of excitatory drive from pyramidal cells in layers deep 3-4, and in turn, lead to overall reduced activity of the PFC and lower GAD67 expression in neurons that may not receive direct inputs from layers deep 3-4 pyramidal cells.

6.2.2 Extrinsic excitatory afferent projections

Dendritic spines of layers deep 3-4 pyramidal cells are the principal targets of the vast majority of thalamo-cortical (Giguere and Goldman-Rakic, 1988; Jones and Hendry, 1989) and cortico-cortical projections (Medalla and Barbas, 2009; Melchitzky et al., 2001); however, afferent projections from distinct brain regions preferentially innervate distinct subtypes of GABA neurons. In rat, afferent projections from the mediodorsal thalamic nuclei to the PFC predominantly target PV neurons (Rotaru et al., 2005). In monkey PFC, CB neurons are the predominant GABAergic subtype that receives projections from the ACC (Medalla and Barbas, 2009; Medalla and Barbas, 2010), presumably from layer 3 pyramidal cells (Barbas and Rempel-Clower, 1997), whereas CR neurons are the predominant GABAergic subtype that receives layer 3 projections from pyramidal cells in adjacent PFC areas (e.g. projections in area 46 to area 9) (Medalla and Barbas, 2009). This connectivity pattern suggests that deficits in excitatory drive from extrinsic brain regions may contribute to lower GAD67 expression in PV, CB, and CR neurons in the PFC of schizophrenia subjects.

Indeed, deficits in total neuron number and volume of the mediodorsal thalamic nuclei, the number of putative thalamic projections to the PFC, and transcripts encoding glutamate receptor subunits in the thalamus are reduced in schizophrenia (Byne et al., 2001; Byne et al., 2002; Gilbert et al., 2001; Lewis et al., 2001; Pakkenberg, 1990; Popken et al., 2000; Sodhi et al., 2011;

Young et al., 2000); therefore, reduced excitatory drive from the thalamus may contribute to lower GAD67 levels in PV neurons (**Figure 6.1**). It is currently unknown if thalamic projections preferentially innervate PV basket or chandelier cells; however, considering that the highest density of chandelier cells is in layers 2 and 6 (Taniguchi et al., 2013), the highest density of all PV neurons is in layers deep 3-4 (Conde et al., 1994), and thalamic inputs predominantly innervate layers deep 3-4 (Giguere and Goldman-Rakic, 1988; Jones and Hendry, 1989), PV basket cells may receive a greater density of thalamic inputs compared to chandelier cells. Therefore, a greater magnitude reduction in GAD67 protein levels in boutons from PV basket cells than chandelier cells may be a consequence of deficits in the strength of thalamic afferents in combination with reduced drive from local pyramidal cells.

Similar to the PFC, morphological deficits in layer 3 pyramidal cells of the ACC are reported in schizophrenia (Broadbelt et al., 2002), and numerous functional imaging studies suggest that the activity of both of these brain regions is altered in schizophrenia patients during cognitive control tasks (Allen et al., 2007; Cho et al., 2006; Ikuta et al., 2012; Kerns et al., 2005; Minzenberg et al., 2010; Quintana et al., 2004; Schultz et al., 2012; Yucel et al., 2007). Therefore, lower excitatory drive from the ACC may contribute to lower GAD67 expression in CB neurons, and reduced excitatory drive from other nearby PFC areas may contribute to lower GAD67 expression in CR neurons.

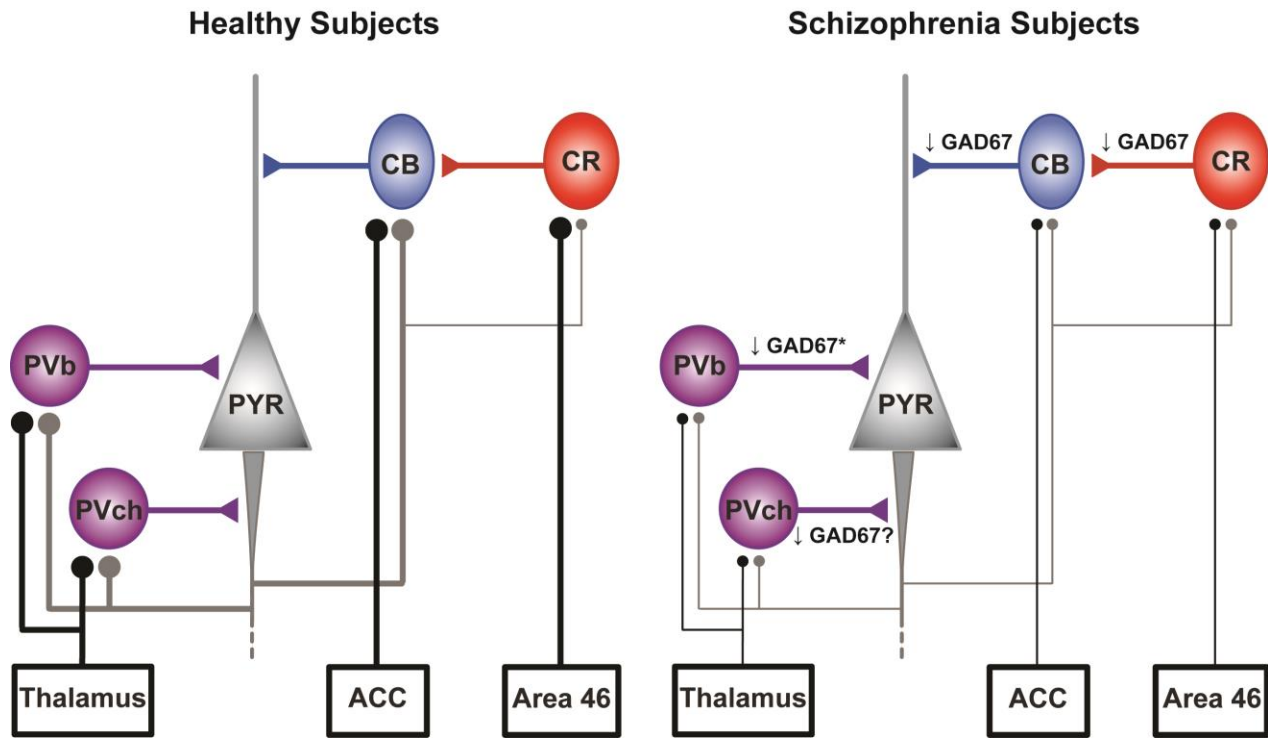


Figure 6.1. Schematic diagram of GAD67 expression alterations in GABA neuron subtypes of PFC area 9 in response to reduced local excitatory drive from layers deep 3-4 pyramidal cells and extrinsic brain regions. The asterisk indicates GAD67 protein level findings in boutons from PV basket cells (PVb) in PFC layers 3-4 of schizophrenia subjects (Curley et al., 2011). Bouton GAD67 expression levels from PV chandelier (PVch), CB, and CR neurons are reported in 4.0 and 5.0. The thicker lines from the pyramidal cell (PYR), thalamus, anterior cingulate cortex (ACC), and PFC area 46 depict greater strength of excitatory drive to PV, CB, and CR neurons.

6.2.3 Lower expression of several GABA-related markers

Converging evidence suggests that reduced expression of various other activity-dependent GABA-related markers accompany lower GAD67 expression in schizophrenia. For example, monocular deprivation in monkeys result in lower PV and CB immunoreactivity (Carder et al., 1996), and similar reductions in PV and CB protein levels are observed in rat olfactory bulb upon olfactory deprivation (Philpot et al., 1997). In schizophrenia subjects, PV mRNA expression (Fung et al., 2010; Hashimoto et al., 2008; Hashimoto et al., 2003; Mellios et al., 2009) and bouton PV levels (Glausier et al., 2014) are reduced in the PFC, and we report here that bouton CB protein levels are also lower (**5.0**). Moreover, GAD65 protein levels are reduced under conditions of chronic network inactivity (Hartman et al., 2006). In the primary auditory cortex of schizophrenia subjects, bouton GAD65 protein levels are reduced and correlate with a lower density of dendritic spines in layer deep 3 (Moyer et al., 2012). Similarly, we found that bouton levels of GAD65 protein are significantly lower in the PFC of schizophrenia subjects (**Appendix F Figure F.1**). Consistent with this finding, GAD65 protein levels are significantly lower in boutons from CB and CR neurons (**Appendix F Figure F.2**). Although GAD65 mRNA and total gray matter GAD65 protein expression, and GAD65 levels in PV basket cell boutons in PFC layer deep 3 were previously reported to be unchanged in the PFC of schizophrenia (Guidotti et al., 2000; Hashimoto et al., 2008; Impagnatiello et al., 1998), GAD65 mRNA and total gray matter protein expression is lower in the PFC of subjects diagnosed with schizoaffective disorder (Glausier et al., 2015). Our findings of lower bouton GAD65 levels were not a consequence of schizoaffective diagnosis (**Appendix F Figure F.1**), suggesting that within boutons lower GAD65 protein levels accompany lower GAD67 levels, at least for some GABA neuron subtypes.

GABA receptors are also responsive to activity-dependent network changes. For example, decreased activity in cultured visual cortex and hippocampal neurons results in reduced amplitude of miniature inhibitory postsynaptic currents, which is associated with reductions in the number of detectable GABA A receptors and lower protein levels of membrane-bound GABA A receptors (Kilman et al., 2002; Swanwick et al., 2006). In schizophrenia, lower mRNA expression for the $\alpha 1$ and $\alpha 5$ subunits of the GABA A receptor, and lower protein levels for the 1a subtype of the GABA B receptor are reported in the PFC (Beneyto et al., 2011; Duncan et al., 2010; Glausier and Lewis, 2011; Ishikawa et al., 2005).

6.3 FUNCTIONAL IMPLICATIONS OF LOWER BOUTON GAD67 PROTEIN LEVELS IN GABA NEURON SUBTYPES IN THE PREFRONTAL CORTEX OF SCHIZOPHRENIA

6.3.1 Chandelier cells

Although GAD67 protein levels in boutons from chandelier cells are trending lower in schizophrenia, downregulation of GAT1, which appears to be specific to chandelier cell boutons (Woo et al., 1998), may enhance their signaling effects rather than compensate for reduced GABA signaling as previously hypothesized (Volk et al., 2002). For example, pharmacological blockade of GAT1 increases the latency of postsynaptic responses upon GABA release at rat hippocampal synapses (Overstreet and Westbrook, 2003). Considering that GAD67 protein levels are only trending lower, vGAT protein levels are unaltered, and GAT1 levels are significantly

reduced at some chandelier cell inputs, similar effects may occur at chandelier cell synapses in the illness.

PV neurons, including chandelier cells, are critically involved in the generation and maintenance of gamma-frequency oscillations (Cardin et al., 2009; Fuchs et al., 2007; Sohal et al., 2009) and altered inhibitory signaling from chandelier cells is hypothesized to contribute to altered gamma synchrony; however, signaling from chandelier cells may enhance pyramidal cell excitability (reviewed in Lewis, 2011). The postsynaptic responses from chandelier cells are highly responsive to network activity. While the synaptic effects of chandelier cells appear to be mainly inhibitory under physiological conditions (Woodruff et al., 2011), multiple studies have reported that they can also depolarize cortical and hippocampal pyramidal cells (Molnar et al., 2008; Sauer et al., 2012; Szabadics et al., 2006; Woodruff et al., 2011). The effects from chandelier cell inputs are hyperpolarizing when the state of the network is highly active and depolarizing when the network is relatively quiescent (Woodruff et al., 2011). Considering that activity within the PFC is reduced in schizophrenia (Minzenberg et al., 2009) signaling from chandelier cells may favor depolarizing responses.

6.3.2 CB neurons

CB/SST neurons regulate the integration of cortico-cortical and thalamo-cortical excitatory projections to pyramidal cells (Kapfer et al., 2007; Lovett-Barron et al., 2012; Xu et al., 2013), and provide a layer of tonic inhibition via activation of GABA B receptors over the cortical network (Urban-Ciecko et al., 2015). Reductions in the strength of signaling from CB neurons may increase the gain of local pyramidal cells in the PFC of schizophrenia. Indeed, suppressing the activity of SST neurons using optogenetic techniques increases the overall excitability of the

network (Urban-Ciecko et al., 2015). Consistent with reduced GABA signaling from CB neurons, protein levels for GABA B receptor subunits are reduced in the PFC (Ishikawa et al., 2005) as well as mRNA expression for $\alpha 5$ -containing GABA A receptors (Beneyto et al., 2011), which are enriched at synapses from SST neurons (Ali and Thomson, 2008; Serwanski et al., 2006).

6.3.3 CR neurons

In contrast to CB neurons, lower GABA signaling from CR/VIP neurons would presumably decrease the activity of the PFC. By predominantly innervating the dendrites and soma of GABA neurons (Melchitzky et al., 2005; Melchitzky and Lewis, 2008), the majority of which are SST neurons (Pfeffer et al., 2013), CR neurons mediate disinhibitory control of pyramidal cells, and thereby control the overall gain within the PFC (Pi et al., 2013). Reduced signaling from CR neurons would therefore result in less inhibition of CB neurons and, in turn, reduce the excitability of pyramidal cells.

Activity of CR/VIP neurons has been shown to be important for a number of sensory and cognitive processes. For example, selective activation of VIP neurons by optogenetic techniques in mice increases the efficiency of tone discrimination in the auditory cortex during an auditory discrimination task (Pi et al., 2013). Locomotion induced activation of VIP neurons in mouse primary visual cortex enhances visual responses (Fu et al., 2014), and activation of VIP neurons via afferents from motor cortex silences SST neurons, and to a lesser extent PV cells, in somatosensory cortex during active whisking, which increases the efficacy of sensory responses in this brain region (Lee et al., 2013). Moreover, VIP neuron inhibition of PV cells in mouse hippocampus modulates learning induced synaptic plasticity during a fear-conditioning paradigm (Donato et al., 2013).

Impairments in many of these sensory and cognitive modalities are disrupted in schizophrenia. For example, schizophrenia subjects exhibit deficits in tone discrimination (Holcomb et al., 1995; Strous et al., 1995), mismatch negativity (Javitt, 2000), and speech prosody, which is the ability to recognize discrete tones associated with a wide range of emotional states (Leitman et al., 2010). Deficits in orientation surround suppression are reported in the illness (Yoon et al., 2009), and correlate with lower GABA levels in the visual cortex (Yoon et al., 2010). In monkey, CR neurons receive excitatory projections from brain regions that are functionally similar. For example, CR neurons in PFC area 9 receive afferent projections from pyramidal cells in PFC area 46 (Medalla and Barbas, 2009), and both brain areas are critically involved in working memory tasks (Levy and Goldman-Rakic, 1999; Petrides, 2000; Tanila et al., 1992; Tanji and Hoshi, 2008). By disinhibiting pyramidal cells CR neurons increase the efficacy of excitatory inputs between nearby brain areas that perform similar functions. Altered activity of the PFC is widely reported in schizophrenia subjects during cognitive control tasks (Berman et al., 1986; Glahn et al., 2005; Minzenberg et al., 2009; Perlstein et al., 2003; Weinberger et al., 1988; Weinberger et al., 1986), and reduced strength of signaling from CR neurons may result in weaker recruitment of neural networks involved in similar cognitive processes.

6.4 EXPERIMENTAL CONSIDERATIONS

6.4.1 Data segmentation

Because previous findings suggested that levels of some proteins are significantly lower in the PFC of schizophrenia subjects (i.e. GAD67), the methods used here to assess bouton density and

bouton protein content were done to maximize the detectability of immunoreactive objects. This approach included using optimal image capture settings for each image acquisition (2.4.2) and applying an optimal initial threshold value for data segmentation for each image stack (2.5.2). Importantly, the same parameters were used to determine the optimal initial threshold value. There are several advantages of using this approach. For example, there is a greater chance of under- or over-exposing image stacks, which may result in an underestimate of immunoreactive objects or saturated pixels, respectively, when using constant rather than optimal exposure settings. Applying an optimal initial threshold value for data segmentation for each image stack maximizes the detectability of immunoreactive objects across image stacks with variable intensity levels, which can arise from several factors including differences in protein content across cortical layers and differences in the density of immunoreactive objects. Because using a consistent way of determining an optimal initial threshold value maintains a constant level of sensitivity across image stacks, a lower density of objects is attributable to undetectable immunoreactivity, and lower intensity levels are due to less protein content in the detectable objects. By contrast, when using a constant initial threshold value only objects with relatively similar intensity levels are detectable, and therefore changes in intensity levels between conditions may not be found if the threshold value used to define the objects is too high; however, if protein content in these objects were in fact different between conditions (e.g. schizophrenia and comparison subjects) despite a change in intensity levels between the detectable objects, the density of objects would presumably be different. A caveat to using an optimal initial threshold value for each stack is that lower protein content (e.g. GAD67 protein levels between schizophrenia and comparison subjects) can theoretically result in a much lower threshold value and, in turn, a higher density of objects, which may include false positives. However, this did not appear to be the case for our data

segmentation procedure since bouton GAD67 protein levels and the density of vGAT+/GAD67-IR boutons were significantly lower in schizophrenia subjects (3.0), and since the density of CB+/vGAT+/GAD67+ boutons and CR+/vGAT+/GAD67+ boutons were unchanged and significantly lower, respectively, even though both bouton subtypes had significantly lower GAD67 protein levels (5.0).

6.4.2 Other microscopy techniques for assessing synaptic protein levels

In contrast to protein immunoblotting techniques (i.e. Western blot), which typically require tissue homogenates, the confocal microscopy techniques used here allowed for the simultaneous detection of multiple proteins within axonal boutons. The colocalization of vGAT and GAD67 presumably designated presynaptic terminals; though, it is unknown if all of these boutons were truly presynaptic to postsynaptic elements. Additional techniques which provide a significant increase in the resolving power of neuronal structures within tissue sections or an increase in the number of synaptic proteins that can be assessed may be used to quantify the proteins assessed here that are specifically apposed to postsynaptic structures. For example, studies using electron microscopy (EM) provide the highest level of resolution for assessing neuronal ultrastructure including synapses in postmortem tissue sections. With EM techniques, multiple proteins can be simultaneously quantified within presynaptic terminals using different size metallic nanoparticles; however, multi-label EM studies are currently able to only reliably differentiate ~2 specific proteins (Bleher et al., 2008). Other microscopy techniques provide the same image resolution used here but allow for the detection of a greater number of proteins. For example, with array tomography, multiple proteins within serial ultrathin tissue sections can be labeled, imaged, and then removed, and a new set of several other proteins can be labeled and imaged within the same

tissue section (Micheva and Smith, 2007). The images containing the different labeled proteins can then be collated and aligned. Therefore, multiple apposed presynaptic and postsynaptic proteins can be simultaneously quantified within the same tissue sections. Moving forward, studies using other techniques than those used here, such as EM and array tomography will be important for testing the reproducibility of our results and for simultaneously assessing a greater number of pre- and postsynaptic proteins involved in GABA signaling in schizophrenia.

6.5 SUMMARY

This dissertation provides the first direct assessment of GAD67 expression levels in chandelier, CB, and CR neurons in schizophrenia with the goal of identifying which subtypes are affected by lower bouton GAD67 protein levels. First, we determined that reduced GAD67 mRNA expression in only a subset of neurons in the PFC of schizophrenia subjects is associated with lower GAD67 protein levels in only a subset of axonal boutons (**3.0**). Investigation of GAD67 protein levels within GABA neuron subtypes found that GAD67 levels in boutons from chandelier cells were only trending lower in schizophrenia (**4.0**). By contrast, boutons from CB neurons had significantly lower GAD67 levels. Some boutons arising from CR neurons lacked detectable GAD67 protein levels, and GAD67 levels were significantly lower in the CR boutons that contained GAD67 (**5.0**). These findings suggest that lower GAD67 expression in the PFC of schizophrenia subjects is not restricted to a specific subtype of GABA neuron, but rather lower GAD67 expression affects a proportion of several subtypes, which may be a consequence of lower PFC activity. GABA neurons play unique functional roles within cortical networks and these findings shed light on the pathophysiological changes in the PFC of schizophrenia subjects.

APPENDIX A

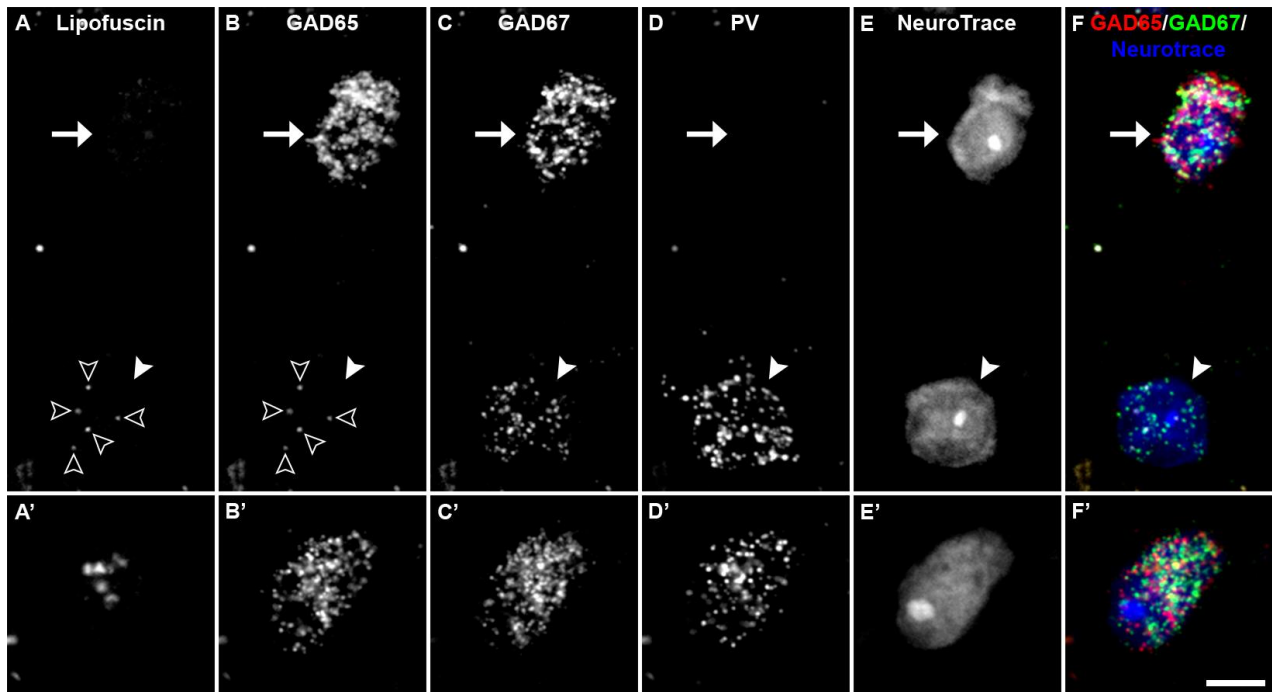


Figure A.1. PV neurons are distinguishable by their GAD65 and GAD67 mRNA content. Single plane image of a human PFC tissue section labeled for GAD65, GAD67, and PV mRNAs, and counterstained with NeuroTrace. Single channel images of lipofuscin autofluorescence (A, A'), GAD65 mRNA (B, B'), GAD67 mRNA (C, C'), PV mRNA (D, D'), and NeuroTrace (E, E'). (F, F') Merged channels image of B (B'), C (C'), and E (E'). (A-F) Arrows depict a GAD65/GAD67 mRNA expressing neuron (arrow) and a GAD67/PV mRNA expressing neuron (solid arrowhead). The open arrowheads in A and B identify lipofuscin autofluorescence in the GAD67/PV mRNA expressing neuron. (A'-F') Neuron expressing GAD65/GAD67/PV mRNA. Bar = 10 μ m.

APPENDIX B

CHAPTER 2 SUPPLEMENTAL MATERIALS

B.1 SUPPLEMENTAL METHODS

Table B.1. Detailed demographic and postmortem characteristics of human subjects. ^aPMI, postmortem interval (hours); ^bYears stored in 30% glycerin/30% ethylene glycol solution at -30°C. Abbreviations: M, male; F, female; W, white; B, black; ASCVD, arteriosclerotic cardiovascular disease; AAR, alcohol abuse, in remission at time of death; ADC, alcohol dependence, current at time of death; ADR, alcohol dependence, in remission at time of death; OAR, ATOD, at time of death; CO, carbon monoxide; U, unknown.

Healthy Comparison Subjects							Subjects with Schizophrenia										
Pair	Case	Sex/Race	Age (years)	PMI ^a	Storage Time ^b	Cause of Death	Case	DSM IV diagnosis	Sex/Race	Age (years)	PMI ^a	Storage Time ^b	Cause of Death	Antipsychotic ATOD	Antidepressant ATOD	Benzodiazepine/Anticonvulsant ATOD	Nicotine Use ATOD
1	727	M/B	19	7.00	12.90	Trauma	829	Schizoaffective disorder; ADC; OAR	M/W	25	5.00	11.34	Suicide by salicylate overdose	N	N	Y	Y
2	852	M/W	54	8.00	10.90	Cardiac tamponade	781	Schizoaffective disorder; ADR	M/B	52	8.00	12.16	Peritonitis	Y	Y	N	Y
3	1307	M/B	32	4.80	5.20	ASCVD	10024	Paranoid schizophrenia	M/B	37	5.98	5.96	ASCVD	N	N	N	N
4	567	F/W	46	15.00	14.80	Mitral valve prolapse	537	Schizoaffective disorder	F/W	37	14.50	15.25	Suicide by hanging	N	N	N	U
5	1047	M/W	43	13.80	8.10	ASCVD	1209	Schizoaffective disorder	M/W	35	9.1	6.50	Suicide by diphenhydramine overdose	Y	N	N	N
6	739	M/W	40	15.8	13	ASCVD	933	Disorganized schizophrenia	M/W	44	8.30	9.66	Myocarditis	Y	Y	Y	N
7	451	M/W	48	12.00	16.30	ASCVD	317	Chronic undifferentiated schizophrenia	M/W	48	8.30	18.9	Bronchopneumonia	Y	Y	N	N
8	178	M/W	48	7.80	20.50	ASCVD	377	Chronic undifferentiated schizophrenia	M/W	52	10.00	18.1	Gastrointestinal bleeding	Y	N	N	N
9	452	F/W	40	14.30	16.30	ASCVD	341	Chronic undifferentiated schizophrenia	F/W	47	14.50	18.6	Suicide, chlorpromazine overdose	Y	N	N	Y
10	449	F/W	47	4.30	16.30	Accidental CO poisoning	517	Chronic disorganized schizophrenia	F/W	48	3.70	15.10	Intracerebral hemorrhage	Y	N	N	Y
11	681	M/W	51	11.60	14.10	Hypertrophic cardiomyopathy	234	Chronic paranoid schizophrenia	M/W	51	12.80	21.00	Cardiomyopathy	N	N	N	N
12	395	M/W	42	12.30	18.80	Pericardial tamponade	322	Chronic undifferentiated schizophrenia	M/W	40	8.50	20.20	Suicide, combined drug overdose	Y	Y	N	N
13	575	F/B	55	11.30	15.40	ASCVD	597	Schizoaffective disorder	F/W	46	10.10	15.1	Pneumonia	Y	Y	N	Y
14	278	M/W	50	4.50	20.40	ASCVD	640	Chronic paranoid schizophrenia	M/W	49	5.20	14.5	Pulmonary Embolism	Y	Y	N	U
15	1284	M/W	55	6.40	5.60	ASCVD	1105	Schizoaffective disorder	M/W	53	7.90	7.47	ASCVD	Y	N	N	Y
16	1122	M/W	55	15.40	7.30	Cardiac Tamponade	930	Disorganized schizophrenia; ADR; OAR	M/W	47	15.30	9.70	ASCVD	Y	N	Y	Y
17	250	F/W	47	5.30	19.70	ASCVD	398	Schizoaffective disorder	F/W	41	10.30	17.7	Pulmonary embolus	Y	N	Y	U
18	412	M/W	42	14.20	17.50	Aortic stenosis	422	Chronic paranoid schizophrenia	M/W	54	11.00	17.20	ASCVD	Y	N	Y	U
19	344	M/W	50	6.80	18.60	ASCVD	1296	Undifferentiated schizophrenia	M/W	48	7.80	5.42	Pneumonia	Y	Y	N	Y
20	1391	F/W	51	7.8	4	ASCVD	1189	Schizoaffective disorder; AAR	F/W	47	14.4	7	Suicide by combined drug overdose	Y	Y	Y	Y

APPENDIX C

CHAPTER 3 SUPPLEMENTAL MATERIALS

C.1 SUPPLEMENTAL RESULTS

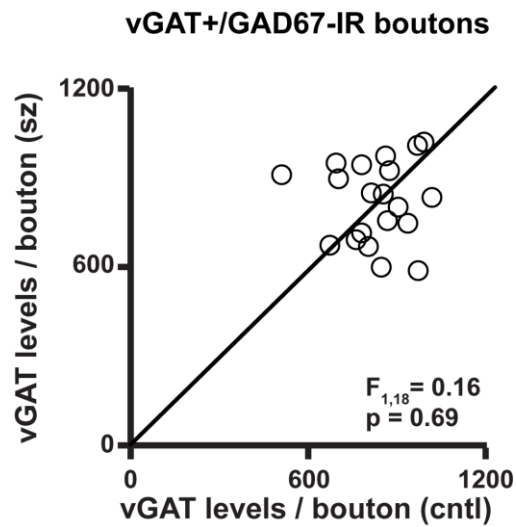


Figure C.1. vGAT+/GAD67-IR bouton vGAT protein levels. vGAT protein levels per bouton in total gray matter. The data points in each scatterplot represent a matched pair of schizophrenia (sz) and comparison (cntl) subject. Points below the unity line reflect pairs in which the measures are lower for the schizophrenia relative to the comparison subject.

APPENDIX D

CHAPTER 4 SUPPLEMENTAL MATERIALS

D.1 SUPPLEMENTAL RESULTS

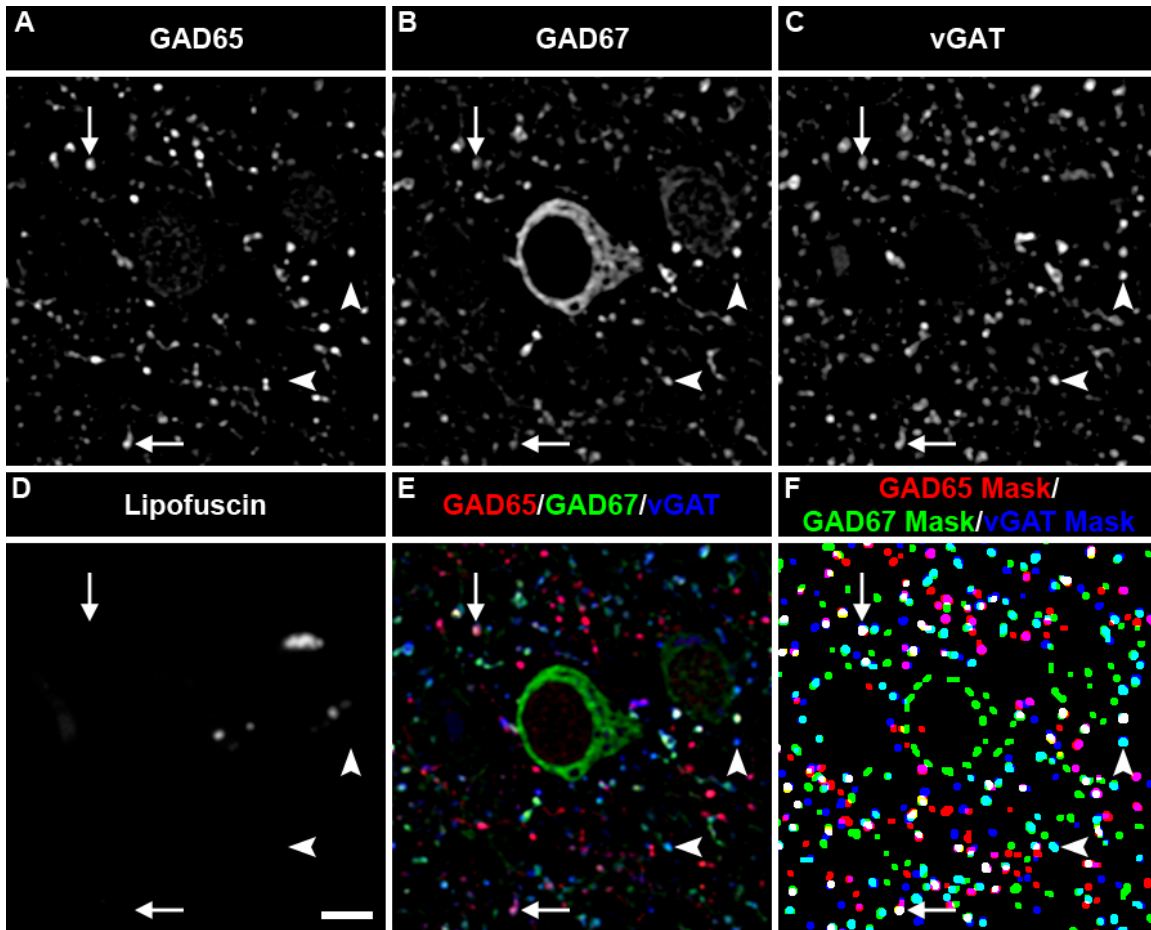


Figure D.1. Examples of vGAT+/GAD67+ and vGAT+/GAD65+/GAD67+ boutons. Projection image (3 z-planes taken 0.25 μm apart) of a human PFC tissue section immunolabeled for vGAT, GAD65, and GAD67. Single channel images of (A) GAD65, (B) GAD67, (C) vGAT, and (D) lipofuscin autofluorescence. (E) Merged image of A, B, and C. (F) Object masks corresponding to A, B, and C. Arrows indicate vGAT+/GAD67+ (arrowheads) and vGAT+/GAD65+/GAD67+ (arrows) boutons. Bar = 10 μm .

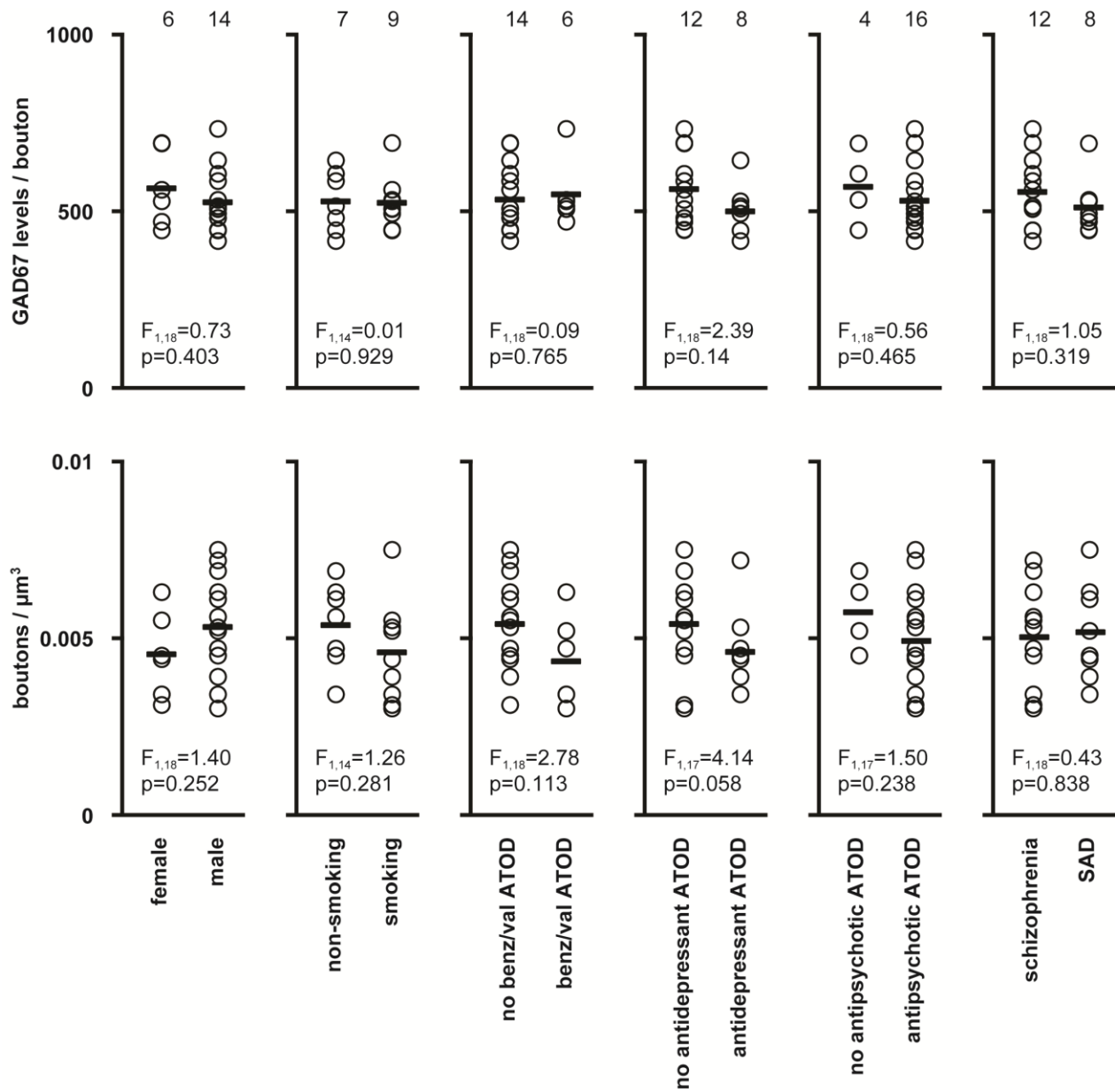


Figure D.2. Effects of potential comorbid factors on the density and levels of GAD67 from vGAT+/GAD67+ boutons in schizophrenia. The number of schizophrenia subjects in each comparison group is indicated at the top of each graph. Bolded values indicate significant differences between groups. ATOD, at time of death; benz/val; benzodiazepines/valproic acid; SAD, schizoaffective disorder.

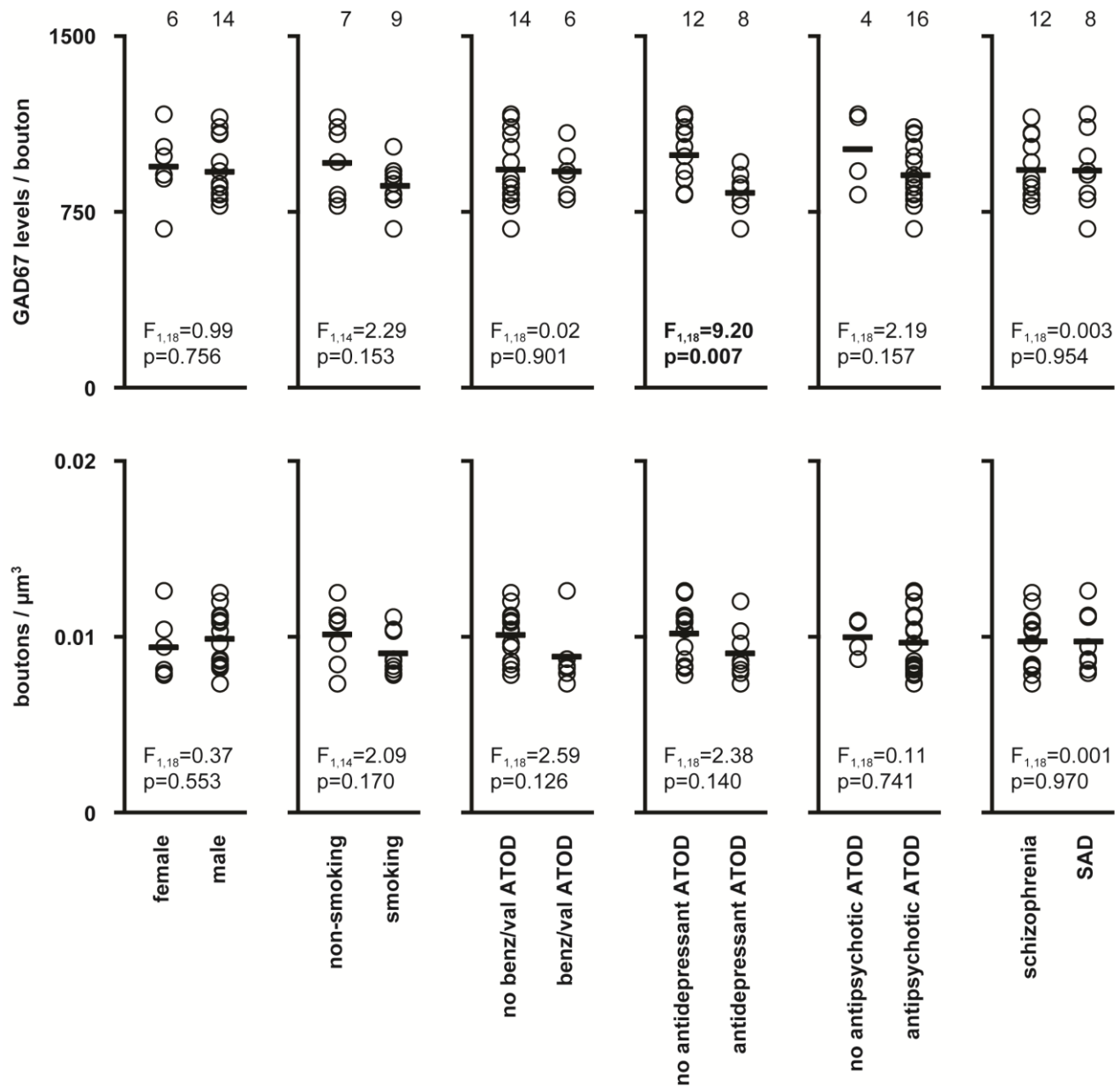


Figure D.3. Effects of potential comorbid factors on the density and levels of GAD67 from vGAT+/GAD65+/GAD67+ boutons in schizophrenia. The number of schizophrenia subjects in each comparison group is indicated at the top of each graph. Bolded values indicate significant differences between groups. ATOD, at time of death; benz/val; benzodiazepines/valproic acid; SAD, schizoaffective disorder.

APPENDIX E

CHAPTER 5 SUPPLEMENTAL MATERIALS

E.1 SUPPLEMENTAL RESULTS

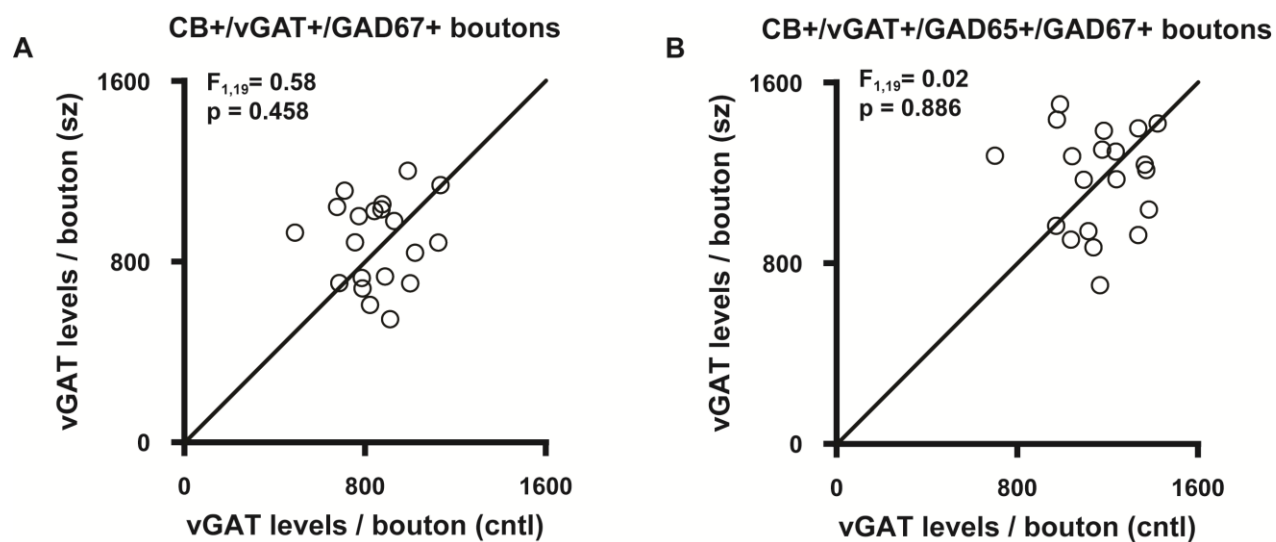


Figure E.1. CB+/vGAT+/GAD67+ and CB+/vGAT+/GAD65+/GAD67+ bouton vGAT protein levels between diagnostic groups. Mean vGAT protein levels in CB+/vGAT+/GAD67+ (A) and CB+/vGAT+/GAD65+/GAD67+ (B) boutons in total gray matter.

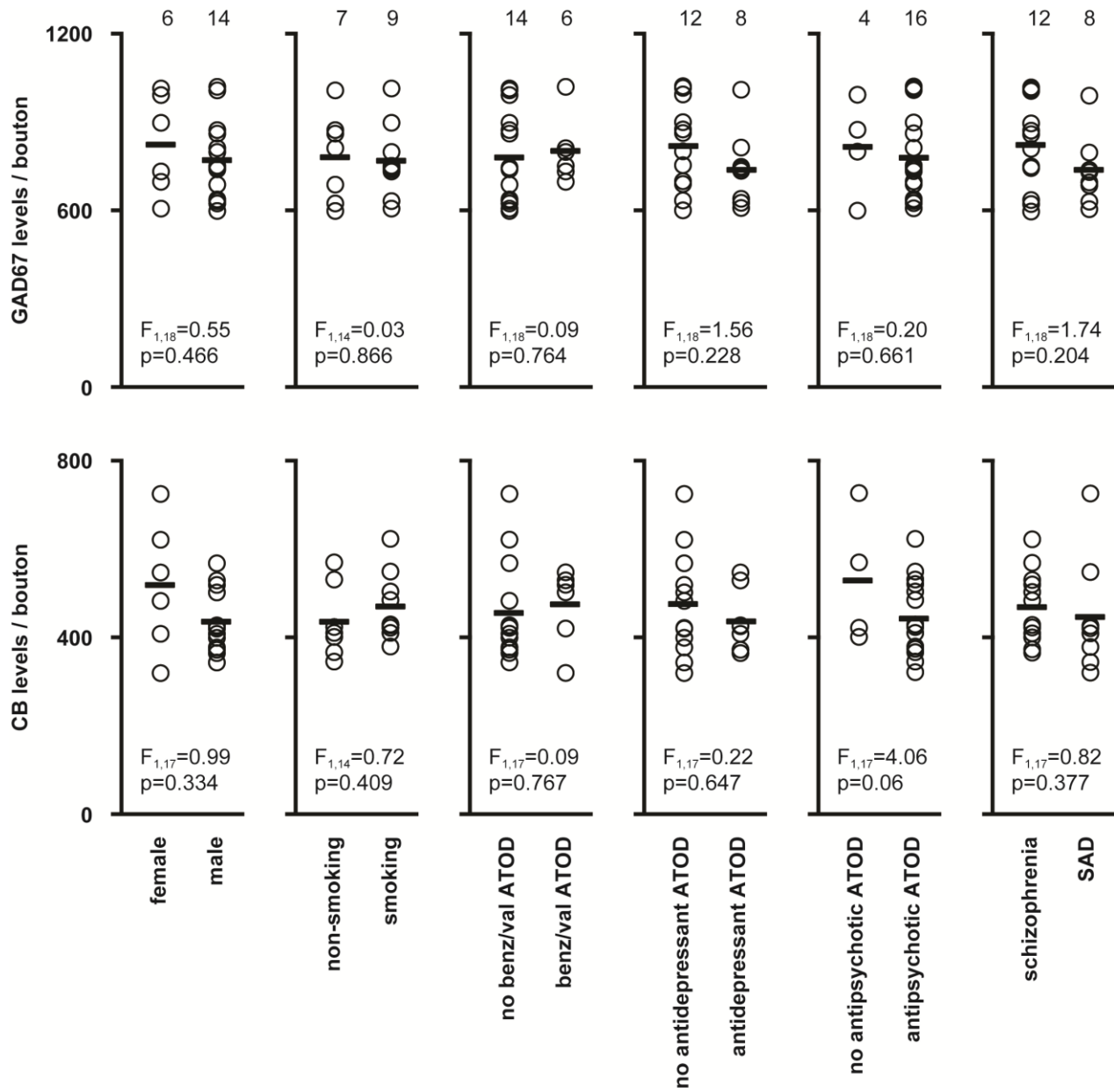


Figure E.2. Effects of potential comorbid factors on levels of GAD67 and CB from CB+/vGAT+/GAD67+ boutons in schizophrenia. The number of schizophrenia subjects in each comparison group is indicated at the top of each graph. Bolded values indicate significant differences between groups. ATOD, at time of death; benz/val; benzodiazepines/valproic acid; SAD, schizoaffective disorder.

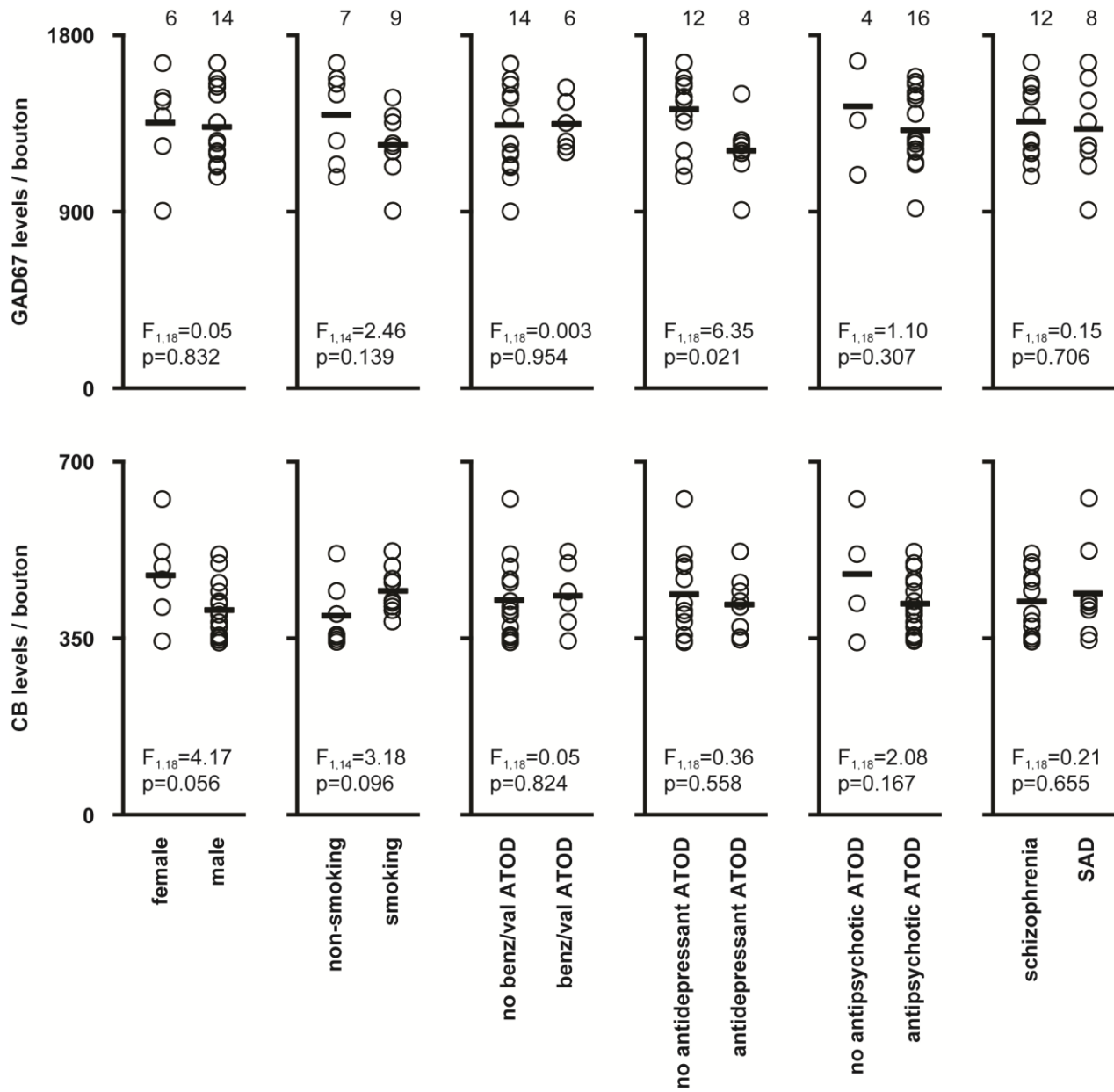


Figure E.3. Effects of potential comorbid factors on levels of GAD67 and CB from CB+/vGAT+/GAD65+/GAD67+ boutons in schizophrenia. The number of schizophrenia subjects in each comparison group is indicated at the top of each graph. Bolded values indicate significant differences between groups. ATOD, at time of death; benz/val; benzodiazepines/valproic acid; SAD, schizoaffective disorder.

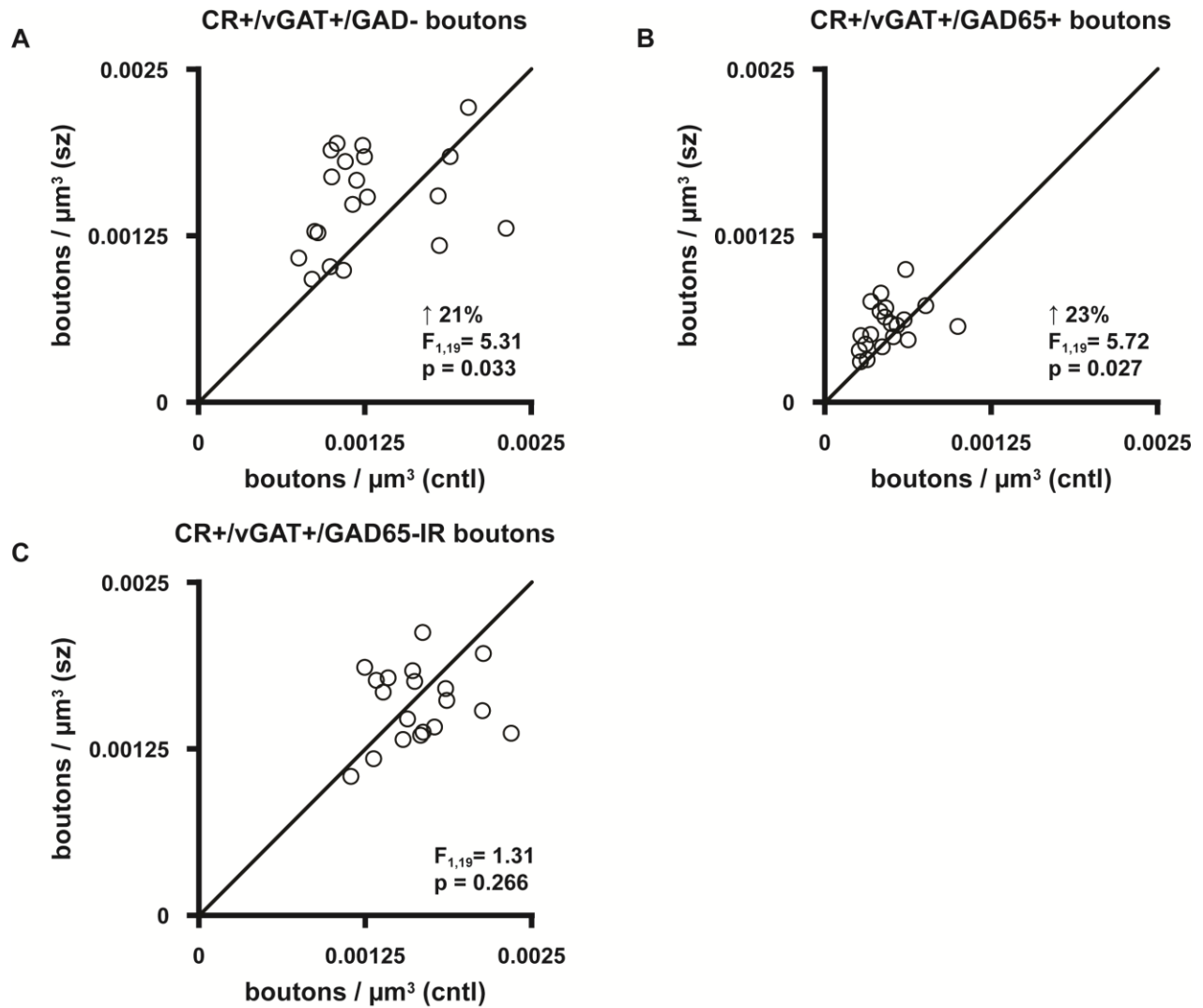


Figure E.4. CR+/vGAT+/GAD67-, CR+/vGAT+/GAD65+, and CR+/vGAT+/GAD65-IR bouton density between diagnostic groups. Mean density of CR+/vGAT+ boutons that lacked GAD65 and/or GAD67 immunoreactivity (CR+/vGAT+/GAD-; A), CR+/vGAT+/GAD65+ boutons (B), and all CR+/vGAT+ boutons that contained GAD65 immunoreactivity (i.e. CR+/vGAT+/GAD65+ and CR+/vGAT+/GAD65+/GAD67+ boutons; CR+/vGAT+/GAD65-IR; C) in total gray matter.

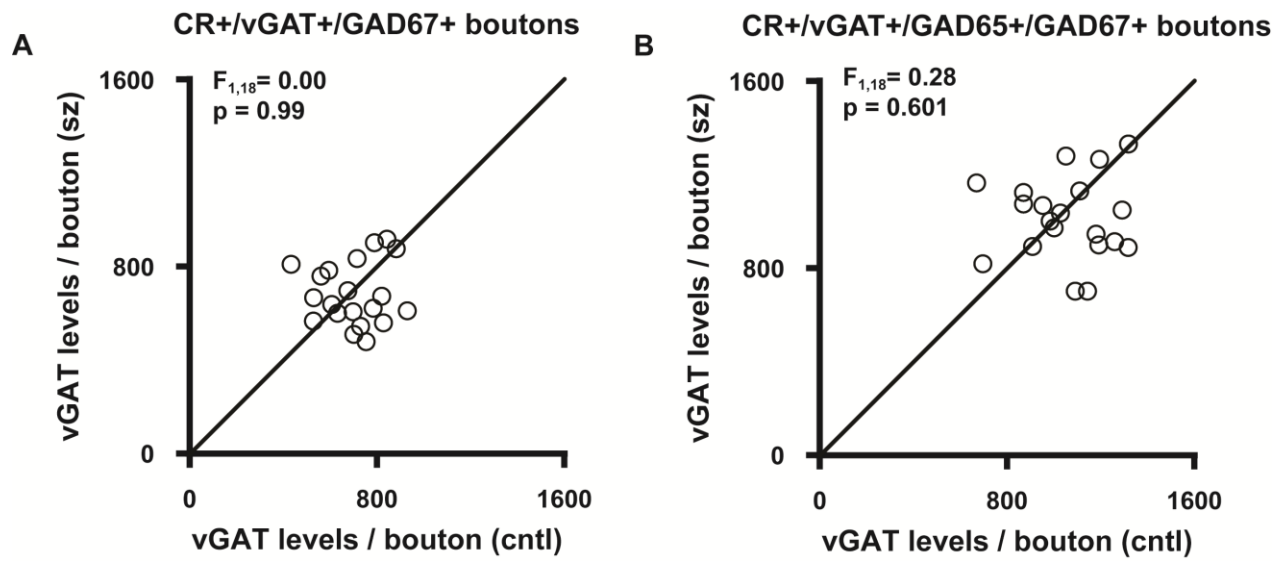


Figure E.5. CR+/vGAT+/GAD67+ and CR+/vGAT+/GAD65+/GAD67+ bouton vGAT protein levels between diagnostic groups. Mean vGAT protein levels in CR+/vGAT+/GAD67+ (A) and CR+/vGAT+/GAD65+/GAD67+ (B) boutons in total gray matter.

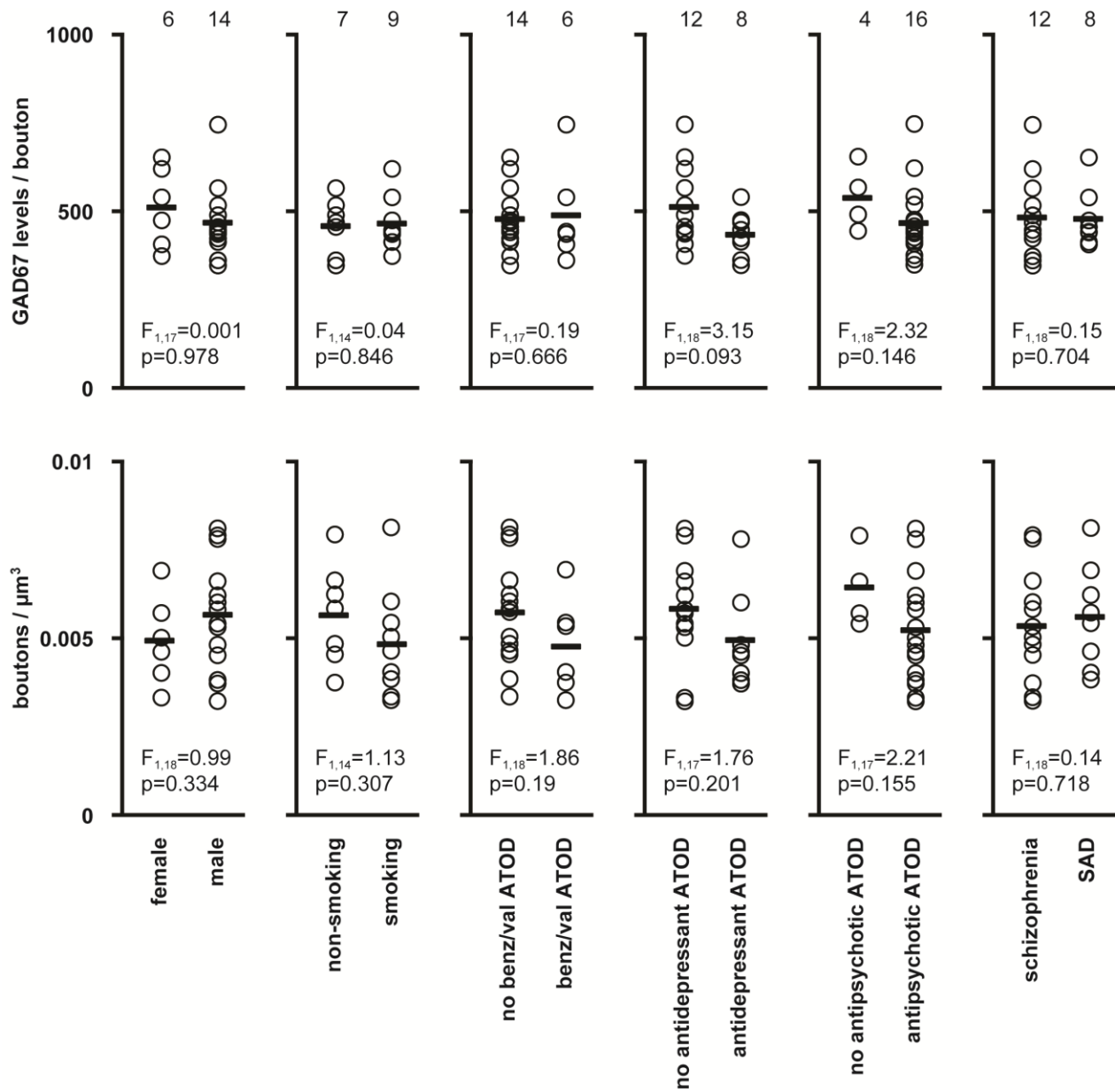


Figure E.6. Effects of potential comorbid factors on the density and levels of GAD67 from CR+/vGAT+/GAD67+ boutons in schizophrenia. The number of schizophrenia subjects in each comparison group is indicated at the top of each graph. Bolded values indicate significant differences between groups. ATOD, at time of death; benz/val; benzodiazepines/valproic acid; SAD, schizoaffective disorder.

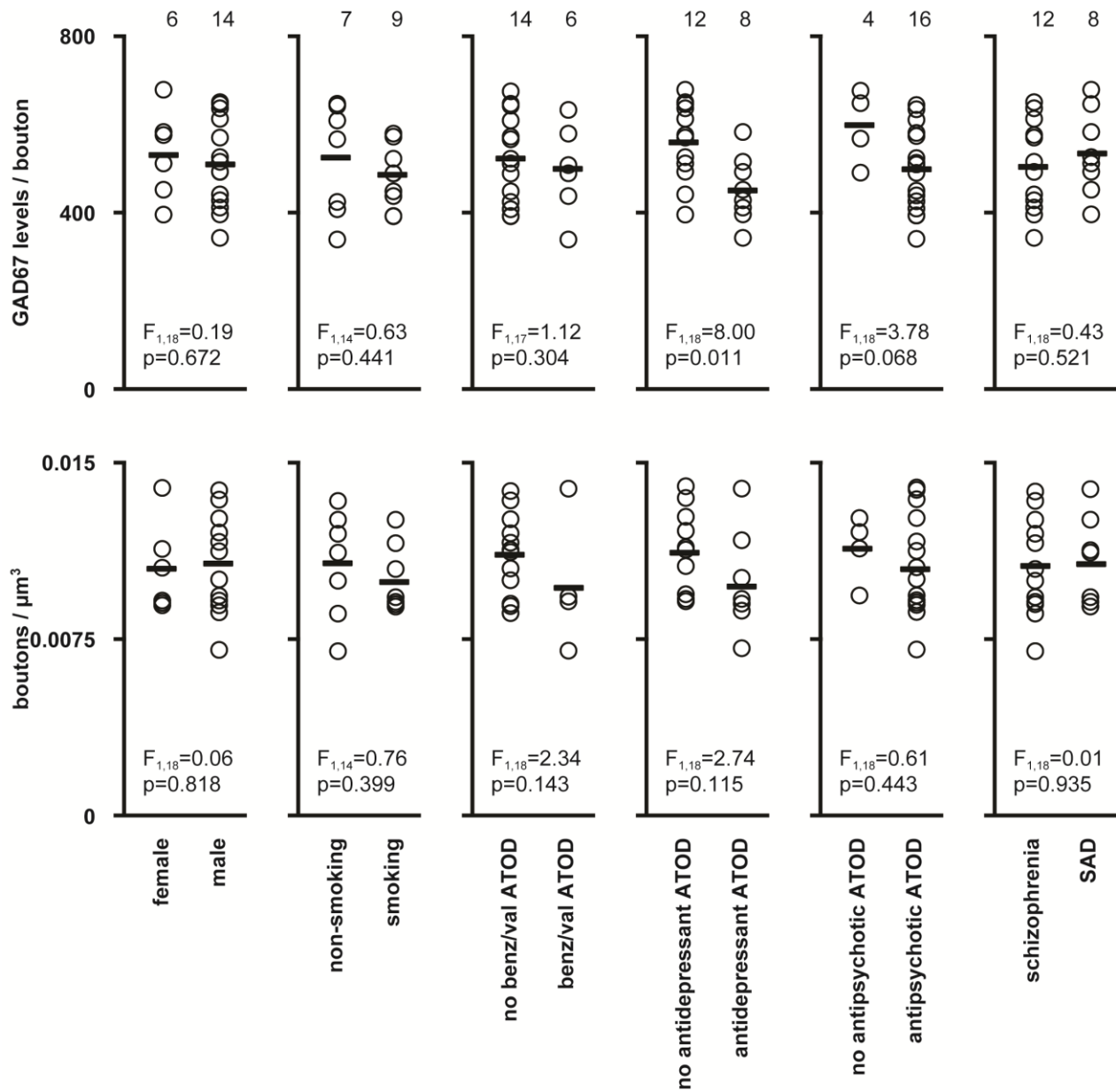


Figure E.7. Effects of potential comorbid factors on the density and levels of GAD67 from CR+/vGAT+/GAD65+/GAD67+ boutons in schizophrenia. The number of schizophrenia subjects in each comparison group is indicated at the top of each graph. Bolded values indicate significant differences between groups. ATOD, at time of death; benz/val; benzodiazepines/valproic acid; SAD, schizoaffective disorder.

APPENDIX F

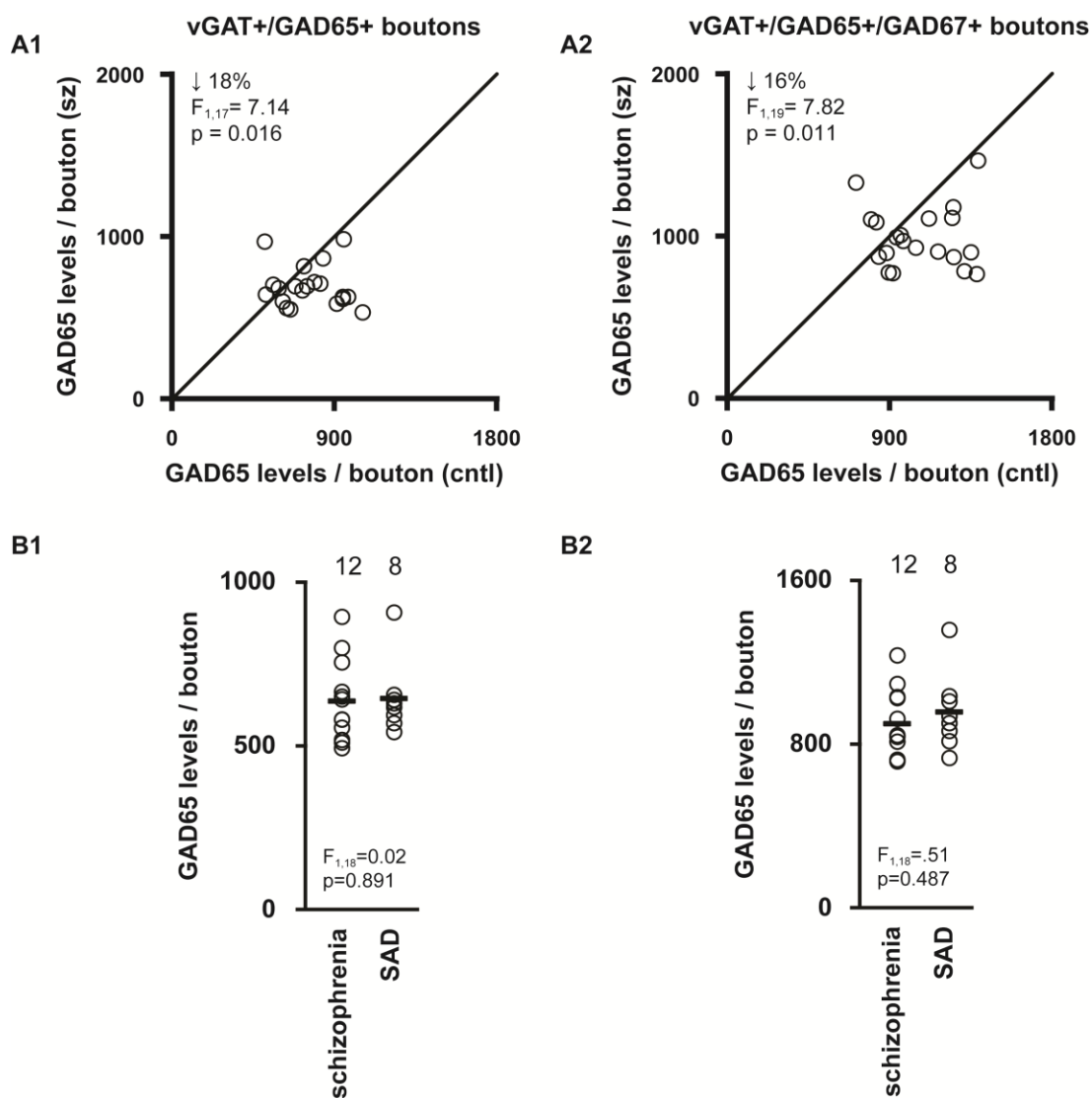


Figure F.1. vGAT+/GAD65+ and vGAT+/GAD65+/GAD67+ bouton GAD65 protein levels between diagnostic groups and effects of schizoaffective diagnosis. Mean GAD65 protein levels in vGAT+/GAD65+ (A1) and

vGAT+/GAD65+/GAD67+ (A2) boutons between schizophrenia (sz) and comparison (cntl) subjects in total gray matter. Mean GAD65 protein levels in vGAT+/GAD65+ (B1) and vGAT+/GAD65+/GAD67+ (B2) boutons between schizophrenia subjects and subjects diagnosed with schizoaffective disorder (SAD).

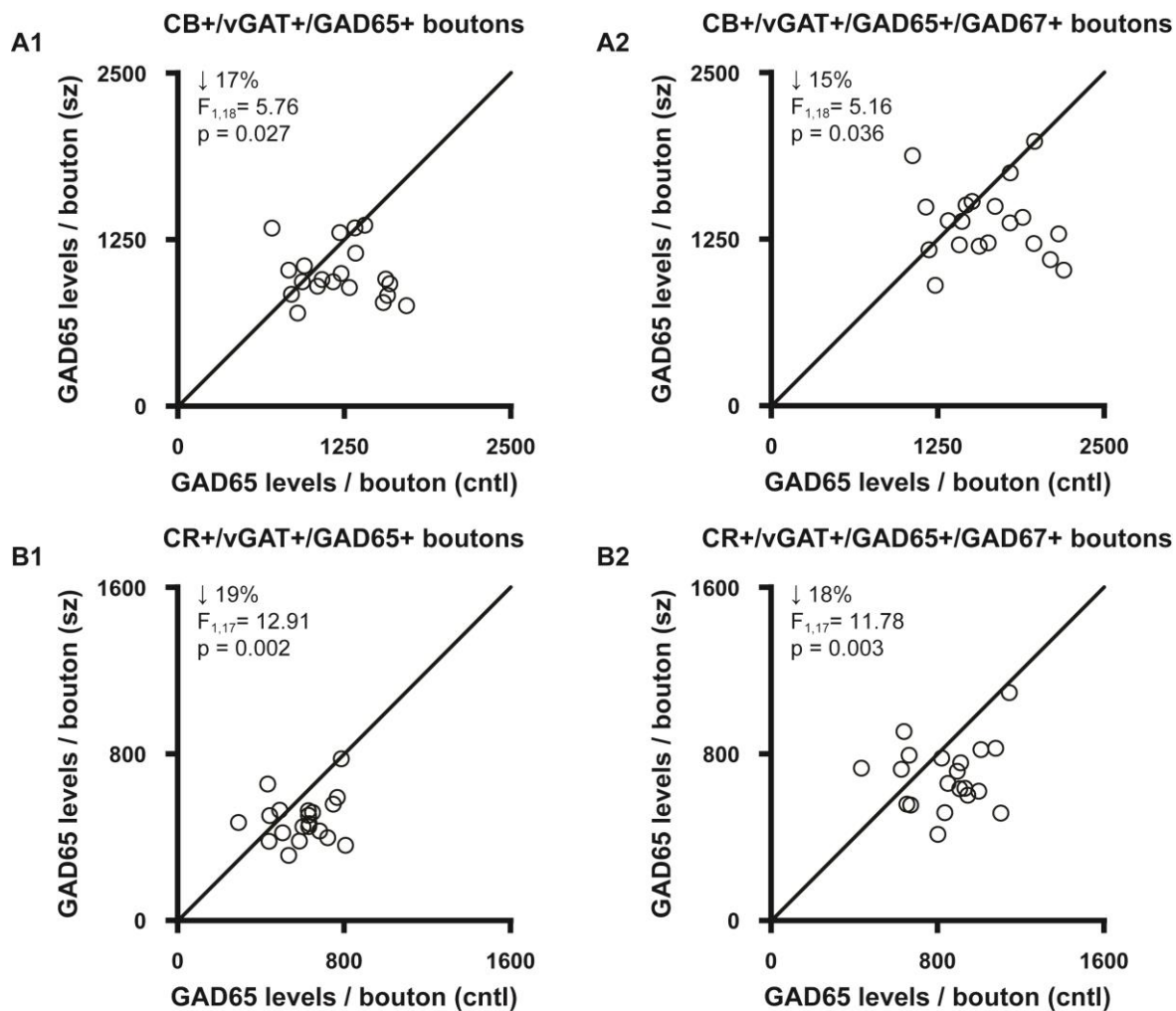


Figure F.2. CB bouton and CR bouton GAD65 protein levels between diagnostic groups. Mean GAD65 protein levels in vGAT+/GAD65+ boutons (A1 and B1) and vGAT+/GAD65+/GAD67+ boutons (A2 and B2) from CB neurons (A) and CR neurons (B) in total gray matter.

REFERENCES

- Addington, A. M., Gornick, M., Duckworth, J., Sporn, A., Gogtay, N., Bobb, A., Greenstein, D., Lenane, M., Gochman, P., Baker, N., Balkissoon, R., Vakkalanka, R. K., Weinberger, D. R., Rapoport, J. L., Straub, R. E. (2005). GAD1 (2q31.1), which encodes glutamic acid decarboxylase (GAD(67)), is associated with childhood-onset schizophrenia and cortical gray matter volume loss. *Molecular Psychiatry*, 10(6), 581-588.
- Ago, Y., Condro, M. C., Tan, Y. V., Ghiani, C. A., Colwell, C. S., Cushman, J. D., Fanselow, M. S., Hashimoto, H., Waschek, J. A. (2015). Reductions in synaptic proteins and selective alteration of prepulse inhibition in male C57BL/6 mice after postnatal administration of a VIP receptor (VIPR2) agonist. *Psychopharmacology (Berl)*.
- Ahmed, B., Anderson, J. C., Douglas, R. J., Martin, K. A. C., Nelson, J. C. (1994). Polyneuronal innervation of spiny stellate neurons in cat visual cortex. *The Journal of Comparative Neurology*, 341, 39-49.
- Akbarian, S., Kim, J. J., Potkin, S. G., Hagman, J. O., Tafazzoli, A., Bunney, W. E., Jr., Jones, E. G. (1995). Gene expression for glutamic acid decarboxylase is reduced without loss of neurons in prefrontal cortex of schizophrenics. *Arch Gen Psychiatry*, 52(4), 258-266.
- Ali, A. B., Thomson, A. M. (2008). Synaptic alpha 5 subunit-containing GABAA receptors mediate IPSPs elicited by dendrite-preferring cells in rat neocortex. *Cereb Cortex*, 18(6), 1260-1271.
- Allen, P., Amaro, E., Fu, C. H., Williams, S. C., Brammer, M. J., Johns, L. C., McGuire, P. K. (2007). Neural correlates of the misattribution of speech in schizophrenia. *The British journal of psychiatry : the journal of mental science*, 190, 162-169.
- Anderson, S. A., Classey, J. D., Conde, F., Lund, J. S., Lewis, D. A. (1995). Synchronous development of pyramidal neuron dendritic spines and parvalbumin-immunoreactive chandelier neuron axon terminals in layer III of monkey prefrontal cortex. *Neuroscience*, 67(1), 7-22.
- Asaad, W. F., Rainer, G., Miller, E. K. (1998). Neural activity in the primate prefrontal cortex during associative learning. *Neuron*, 21(6), 1399-1407.
- Auquier, P., Lancon, C., Rouillon, F., Lader, M. (2007). Mortality in schizophrenia. *Pharmacoepidemiology and drug safety*, 16(12), 1308-1312.

- Barbas, H., Rempel-Clower, N. (1997). Cortical structure predicts the pattern of corticocortical connections. *Cereb Cortex*, 7(7), 635-646.
- Battaglioli, G., Liu, H., Martin, D. L. (2003). Kinetic differences between the isoforms of glutamate decarboxylase: implications for the regulation of GABA synthesis. *J Neurochem*, 86(4), 879-887.
- Benes, F. M., Todtenkopf, M. S., Logiotatos, P., Williams, M. (2000). Glutamate decarboxylase(65)-immunoreactive terminals in cingulate and prefrontal cortices of schizophrenic and bipolar brain. *J Chem Neuroanat*, 20(3-4), 259-269.
- Beneyto, M., Abbott, A., Hashimoto, T., Lewis, D. A. (2011). Lamina-Specific Alterations in Cortical GABAA Receptor Subunit Expression in Schizophrenia. *Cereb Cortex*, 21(5), 999-1011.
- Beneyto, M., Sibille, E., Lewis, D. (2008). Human postmortem brain research in mental illness syndromes, in *Neurobiology of Mental Illness*. Edited by Charney DS, Nestler E. New York, Oxford University Press. 202-214.
- Berman, K. F., Zec, R. F., Weinberger, D. R. (1986). Physiological dysfunction of dorsolateral prefrontal cortex in schizophrenia. II. Role of neuroleptic treatment, attention and mental effort. *Archives of General Psychiatry*, 43, 126-135.
- Bharadwaj, R., Jiang, Y., Mao, W., Jakovcevski, M., Dincer, A., Krueger, W., Garbett, K., Whittle, C., Tushir, J. S., Liu, J., Sequeira, A., Vawter, M. P., Gardner, P. D., Casaccia, P., Rasmussen, T., Bunney, W. E., Jr., Mirnics, K., Futai, K., Akbarian, S. (2013). Conserved chromosome 2q31 conformations are associated with transcriptional regulation of GAD1 GABA synthesis enzyme and altered in prefrontal cortex of subjects with schizophrenia. *J Neurosci*, 33(29), 11839-11851.
- Bitanhirwe, B. K., Woo, T. U. (2014). Transcriptional dysregulation of gamma-aminobutyric acid transporter in parvalbumin-containing inhibitory neurons in the prefrontal cortex in schizophrenia. *Psychiatry Res*.
- Bleher, R., Kandela, I., Meyer, D. A., Albrecht, R. M. (2008). Immuno-EM using colloidal metal nanoparticles and electron spectroscopic imaging for co-localization at high spatial resolution. *J Microsc*, 230(Pt 3), 388-395.
- Bowie, C. R., Reichenberg, A., Patterson, T. L., Heaton, R. K., Harvey, P. D. (2006). Determinants of real-world functional performance in schizophrenia subjects: correlations with cognition, functional capacity, and symptoms. *Am J Psychiatry*, 163(3), 418-425.
- Braff, D. L., Swerdlow, N. R., Geyer, M. A. (1999). Symptom correlates of prepulse inhibition deficits in male schizophrenic patients. *Am J Psychiatry*, 156(4), 596-602.
- Braver, T. S., Cohen, J. D., Nystrom, L. E., Jonides, J., Smith, E. E., Noll, D. C. (1997). A parametric study of prefrontal cortex involvement in human working memory. *Neuroimage*, 5(1), 49-62.

- Broadbelt, K., Byne, W., Jones, L. B. (2002). Evidence for a decrease in basilar dendrites of pyramidal cells in schizophrenic medial prefrontal cortex. *Schizophrenia Research*, 58(1), 75-81.
- Brody, H. (1960). The deposition of aging pigment in the human cerebral cortex. *Journal of gerontology*, 15, 258-261.
- Byne, W., Buchsbaum, M. S., Kemether, E., Hazlett, E. A., Shinwari, A., Mitropoulou, V., Siever, L. J. (2001). Magnetic resonance imaging of the thalamic mediodorsal nucleus and pulvinar in schizophrenia and schizotypal personality disorder. *Arch Gen Psychiatry*, 58(2), 133-140.
- Byne, W., Buchsbaum, M. S., Mattiace, L. A., Hazlett, E. A., Kemether, E., Elhakem, S. L., Purohit, D. P., Haroutunian, V., Jones, L. (2002). Postmortem assessment of thalamic nuclear volumes in subjects with schizophrenia. *Am J Psychiatry*, 159(1), 59-65.
- Carder, R. K., Leclerc, S. S., Hendry, S. H. (1996). Regulation of calcium-binding protein immunoreactivity in GABA neurons of macaque primary visual cortex. *Cereb Cortex*, 6(2), 271-287.
- Cardin, J. A., Carlen, M., Meletis, K., Knoblich, U., Zhang, F., Deisseroth, K., Tsai, L. H., Moore, C. I. (2009). Driving fast-spiking cells induces gamma rhythm and controls sensory responses. *Nature*, 459(7247), 663-667.
- Carpenter, W. T., Koenig, J. I. (2008). The evolution of drug development in schizophrenia: past issues and future opportunities. *Neuropsychopharmacology*, 33(9), 2061-2079.
- Chattopadhyaya, B., Di Cristo, G., Wu, C. Z., Knott, G., Kuhlman, S., Fu, Y., Palmiter, R. D., Huang, Z. J. (2007). GAD67-mediated GABA synthesis and signaling regulate inhibitory synaptic innervation in the visual cortex. *Neuron*, 54(6), 889-903.
- Chaudhry, F. A., Reimer, R. J., Bellocchio, E. E., Danbolt, N. C., Osen, K. K., Edwards, R. H., Storm-Mathisen, J. (1998). The vesicular GABA transporter, VGAT, localizes to synaptic vesicles in sets of glycinergic as well as GABAergic neurons. *The Journal of Neuroscience*, 18, 9733-9750.
- Chertkow, Y., Weinreb, O., Youdim, M. B., Silver, H. (2006). The effect of chronic co-administration of fluvoxamine and haloperidol compared to clozapine on the GABA system in the rat frontal cortex. *Int J Neuropsychopharmacol*, 9(3), 287-296.
- Cho, R. Y., Konecky, R. O., Carter, C. S. (2006). Impairments in frontal cortical gamma synchrony and cognitive control in schizophrenia. *Proc.Natl.Acad.Sci U.S.A*, 103(52), 19878-19883.
- Cohen, J. D., Perlstein, W. M., Braver, T. S., Nystrom, L. E., Noll, D. C., Jonides, J., Smith, E. E. (1997). Temporal dynamics of brain activation during a working memory task. *Nature*, 386(6625), 604-608.

- Conde, F., Lund, J. S., Jacobowitz, D. M., Baimbridge, K. G., Lewis, D. A. (1994). Local circuit neurons immunoreactive for calretinin, calbindin D-28k or parvalbumin in monkey prefrontal cortex: distribution and morphology. *J Comp Neurol*, 341(1), 95-116.
- Constantinidis, C., Williams, G. V., Goldman-Rakic, P. S. (2002). A role for inhibition in shaping the temporal flow of information in prefrontal cortex. *Nature Neuroscience*, 5, 175-180.
- Cruz, D. A., Eggan, S. M., Lewis, D. A. (2003). Postnatal development of pre- and postsynaptic GABA markers at chandelier cell connections with pyramidal neurons in monkey prefrontal cortex. *J Comp Neurol*, 465(3), 385-400.
- Curley, A. A., Arion, D., Volk, D. W., Asafu-Adjei, J. K., Sampson, A. R., Fish, K. N., Lewis, D. A. (2011). Cortical deficits of glutamic acid decarboxylase 67 expression in schizophrenia: clinical, protein, and cell type-specific features. *Am J Psychiatry*, 168(9), 921-929.
- DeFelipe, J., del Carmen Gonzalez-Albo, M. (1998). Chandelier cell axons are immunoreactive for GAT-1 in the human neocortex. *NeuroReport*, 9, 467-470.
- DeFelipe, J., Hendry, S. H., Jones, E. G. (1989). Visualization of chandelier cell axons by parvalbumin immunoreactivity in monkey cerebral cortex. *Proc Natl Acad Sci U S A*, 86(6), 2093-2097.
- DeFelipe, J., Hendry, S. H. C., Jones, E. G. (1989). Synapses of double bouquet cells in monkey cerebral cortex visualized by calbindin immunoreactivity. *Brain Res*, 503, 49-54.
- del Rio, M. R., DeFelipe, J. (1996). Colocalization of calbindin D-28k, calretinin, and GABA immunoreactivities in neurons of the human temporal cortex. *The Journal of Comparative Neurology*, 369, 472-482.
- Dickson, H., Laurens, K. R., Cullen, A. E., Hodgins, S. (2012). Meta-analyses of cognitive and motor function in youth aged 16 years and younger who subsequently develop schizophrenia. *Psychol Med*, 42(4), 743-755.
- Dold, M., Leucht, S. (2014). Pharmacotherapy of treatment-resistant schizophrenia: a clinical perspective. *Evidence-based mental health*, 17(2), 33-37.
- Donato, F., Rompani, S. B., Caroni, P. (2013). Parvalbumin-expressing basket-cell network plasticity induced by experience regulates adult learning. *Nature*, 504(7479), 272-276.
- Duncan, C. E., Webster, M. J., Rothmond, D. A., Bahn, S., Elashoff, M., Shannon Weickert, C. (2010). Prefrontal GABA(A) receptor alpha-subunit expression in normal postnatal human development and schizophrenia. *J Psychiatr Res*, 44(10), 673-681.
- Erickson, S. L., Lewis, D. A. (2004). Cortical connections of the lateral mediodorsal thalamus in cynomolgus monkeys. *J Comp Neurol*, 473(1), 107-127.

- Erlander, M. G., Tillakaratne, N. J., Feldblum, S., Patel, N., Tobin, A. J. (1991). Two genes encode distinct glutamate decarboxylases. *Neuron*, 7(1), 91-100.
- Felleman, D. J., Van Essen, D. C. (1991). Distributed hierarchical processing in the primate cerebral cortex. *Cereb Cortex*, 1(1), 1-47.
- Fish, K. N., Hoftman, G. D., Sheikh, W., Kitchens, M., Lewis, D. A. (2013). Parvalbumin-containing chandelier and basket cell boutons have distinctive modes of maturation in monkey prefrontal cortex. *J Neurosci*, 33(19), 8352-8358.
- Fish, K. N., Sweet, R. A., Deo, A. J., Lewis, D. A. (2008). An automated segmentation methodology for quantifying immunoreactive puncta number and fluorescence intensity in tissue sections. *Brain Res*, 1240, 62-72.
- Fish, K. N., Sweet, R. A., Lewis, D. A. (2011). Differential distribution of proteins regulating GABA synthesis and reuptake in axon boutons of subpopulations of cortical interneurons. *Cereb Cortex*, 21(11), 2450-2460.
- Freund, T. F., Busz̄ki, G., Leon, A., Baimbridge, K. G., Somogyi, P. (1990). Relationship of neuronal vulnerability and calcium binding protein immunoreactivity in ischemia. *Experimental Brain Research*, 83, 55-66.
- Fries, P. (2009). Neuronal gamma-band synchronization as a fundamental process in cortical computation. *Annu Rev Neurosci*, 32, 209-224.
- Fu, Y., Tucciarone, J. M., Espinosa, J. S., Sheng, N., Darcy, D. P., Nicoll, R. A., Huang, Z. J., Stryker, M. P. (2014). A cortical circuit for gain control by behavioral state. *Cell*, 156(6), 1139-1152.
- Fuchs, E. C., Zivkovic, A. R., Cunningham, M. O., Middleton, S., LeBeau, F. E., Bannerman, D. M., Rozov, A., Whittington, M. A., Traub, R. D., Rawlins, J. N., Monyer, H. (2007). Recruitment of parvalbumin-positive interneurons determines hippocampal function and associated behavior. *Neuron*, 53(4), 591-604.
- Fuller, R., Nopoulos, P., Arndt, S., O'Leary, D., Ho, B. C., Andreasen, N. C. (2002). Longitudinal assessment of premorbid cognitive functioning in patients with schizophrenia through examination of standardized scholastic test performance. *Am J Psychiatry*, 159(7), 1183-1189.
- Fung, S. J., Sivagnanasundaram, S., Weickert, C. S. (2011). Lack of change in markers of presynaptic terminal abundance alongside subtle reductions in markers of presynaptic terminal plasticity in prefrontal cortex of schizophrenia patients. *Biol Psychiatry*, 69(1), 71-79.
- Fung, S. J., Webster, M. J., Sivagnanasundaram, S., Duncan, C., Elashoff, M., Weickert, C. S. (2010). Expression of interneuron markers in the dorsolateral prefrontal cortex of the developing human and in schizophrenia. *Am J Psychiatry*, 167(12), 1479-1488.

- Fung, S. J., Webster, M. J., Weickert, C. S. (2011). Expression of VGluT1 and VGAT mRNAs in human dorsolateral prefrontal cortex during development and in schizophrenia. *Brain Res*, 1388, 22-31.
- Gabbott, P. L., Bacon, S. J. (1996). Local circuit neurons in the medial prefrontal cortex (areas 24a,b,c, 25 and 32) in the monkey: II. Quantitative areal and laminar distributions. *J Comp Neurol*, 364(4), 609-636.
- Gabbott, P. L., Bacon, S. J. (1997). Vasoactive intestinal polypeptide containing neurones in monkey medial prefrontal cortex (mPFC): colocalisation with calretinin. *Brain Res*, 744(1), 179-184.
- Gabriel, S. M., Davidson, M., Haroutunian, V., Powchik, P., Bierer, L. M., Purohit, D. P., Perl, D. P., Davis, K. L. (1996). Neuropeptide deficits in schizophrenia vs. Alzheimer's disease cerebral cortex. *Biological Psychiatry*, 39(2), 82-91.
- Garey, L. J., Ong, W. Y., Patel, T. S., Kanani, M., Davis, A., Mortimer, A. M., Barnes, T. R., Hirsch, S. R. (1998). Reduced dendritic spine density on cerebral cortical pyramidal neurons in schizophrenia. *J Neurol Neurosurg Psychiatry*, 65(4), 446-453.
- Gentet, L. J., Kremer, Y., Taniguchi, H., Huang, Z. J., Staiger, J. F., Petersen, C. C. (2012). Unique functional properties of somatostatin-expressing GABAergic neurons in mouse barrel cortex. *Nat Neurosci*, 15(4), 607-612.
- Gibbons, J. S., Horn, S. H., Powell, J. M., Gibbons, J. L. (1984). Schizophrenic patients and their families. A survey in a psychiatric service based on a DGH unit. *The British journal of psychiatry : the journal of mental science*, 144, 70-77.
- Giguere, M., Goldman-Rakic, P. S. (1988). Mediodorsal nucleus: areal, laminar, and tangential distribution of afferents and efferents in the frontal lobe of rhesus monkeys. *J Comp Neurol*, 277(2), 195-213.
- Gilbert, A. R., Rosenberg, D. R., Harenski, K., Spencer, S., Sweeney, J. A., Keshavan, M. S. (2001). Thalamic volumes in patients with first-episode schizophrenia. *American Journal of Psychiatry*, 158, 618-624.
- Gilbert, C. D., Kelly, J. P. (1975). The projections of cells in different layers of the cat's visual cortex. *The Journal of Comparative Neurology*, 63, 81-106.
- Glahn, D. C., Ragland, J. D., Abramoff, A., Barrett, J., Laird, A. R., Bearden, C. E., Velligan, D. I. (2005). Beyond hypofrontality: a quantitative meta-analysis of functional neuroimaging studies of working memory in schizophrenia. *Hum Brain Mapp*, 25(1), 60-69.
- Glantz, L. A., Lewis, D. A. (1997). Reduction of synaptophysin immunoreactivity in the prefrontal cortex of subjects with schizophrenia. Regional and diagnostic specificity. *Arch Gen Psychiatry*, 54(10), 943-952.

- Glantz, L. A., Lewis, D. A. (2000). Decreased dendritic spine density on prefrontal cortical pyramidal neurons in schizophrenia. *Arch Gen Psychiatry*, 57(1), 65-73.
- Glausier, J. R., Fish, K. N., Lewis, D. A. (2014). Altered parvalbumin basket cell inputs in the dorsolateral prefrontal cortex of schizophrenia subjects. *Mol Psychiatry*, 19(1), 30-36.
- Glausier, J. R., Fish, K. N., Lewis, D. A. (2014). Altered parvalbumin basket cell inputs in the dorsolateral prefrontal cortex of schizophrenia subjects. *Mol Psychiatry*, 19(1), 140.
- Glausier, J. R., Kimoto, S., Fish, K. N., Lewis, D. A. (2015). Lower Glutamic Acid Decarboxylase 65-kDa Isoform Messenger RNA and Protein Levels in the Prefrontal Cortex in Schizoaffective Disorder but Not Schizophrenia. *Biol Psychiatry*, 77(2), 167-176.
- Glausier, J. R., Lewis, D. A. (2011). Selective pyramidal cell reduction of GABA(A) receptor alpha1 subunit messenger RNA expression in schizophrenia. *Neuropsychopharmacology*, 36(10), 2103-2110.
- Glausier, J. R., Lewis, D. A. (2013). Dendritic spine pathology in schizophrenia. *Neuroscience*, 251, 90-107.
- Glickfeld, L. L., Roberts, J. D., Somogyi, P., Scanziani, M. (2009). Interneurons hyperpolarize pyramidal cells along their entire somatodendritic axis. *Nat Neurosci*, 12(1), 21-23.
- Goldman-Rakic, P. S. (1995). Cellular basis of working memory. *Neuron*, 14(3), 477-485.
- Goldman-Rakic, P. S. (1995). Cellular basis of working memory. *Neuron*, 14, 477-485.
- Goldman-Rakic, P. S., Porrino, L. J. (1985). The primate mediodorsal (MD) nucleus and its projection to the frontal lobe. *J Comp Neurol*, 242(4), 535-560.
- Gonchar, Y., Burkhalter, A. (1997). Three distinct families of GABAergic neurons in rat visual cortex. *Cereb Cortex*, 7(4), 347-358.
- Gonchar, Y., Burkhalter, A. (2003). Distinct GABAergic targets of feedforward and feedback connections between lower and higher areas of rat visual cortex. *J Neurosci*, 23(34), 10904-10912.
- Gonzalez-Albo, M. C., Elston, G. N., DeFelipe, J. (2001). The human temporal cortex: characterization of neurons expressing nitric oxide synthase, neuropeptides and calcium-binding proteins, and their glutamate receptor subunit profiles. *Cereb Cortex*, 11(12), 1170-1181.
- Green, M. F. (2006). Cognitive impairment and functional outcome in schizophrenia and bipolar disorder. *J Clin Psychiatry*, 67(10), e12.
- Green, M. F., Nuechterlein, K. H., Gold, J. M., Barch, D. M., Cohen, J., Essock, S., Fenton, W. S., Frese, F., Goldberg, T. E., Heaton, R. K., Keefe, R. S., Kern, R. S., Kraemer, H.,

- Stover, E., Weinberger, D. R., Zalcman, S., Marder, S. R. (2004). Approaching a consensus cognitive battery for clinical trials in schizophrenia: the NIMH-MATRICES conference to select cognitive domains and test criteria. *Biol Psychiatry*, 56(5), 301-307.
- Guidotti, A., Auta, J., Davis, J. M., Di-Giorgi-Gerevini, V., Dwivedi, Y., Grayson, D. R., Impagnatiello, F., Pandey, G., Pesold, C., Sharma, R., Uzunov, D., Costa, E. (2000). Decrease in reelin and glutamic acid decarboxylase67 (GAD67) expression in schizophrenia and bipolar disorder: a postmortem brain study. *Arch Gen Psychiatry*, 57(11), 1061-1069.
- Guillozet-Bongaarts, A. L., Hyde, T. M., Dalley, R. A., Hawrylycz, M. J., Henry, A., Hof, P. R., Hohmann, J., Jones, A. R., Kuan, C. L., Royall, J., Shen, E., Swanson, B., Zeng, H., Kleinman, J. E. (2014). Altered gene expression in the dorsolateral prefrontal cortex of individuals with schizophrenia. *Mol Psychiatry*, 19(4), 478-485.
- Guo, C., Stella, S. L., Jr., Hirano, A. A., Brecha, N. C. (2009). Plasmalemmal and vesicular gamma-aminobutyric acid transporter expression in the developing mouse retina. *J Comp Neurol*, 512(1), 6-26.
- Hartman, K. N., Pal, S. K., Burrone, J., Murthy, V. N. (2006). Activity-dependent regulation of inhibitory synaptic transmission in hippocampal neurons. *Nat Neurosci*, 9(5), 642-649.
- Hashimoto, T., Arion, D., Unger, T., Maldonado-Aviles, J. G., Morris, H. M., Volk, D. W., Mirnics, K., Lewis, D. A. (2008). Alterations in GABA-related transcriptome in the dorsolateral prefrontal cortex of subjects with schizophrenia. *Mol Psychiatry*, 13(2), 147-161.
- Hashimoto, T., Bazmi, H. H., Mirnics, K., Wu, Q., Sampson, A. R., Lewis, D. A. (2008). Conserved regional patterns of GABA-related transcript expression in the neocortex of subjects with schizophrenia. *Am J Psychiatry*, 165(4), 479-489.
- Hashimoto, T., Volk, D. W., Eggen, S. M., Mirnics, K., Pierri, J. N., Sun, Z., Sampson, A. R., Lewis, D. A. (2003). Gene expression deficits in a subclass of GABA neurons in the prefrontal cortex of subjects with schizophrenia. *J Neurosci*, 23(15), 6315-6326.
- Hayes, T. L., Cameron, J. L., Fernstrom, J. D., Lewis, D. A. (1991). A comparative analysis of the distribution of prosomatostatin-derived peptides in human and monkey neocortex. *J Comp Neurol*, 303(4), 584-599.
- Hayes, T. L., Lewis, D. A. (1992). Nonphosphorylated neurofilament protein and calbindin immunoreactivity in layer III pyramidal neurons of human neocortex. *Cereb Cortex*, 2(1), 56-67.
- Hayes, T. L., Lewis, D. A. (1993). Hemispheric differences in layer III pyramidal neurons of the anterior language areas. *Archives of Neurology*, 50, 501-505.

- Hedman, A. M., van Haren, N. E., van Baal, C. G., Kahn, R. S., Hulshoff Pol, H. E. (2013). IQ change over time in schizophrenia and healthy individuals: a meta-analysis. *Schizophr Res*, 146(1-3), 201-208.
- Hendrickson, A. E., Tillakaratne, N. J., Mehra, R. D., Esclapez, M., Erickson, A., Vician, L., Tobin, A. J. (1994). Differential localization of two glutamic acid decarboxylases (GAD65 and GAD67) in adult monkey visual cortex. *J Comp Neurol*, 343(4), 566-581.
- Hendry, S. H. C., Schwark, H. D., Jones, E. G., Yan, J. (1987). Numbers and proportions of GABA-immunoreactive neurons in different areas of monkey cerebral cortex. *The Journal of Neuroscience*, 7, 1503-1519.
- Hill, J. J., Hashimoto, T., Lewis, D. A. (2006). Molecular mechanisms contributing to dendritic spine alterations in the prefrontal cortex of subjects with schizophrenia. *Mol Psychiatry*, 11(6), 557-566.
- Hof, P. R., Morrison, J. H. (1991). Neocortical neuronal subpopulations labeled by a monoclonal antibody to calbindin exhibit differential vulnerability in Alzheimer's disease. *Exp Neurol*, 111(3), 293-301.
- Hoftman, G. D., Volk, D. W., Bazmi, H. H., Li, S., Sampson, A. R., Lewis, D. A. (2013). Altered Cortical Expression of GABA-Related Genes in Schizophrenia: Illness Progression vs Developmental Disturbance. *Schizophr Bull*.
- Hoftman, G. D., Volk, D. W., Bazmi, H. H., Li, S., Sampson, A. R., Lewis, D. A. (2015). Altered cortical expression of GABA-related genes in schizophrenia: illness progression vs developmental disturbance. *Schizophr Bull*, 41(1), 180-191.
- Holcomb, H. H., Ritzl, E. K., Medoff, D. R., Nevitt, J., Gordon, B., Tamminga, C. A. (1995). Tone discrimination performance in schizophrenic patients and normal volunteers: impact of stimulus presentation levels and frequency differences. *Psychiatry Res*, 57(1), 75-82.
- Howard, M. W., Rizzuto, D. S., Caplan, J. B., Madsen, J. R., Lisman, J., Aschenbrenner-Scheibe, R., Schulze-Bonhage, A., Kahana, M. J. (2003). Gamma oscillations correlate with working memory load in humans. *Cereb Cortex*, 13(12), 1369-1374.
- Huang, H. S., Matevossian, A., Whittle, C., Kim, S. Y., Schumacher, A., Baker, S. P., Akbarian, S. (2007). Prefrontal dysfunction in schizophrenia involves mixed-lineage leukemia 1-regulated histone methylation at GABAergic gene promoters. *J Neurosci*, 27(42), 11254-11262.
- Huang, Z. J. (2009). Activity-dependent development of inhibitory synapses and innervation pattern: role of GABA signalling and beyond. *J Physiol*, 587(Pt 9), 1881-1888.
- Hyde, T. M., Lipska, B. K., Ali, T., Mathew, S. V., Law, A. J., Metitiri, O. E., Straub, R. E., Ye, T., Colantuoni, C., Herman, M. M., Bigelow, L. B., Weinberger, D. R., Kleinman, J. E. (2011). Expression of GABA signaling molecules KCC2, NKCC1, and GAD1 in cortical development and schizophrenia. *J Neurosci*, 31(30), 11088-11095.

- Ide, M., Lewis, D. A. (2010). Altered cortical CDC42 signaling pathways in schizophrenia: implications for dendritic spine deficits. *Biol Psychiatry*, 68(1), 25-32.
- Ikuta, T., Szeszko, P. R., Gruner, P., DeRosse, P., Gallego, J., Malhotra, A. K. (2012). Abnormal anterior cingulate cortex activity predicts functional disability in schizophrenia. *Schizophr Res*, 137(1-3), 267-268.
- Impagnatiello, F., Guidotti, A. R., Pesold, C., Dwivedi, Y., Caruncho, H., Pisu, M. G., Uzunov, D. P., Smalheiser, N. R., Davis, J. M., Pandey, G. N., Pappas, G. D., Tueting, P., Sharma, R. P., Costa, E. (1998). A decrease of reelin expression as a putative vulnerability factor in schizophrenia. *Proc Natl Acad Sci U S A*, 95(26), 15718-15723.
- Insel, T. R., Scolnick, E. M. (2006). Cure therapeutics and strategic prevention: raising the bar for mental health research. *Molecular Psychiatry*, 11(1), 11-17.
- Ishikawa, M., Mizukami, K., Iwakiri, M., Asada, T. (2005). Immunohistochemical and immunoblot analysis of gamma-aminobutyric acid B receptor in the prefrontal cortex of subjects with schizophrenia and bipolar disorder. *Neurosci Lett*, 383(3), 272-277.
- Jacobs, B., Driscoll, L., Schall, M. (1997). Life-span dendritic and spine changes in areas 10 and 18 of human cortex: A quantitative Golgi study. *The Journal of Comparative Neurology*, 386, 661-680.
- Javitt, D. C. (2000). Intracortical mechanisms of mismatch negativity dysfunction in schizophrenia. *Audiology & neuro-otology*, 5(3-4), 207-215.
- Jiao, Y., Sun, Z., Lee, T., Fusco, F. R., Kimble, T. D., Meade, C. A., Cuthbertson, S., Reiner, A. (1999). A simple and sensitive antigen retrieval method for free-floating and slide-mounted tissue sections. *J Neurosci Methods*, 93(2), 149-162.
- Jones, E. G., Hendry, S. H. C. (1989). Differential calcium binding protein immunoreactivity distinguishes classes of relay neurons in monkey thalamic nuclei. *European Journal of Neuroscience*, 1, 222-246.
- Jones, L. B., Johnson, N., Byne, W. (2002). Alterations in MAP2 immunocytochemistry in areas 9 and 32 of schizophrenic prefrontal cortex. *Psychiatry Res*, 114(3), 137-148.
- Kahn, R. S., Keefe, R. S. (2013). Schizophrenia is a cognitive illness: time for a change in focus. *JAMA psychiatry*, 70(10), 1107-1112.
- Kalus, P., MÅller, T. J., Zuschratter, W., Senitz, D. (2000). The dendritic architecture of prefrontal pyramidal neurons in schizophrenic patients. *NeuroReport*, 11, 3621-3625.
- Kapfer, C., Glickfeld, L. L., Atallah, B. V., Scanziani, M. (2007). Supralinear increase of recurrent inhibition during sparse activity in the somatosensory cortex. *Nat Neurosci*, 10(6), 743-753.

- Kato, H. K., Gillet, S. N., Peters, A. J., Isaacson, J. S., Komiyama, T. (2013). Parvalbumin-expressing interneurons linearly control olfactory bulb output. *Neuron*, 80(5), 1218-1231.
- Kawaguchi Y, K. Y. (1996). Physiological and morphological identification of somatostatin- or vasoactive intestinal polypeptide-containing cells among GABAergic cell subtypes in rat frontal cortex. *J Neurosci*, 16(8), 2701-2715.
- Keefe, R. S., Malhotra, A. K., Meltzer, H. Y., Kane, J. M., Buchanan, R. W., Murthy, A., Sovel, M., Li, C., Goldman, R. (2008). Efficacy and safety of donepezil in patients with schizophrenia or schizoaffective disorder: significant placebo/practice effects in a 12-week, randomized, double-blind, placebo-controlled trial. *Neuropsychopharmacology*, 33(6), 1217-1228.
- Kerns, J. G., Cohen, J. D., MacDonald, A. W., 3rd, Johnson, M. K., Stenger, V. A., Aizenstein, H., Carter, C. S. (2005). Decreased conflict- and error-related activity in the anterior cingulate cortex in subjects with schizophrenia. *Am J Psychiatry*, 162(10), 1833-1839.
- Kilman, V., van Rossum, M. C., Turrigiano, G. G. (2002). Activity deprivation reduces miniature IPSC amplitude by decreasing the number of postsynaptic GABA(A) receptors clustered at neocortical synapses. *J Neurosci*, 22(4), 1328-1337.
- Kimoto, S., Bazmi, H. H., Lewis, D. A. (2014). Lower Expression of Glutamic Acid Decarboxylase 67 in the Prefrontal Cortex in Schizophrenia: Contribution of Altered Regulation by Zif268. *Am J Psychiatry*.
- Knapp, M., Mangalore, R., Simon, J. (2004). The global costs of schizophrenia. *Schizophr Bull*, 30(2), 279-293.
- Kole, M. H., Ilschner, S. U., Kampa, B. M., Williams, S. R., Ruben, P. C., Stuart, G. J. (2008). Action potential generation requires a high sodium channel density in the axon initial segment. *Nat Neurosci*, 11(2), 178-186.
- Kolluri, N., Sun, Z., Sampson, A. R., Lewis, D. A. (2005). Lamina-specific reductions in dendritic spine density in the prefrontal cortex of subjects with schizophrenia. *Am J Psychiatry*, 162(6), 1200-1202.
- Konopaske, G. T., Lange, N., Coyle, J. T., Benes, F. M. (2014). Prefrontal cortical dendritic spine pathology in schizophrenia and bipolar disorder. *JAMA psychiatry*, 71(12), 1323-1331.
- Konopaske, G. T., Subburaju, S., Coyle, J. T., Benes, F. M. (2015). Altered prefrontal cortical MARCKS and PPP1R9A mRNA expression in schizophrenia and bipolar disorder. *Schizophr Res*, 164(1-3), 100-108.
- Kristiansen, L. V., Beneyto, M., Haroutunian, V., Meador-Woodruff, J. H. (2006). Changes in NMDA receptor subunits and interacting PSD proteins in dorsolateral prefrontal and anterior cingulate cortex indicate abnormal regional expression in schizophrenia. *Molecular Psychiatry*, 11, 737-747.

- Kubota, Y., Hattori, R., Yui, Y. (1994). Three distinct subpopulations of GABAergic neurons in rat frontal agranular cortex. *Brain Res*, 649(1-2), 159-173.
- Lau, C. G., Murthy, V. N. (2012). Activity-dependent regulation of inhibition via GAD67. *J Neurosci*, 32(25), 8521-8531.
- Lee, S., Kruglikov, I., Huang, Z. J., Fishell, G., Rudy, B. (2013). A disinhibitory circuit mediates motor integration in the somatosensory cortex. *Nat Neurosci*, 16(11), 1662-1670.
- Leitman, D. I., Laukka, P., Juslin, P. N., Saccente, E., Butler, P., Javitt, D. C. (2010). Getting the cue: sensory contributions to auditory emotion recognition impairments in schizophrenia. *Schizophr Bull*, 36(3), 545-556.
- Lesh, T. A., Niendam, T. A., Minzenberg, M. J., Carter, C. S. (2011). Cognitive control deficits in schizophrenia: mechanisms and meaning. *Neuropsychopharmacology*, 36(1), 316-338.
- Levinson, D. F., Duan, J., Oh, S., Wang, K., Sanders, A. R., Shi, J., Zhang, N., Mowry, B. J., Olincy, A., Amin, F., Cloninger, C. R., Silverman, J. M., Buccola, N. G., Byerley, W. F., Black, D. W., Kendler, K. S., Freedman, R., Dudbridge, F., Pe'er, I., Hakonarson, H., Bergen, S. E., Fanous, A. H., Holmans, P. A., Gejman, P. V. (2011). Copy number variants in schizophrenia: confirmation of five previous findings and new evidence for 3q29 microdeletions and VIPR2 duplications. *Am J Psychiatry*, 168(3), 302-316.
- Levy, R., Goldman-Rakic, P. S. (1999). Association of storage and processing functions in the dorsolateral prefrontal cortex of the nonhuman primate. *J Neurosci*, 19(12), 5149-5158.
- Lewis, D. A. (2011). The chandelier neuron in schizophrenia. *Developmental neurobiology*, 71(1), 118-127.
- Lewis, D. A. (2014). Inhibitory neurons in human cortical circuits: substrate for cognitive dysfunction in schizophrenia. *Curr Opin Neurobiol*, 26, 22-26.
- Lewis, D. A., Cruz, D. A., Melchitzky, D. S., Pierri, J. N. (2001). Lamina-specific deficits in parvalbumin-immunoreactive varicosities in the prefrontal cortex of subjects with schizophrenia: Evidence for fewer projections from the thalamus. *Am J Psychiatry*, 158(9), 1411-1422.
- Lewis, D. A., Curley, A. A., Glausier, J. R., Volk, D. W. (2012). Cortical parvalbumin interneurons and cognitive dysfunction in schizophrenia. *Trends Neurosci*, 35(1), 57-67.
- Lewis, D. A., Hashimoto, T., Volk, D. W. (2005). Cortical inhibitory neurons and schizophrenia. *Nat Rev Neurosci*, 6(4), 312-324.
- Lewis, D. A., Lieberman, J. A. (2000). Catching up on schizophrenia: natural history and neurobiology. *Neuron*, 28(2), 325-334.

- Lewis, D. A., Lund, J. S. (1990). Heterogeneity of chandelier neurons in monkey neocortex: corticotropin-releasing factor- and parvalbumin-immunoreactive populations. *J Comp Neurol*, 293(4), 599-615.
- Lovett-Barron, M., Turi, G. F., Kaifosh, P., Lee, P. H., Bolze, F., Sun, X. H., Nicoud, J. F., Zemelman, B. V., Sternson, S. M., Losonczy, A. (2012). Regulation of neuronal input transformations by tunable dendritic inhibition. *Nat Neurosci*, 15(3), 423-430, S421-423.
- Lund, J. S., Lund, R. D., Hendrickson, A. E., Bunt, A. H., Fuchs, A. F. (1975). The origin of efferent pathways from the primary visual cortex, area 17, of the macaque monkey as shown by retrograde transport of horseradish peroxidase. *The Journal of Comparative Neurology*, 164, 287-304.
- MacCabe, J. H., Lambe, M. P., Cnattingius, S., Torrang, A., Bjork, C., Sham, P. C., David, A. S., Murray, R. M., Hultman, C. M. (2008). Scholastic achievement at age 16 and risk of schizophrenia and other psychoses: a national cohort study. *Psychol Med*, 38(8), 1133-1140.
- MacDonald, A. W., 3rd, Cohen, J. D., Stenger, V. A., Carter, C. S. (2000). Dissociating the role of the dorsolateral prefrontal and anterior cingulate cortex in cognitive control. *Science*, 288(5472), 1835-1838.
- Maletic-Savatic, M., Malinow, R., Svoboda, K. (1999). Rapid dendritic morphogenesis in CA1 hippocampal dendrites induced by synaptic activity. *Science*, 283(5409), 1923-1927.
- McIntire, S. L., Reimer, R. J., Schuske, K., Edwards, R. H., Jorgensen, E. M. (1997). Identification and characterization of the vesicular GABA transporter. *Nature*, 389(6653), 870-876.
- McKinney, R. A., Capogna, M., Durr, R., Gahwiler, B. H., Thompson, S. M. (1999). Miniature synaptic events maintain dendritic spines via AMPA receptor activation. *Nat Neurosci*, 2(1), 44-49.
- Medalla, M., Barbas, H. (2009). Synapses with inhibitory neurons differentiate anterior cingulate from dorsolateral prefrontal pathways associated with cognitive control. *Neuron*, 61(4), 609-620.
- Medalla, M., Barbas, H. (2010). Anterior cingulate synapses in prefrontal areas 10 and 46 suggest differential influence in cognitive control. *J Neurosci*, 30(48), 16068-16081.
- Meeks, J. P., Mennerick, S. (2007). Action potential initiation and propagation in CA3 pyramidal axons. *J Neurophysiol*, 97(5), 3460-3472.
- Melchitzky, D. S., Egan, S. M., Lewis, D. A. (2005). Synaptic targets of calretinin-containing axon terminals in macaque monkey prefrontal cortex. *Neuroscience*, 130(1), 185-195.

- Melchitzky, D. S., Gonzalez-Burgos, G., Barrionuevo, G., Lewis, D. A. (2001). Synaptic targets of the intrinsic axon collaterals of supragranular pyramidal neurons in monkey prefrontal cortex. *J Comp Neurol*, 430(2), 209-221.
- Melchitzky, D. S., Lewis, D. A. (2003). Pyramidal neuron local axon terminals in monkey prefrontal cortex: differential targeting of subclasses of GABA neurons. *Cereb Cortex*, 13, 452-460.
- Melchitzky, D. S., Lewis, D. A. (2008). Dendritic-targeting GABA neurons in monkey prefrontal cortex: comparison of somatostatin- and calretinin-immunoreactive axon terminals. *Synapse*, 62(6), 456-465.
- Melchitzky, D. S., Sesack, S. R., Lewis, D. A. (1999). Parvalbumin-immunoreactive axon terminals in macaque monkey and human prefrontal cortex: laminar, regional, and target specificity of type I and type II synapses. *J Comp Neurol*, 408(1), 11-22.
- Melchitzky, D. S., Sesack, S. R., Pucak, M. L., Lewis, D. A. (1998). Synaptic targets of pyramidal neurons providing intrinsic horizontal connections in monkey prefrontal cortex. *J Comp Neurol*, 390(2), 211-224.
- Mellios, N., Huang, H. S., Baker, S. P., Galdzicka, M., Ginns, E., Akbarian, S. (2009). Molecular determinants of dysregulated GABAergic gene expression in the prefrontal cortex of subjects with schizophrenia. *Biol Psychiatry*, 65(12), 1006-1014.
- Micheva, K. D., Smith, S. J. (2007). Array tomography: a new tool for imaging the molecular architecture and ultrastructure of neural circuits. *Neuron*, 55(1), 25-36.
- Miller, E. K., Cohen, J. D. (2001). An integrative theory of prefrontal cortex function. *Annual Review of Neuroscience*, 24, 167-202.
- Minzenberg, M. J., Firl, A. J., Yoon, J. H., Gomes, G. C., Reinking, C., Carter, C. S. (2010). Gamma oscillatory power is impaired during cognitive control independent of medication status in first-episode schizophrenia. *Neuropsychopharmacology*, 35(13), 2590-2599.
- Minzenberg, M. J., Laird, A. R., Thelen, S., Carter, C. S., Glahn, D. C. (2009). Meta-analysis of 41 functional neuroimaging studies of executive function in schizophrenia. *Arch Gen Psychiatry*, 66(8), 811-822.
- Molnar, G., Olah, S., Komlosi, G., Fule, M., Szabadics, J., Varga, C., Barzo, P., Tamas, G. (2008). Complex events initiated by individual spikes in the human cerebral cortex. *PLoS Biol*, 6(9), e222.
- Morris, H. M., Hashimoto, T., Lewis, D. A. (2008). Alterations in somatostatin mRNA expression in the dorsolateral prefrontal cortex of subjects with schizophrenia or schizoaffective disorder. *Cereb Cortex*, 18(7), 1575-1587.

- Moyer, C. E., Delevich, K. M., Fish, K. N., Asafu-Adjei, J. K., Sampson, A. R., Dorph-Petersen, K. A., Lewis, D. A., Sweet, R. A. (2012). Reduced Glutamate Decarboxylase 65 Protein Within Primary Auditory Cortex Inhibitory Boutons in Schizophrenia. *Biol Psychiatry*.
- Neske, G. T., Patrick, S. L., Connors, B. W. (2015). Contributions of diverse excitatory and inhibitory neurons to recurrent network activity in cerebral cortex. *J Neurosci*, 35(3), 1089-1105.
- Ohnuma, T., Kato, H., Arai, H., Faull, R. L., McKenna, P. J., Emson, P. C. (2000). Gene expression of PSD95 in prefrontal cortex and hippocampus in schizophrenia. *Neuroreport*, 11(14), 3133-3137.
- Overstreet, L. S., Westbrook, G. L. (2003). Synapse density regulates independence at unitary inhibitory synapses. *J Neurosci*, 23(7), 2618-2626.
- Pakkenberg, B. (1990). Pronounced reduction of total neuron number in mediodorsal thalamic nucleus and nucleus accumbens in schizophrenics. *Arch Gen Psychiatry*, 47(11), 1023-1028.
- Palmer, L. M., Stuart, G. J. (2006). Site of action potential initiation in layer 5 pyramidal neurons. *J Neurosci*, 26(6), 1854-1863.
- Patz, S., Wirth, M. J., Gorba, T., Klostermann, O., Wahle, P. (2003). Neuronal activity and neurotrophic factors regulate GAD-65/67 mRNA and protein expression in organotypic cultures of rat visual cortex. *Eur J Neurosci*, 18(1), 1-12.
- Perlstein, W. M., Dixit, N. K., Carter, C. S., Noll, D. C., Cohen, J. D. (2003). Prefrontal cortex dysfunction mediates deficits in working memory and prepotent responding in schizophrenia. *Biol Psychiatry*, 53(1), 25-38.
- Petanjek, Z., Judas, M., Simic, G., Rasin, M. R., Uylings, H. B., Rakic, P., Kostovic, I. (2011). Extraordinary neoteny of synaptic spines in the human prefrontal cortex. *Proc Natl Acad Sci U S A*, 108(32), 13281-13286.
- Petrides, M. (2000). The role of the mid-dorsolateral prefrontal cortex in working memory. *Exp Brain Res*, 133(1), 44-54.
- Petrides, M., Alivisatos, B., Evans, A. C., Meyer, E. (1993). Dissociation of human mid-dorsolateral from posterior dorsolateral frontal cortex in memory processing. *Proceedings of the National Academy of Sciences USA*, 90, 873-877.
- Pfeffer, C. K., Xue, M., He, M., Huang, Z. J., Scanziani, M. (2013). Inhibition of inhibition in visual cortex: the logic of connections between molecularly distinct interneurons. *Nat Neurosci*, 16(8), 1068-1076.
- Philpot, B. D., Lim, J. H., Brunjes, P. C. (1997). Activity-dependent regulation of calcium-binding proteins in the developing rat olfactory bulb. *J Comp Neurol*, 387(1), 12-26.

- Pi, H. J., Hangya, B., Kvitsiani, D., Sanders, J. I., Huang, Z. J., Kepecs, A. (2013). Cortical interneurons that specialize in disinhibitory control. *Nature*.
- Pierri, J. N., Chaudry, A. S., Woo, T. U., Lewis, D. A. (1999). Alterations in chandelier neuron axon terminals in the prefrontal cortex of schizophrenic subjects. *Am J Psychiatry*, 156(11), 1709-1719.
- Pierri, J. N., Volk, C. L., Auh, S., Sampson, A., Lewis, D. A. (2001). Decreased somal size of deep layer 3 pyramidal neurons in the prefrontal cortex of subjects with schizophrenia. *Arch Gen Psychiatry*, 58(5), 466-473.
- Pierri, J. N., Volk, C. L., Auh, S., Sampson, A., Lewis, D. A. (2003). Somal size of prefrontal cortical pyramidal neurons in schizophrenia: differential effects across neuronal subpopulations. *Biol Psychiatry*, 54(2), 111-120.
- Popken, G. J., Bunney, W. E., Jr., Potkin, S. G., Jones, E. G. (2000). Subnucleus-specific loss of neurons in medial thalamus of schizophrenics. *Proc Natl Acad Sci U S A*, 97(16), 9276-9280.
- Quintana, J., Wong, T., Ortiz-Portillo, E., Marder, S. R., Mazziotta, J. C. (2004). Anterior cingulate dysfunction during choice anticipation in schizophrenia. *Psychiatry Res*, 132(2), 117-130.
- Rainer, G., Asaad, W. F., Miller, E. K. (1998). Selective representation of relevant information by neurons in the primate prefrontal cortex. *Nature*, 393, 577-579.
- Rajkowska, G., Selemon, L. D., Goldman-Rakic, P. S. (1998). Neuronal and glial somal size in the prefrontal cortex: a postmortem morphometric study of schizophrenia and Huntington disease. *Arch Gen Psychiatry*, 55(3), 215-224.
- Rao, S. G., Williams, G. V., Goldman-Rakic, P. S. (2000). Destruction and creation of spatial tuning by disinhibition: GABA A blockade of prefrontal cortical neurons engaged by working memory. *The Journal of Neuroscience*, 20, 485-494.
- Reichenberg, A., Caspi, A., Harrington, H., Houts, R., Keefe, R. S., Murray, R. M., Poulton, R., Moffitt, T. E. (2010). Static and dynamic cognitive deficits in childhood preceding adult schizophrenia: a 30-year study. *Am J Psychiatry*, 167(2), 160-169.
- Ridler, T. W., Calvard, S. (1978). Picture thresholding using an iterative selection method. *IEEE Transactions on Systems, Man, and Cybernetics*, SMC-8, 630-632.
- Rimvall, K., Martin, D. L. (1994). The level of GAD67 protein is highly sensitive to small increases in intraneuronal gamma-aminobutyric acid levels. *J Neurochem*, 62(4), 1375-1381.
- Rocco, B. R., Sweet, R. A., Lewis, D. A., Fish, K. N. (2015). GABA synthesizing enzymes in calbindin and calretinin neurons in monkey prefrontal cortex. *Cereb Cortex*, In Press.

- Rocco, B. R., Sweet, R. A., Lewis, D. A., Fish, K. N. (2015). GABA-Synthesizing Enzymes in Calbindin and Calretinin Neurons in Monkey Prefrontal Cortex. *Cereb Cortex*.
- Rogers, J. H. (1992). Immunohistochemical markers in rat cortex: co-localization of calretinin and calbindin-D28k with neuropeptides and GABA. *Brain Res*, 587(1), 147-157.
- Rotaru, D. C., Barrionuevo, G., Sesack, S. R. (2005). Mediodorsal thalamic afferents to layer III of the rat prefrontal cortex: synaptic relationships to subclasses of interneurons. *J Comp Neurol*, 490(3), 220-238.
- Roux, F., Wibral, M., Mohr, H. M., Singer, W., Uhlhaas, P. J. (2012). Gamma-band activity in human prefrontal cortex codes for the number of relevant items maintained in working memory. *J Neurosci*, 32(36), 12411-12420.
- Sauer, J. F., Struber, M., Bartos, M. (2012). Interneurons provide circuit-specific depolarization and hyperpolarization. *J Neurosci*, 32(12), 4224-4229.
- Schizophrenia Working Group of the Psychiatric Genomics, C. (2014). Biological insights from 108 schizophrenia-associated genetic loci. *Nature*, 511(7510), 421-427.
- Schultz, C. C., Koch, K., Wagner, G., Nenadic, I., Schachtzabel, C., Gullmar, D., Reichenbach, J. R., Sauer, H., Schlosser, R. G. (2012). Reduced anterior cingulate cognitive activation is associated with prefrontal-temporal cortical thinning in schizophrenia. *Biol Psychiatry*, 71(2), 146-153.
- Serwanski, D. R., Miralles, C. P., Christie, S. B., Mehta, A. K., Li, X., De Blas, A. L. (2006). Synaptic and nonsynaptic localization of GABAA receptors containing the alpha5 subunit in the rat brain. *J Comp Neurol*, 499(3), 458-470.
- Sheikh, S. N., Martin, D. L. (1998). Elevation of brain GABA levels with vigabatrin (gamma-vinylGABA) differentially affects GAD65 and GAD67 expression in various regions of rat brain. *J Neurosci Res*, 52(6), 736-741.
- Silver, H. (2003). Selective serotonin reuptake inhibitor augmentation in the treatment of negative symptoms of schizophrenia. *Int Clin Psychopharmacol*, 18(6), 305-313.
- Silver, H., Barash, I., Aharon, N., Kaplan, A., Poyurovsky, M. (2000). Fluvoxamine augmentation of antipsychotics improves negative symptoms in psychotic chronic schizophrenic patients: a placebo-controlled study. *Int Clin Psychopharmacol*, 15(5), 257-261.
- Silver, H., Nassar, A. (1992). Fluvoxamine improves negative symptoms in treated chronic schizophrenia: an add-on double-blind, placebo-controlled study. *Biol Psychiatry*, 31(7), 698-704.
- Sodhi, M. S., Simmons, M., McCullumsmith, R., Haroutunian, V., Meador-Woodruff, J. H. (2011). Glutamatergic gene expression is specifically reduced in thalamocortical projecting relay neurons in schizophrenia. *Biol Psychiatry*, 70(7), 646-654.

- Sohal, V. S., Zhang, F., Yizhar, O., Deisseroth, K. (2009). Parvalbumin neurons and gamma rhythms enhance cortical circuit performance. *Nature*, 459(7247), 698-702.
- Somenarain, L., Jones, L. B. (2010). A comparative study of MAP2 immunostaining in areas 9 and 17 in schizophrenia and Huntington chorea. *J Psychiatr Res*, 44(11), 694-699.
- Staiger, J. F., Masannek, C., Schleicher, A., Zuschratter, W. (2004). Calbindin-containing interneurons are a target for VIP-immunoreactive synapses in rat primary somatosensory cortex. *J Comp Neurol*, 468(2), 179-189.
- Stone, D. J., Walsh, J., Benes, F. M. (1999). Localization of cells preferentially expressing GAD(67) with negligible GAD(65) transcripts in the rat hippocampus. A double in situ hybridization study. *Brain Res.Mol.Brain Res.*, 71(2), 201-209.
- Straub, R. E., Lipska, B. K., Egan, M. F., Goldberg, T. E., Callicott, J. H., Mayhew, M. B., Vakkalanka, R. K., Kolachana, B. S., Kleinman, J. E., Weinberger, D. R. (2007). Allelic variation in GAD1 (GAD67) is associated with schizophrenia and influences cortical function and gene expression. *Mol Psychiatry*, 12(9), 854-869.
- Strous, R. D., Cowan, N., Ritter, W., Javitt, D. C. (1995). Auditory sensory ("echoic") memory dysfunction in schizophrenia. *Am J Psychiatry*, 152(10), 1517-1519.
- Sugino, K., Hempel, C. M., Miller, M. N., Hattox, A. M., Shapiro, P., Wu, C., Huang, Z. J., Nelson, S. B. (2006). Molecular taxonomy of major neuronal classes in the adult mouse forebrain. *Nat Neurosci*, 9(1), 99-107.
- Swanwick, C. C., Murthy, N. R., Kapur, J. (2006). Activity-dependent scaling of GABAergic synapse strength is regulated by brain-derived neurotrophic factor. *Mol Cell Neurosci*, 31(3), 481-492.
- Sweet, R. A., Bergen, S. E., Sun, Z., Sampson, A. R., Pierri, J. N., Lewis, D. A. (2004). Pyramidal cell size reduction in schizophrenia: evidence for involvement of auditory feedforward circuits. *Biol Psychiatry*, 55(12), 1128-1137.
- Sweet, R. A., Henteleff, R. A., Zhang, W., Sampson, A. R., Lewis, D. A. (2009). Reduced dendritic spine density in auditory cortex of subjects with schizophrenia. *Neuropsychopharmacology*, 34(2), 374-389.
- Sweet, R. A., Pierri, J. N., Auh, S., Sampson, A. R., Lewis, D. A. (2003). Reduced pyramidal cell somal volume in auditory association cortex of subjects with schizophrenia. *Neuropsychopharmacology*, 28(3), 599-609.
- Swerdlow, N. R., Light, G. A., Cadenhead, K. S., Sprock, J., Hsieh, M. H., Braff, D. L. (2006). Startle gating deficits in a large cohort of patients with schizophrenia: relationship to medications, symptoms, neurocognition, and level of function. *Arch Gen Psychiatry*, 63(12), 1325-1335.

- Szabadics, J., Varga, C., Molnar, G., Olah, S., Barzo, P., Tamas, G. (2006). Excitatory effect of GABAergic axo-axonic cells in cortical microcircuits. *Science*, 311(5758), 233-235.
- Szentagothai, J., Arbib, M. (1974). Conceptual models of neural organization. *Neurosci.Res.Program Bull.*, 12, 307-510.
- Tandon, R., Nasrallah, H. A., Keshavan, M. S. (2009). Schizophrenia, "just the facts" 4. Clinical features and conceptualization. *Schizophr Res*, 110(1-3), 1-23.
- Tang, B., Dean, B., Thomas, E. A. (2011). Disease- and age-related changes in histone acetylation at gene promoters in psychiatric disorders. *Translational psychiatry*, 1, e64.
- Taniguchi, H., Lu, J., Huang, Z. J. (2013). The spatial and temporal origin of chandelier cells in mouse neocortex. *Science*, 339(6115), 70-74.
- Tanila, H., Carlson, S., Linnankoski, I., Lindroos, F., Kahila, H. (1992). Functional properties of dorsolateral prefrontal cortical neurons in awake monkey. *Behav Brain Res*, 47(2), 169-180.
- Tanji, J., Hoshi, E. (2008). Role of the lateral prefrontal cortex in executive behavioral control. *Physiol Rev*, 88(1), 37-57.
- Thune, J. J., Uylings, H. B. M., Pakkenberg, B. (2001). No deficit in total number of neurons in the prefrontal cortex in schizophrenics. *J.Psychiatr.Res.*, 35, 15-21.
- Tobias, T. J. (1975). Afferents to prefrontal cortex from the thalamic mediodorsal nucleus in the rhesus monkey. *Brain Res*, 83(2), 191-212.
- Tyan, L., Chamberland, S., Magnin, E., Camire, O., Francavilla, R., David, L. S., Deisseroth, K., Topolnik, L. (2014). Dendritic inhibition provided by interneuron-specific cells controls the firing rate and timing of the hippocampal feedback inhibitory circuitry. *J Neurosci*, 34(13), 4534-4547.
- Urban-Ciecko, J., Fanselow, E. E., Barth, A. L. (2015). Neocortical Somatostatin Neurons Reversibly Silence Excitatory Transmission via GABA_B Receptors. *Curr Biol*, 25(6), 722-731.
- Vacic, V., McCarthy, S., Malhotra, D., Murray, F., Chou, H. H., Peoples, A., Makarov, V., Yoon, S., Bhandari, A., Corominas, R., Iakoucheva, L. M., Krastoshevsky, O., Krause, V., Larach-Walters, V., Welsh, D. K., Craig, D., Kelsoe, J. R., Gershon, E. S., Leal, S. M., Dell Aquila, M., Morris, D. W., Gill, M., Corvin, A., Insel, P. A., McClellan, J., King, M. C., Karayiorgou, M., Levy, D. L., DeLisi, L. E., Sebat, J. (2011). Duplications of the neuropeptide receptor gene VIPR2 confer significant risk for schizophrenia. *Nature*, 471(7339), 499-503.
- van Oel, C. J., Sitskoorn, M. M., Cremer, M. P., Kahn, R. S. (2002). School performance as a premorbid marker for schizophrenia: a twin study. *Schizophr Bull*, 28(3), 401-414.

- Volk, D. W., Austin, M. C., Pierri, J. N., Sampson, A. R., Lewis, D. A. (2000). Decreased glutamic acid decarboxylase67 messenger RNA expression in a subset of prefrontal cortical gamma-aminobutyric acid neurons in subjects with schizophrenia. *Arch Gen Psychiatry*, 57(3), 237-245.
- Volk, D. W., Matsubara, T., Li, S., Sengupta, E. J., Georgiev, D., Minabe, Y., Sampson, A., Hashimoto, T., Lewis, D. A. (2012). Deficits in transcriptional regulators of cortical parvalbumin neurons in schizophrenia. *Am J Psychiatry*, 169(10), 1082-1091.
- Volk, D. W., Pierri, J. N., Fritschy, J. M., Auh, S., Sampson, A. R., Lewis, D. A. (2002). Reciprocal alterations in pre- and postsynaptic inhibitory markers at chandelier cell inputs to pyramidal neurons in schizophrenia. *Cerebral Cortex*, 12(10), 1063-1070.
- Wang, Y., Toledo-Rodriguez, M., Gupta, A., Wu, C., Silberberg, G., Luo, J., Markram, H. (2004). Anatomical, physiological and molecular properties of Martinotti cells in the somatosensory cortex of the juvenile rat. *J Physiol*, 561(Pt 1), 65-90.
- Watanabe, M. (1990). Prefrontal unit activity during associative learning in the monkey. *Exp Brain Res*, 80(2), 296-309.
- Weinberger, D. R., Berman, K. F., Illowsky, B. P. (1988). Physiological dysfunction of dorsolateral prefrontal cortex in schizophrenia: III. A new cohort and evidence for a monoaminergic mechanism. *Archives of General Psychiatry*, 45, 609-615.
- Weinberger, D. R., Berman, K. F., Zec, R. F. (1986). Physiologic dysfunction of dorsolateral prefrontal cortex in schizophrenia. I. Regional cerebral blood flow evidence. *Archives of General Psychiatry*, 43, 114-124.
- Woo, T. U., Whitehead, R. E., Melchitzky, D. S., Lewis, D. A. (1998). A subclass of prefrontal gamma-aminobutyric acid axon terminals are selectively altered in schizophrenia. *Proc Natl Acad Sci U S A*, 95(9), 5341-5346.
- Woodruff, A. R., McGarry, L. M., Vogels, T. P., Inan, M., Anderson, S. A., Yuste, R. (2011). State-dependent function of neocortical chandelier cells. *J Neurosci*, 31(49), 17872-17886.
- Wu, E. Q., Birnbaum, H. G., Shi, L., Ball, D. E., Kessler, R. C., Moulis, M., Aggarwal, J. (2005). The economic burden of schizophrenia in the United States in 2002. *J Clin Psychiatry*, 66(9), 1122-1129.
- Xie, Z., Haganir, R. L., Penzes, P. (2005). Activity-dependent dendritic spine structural plasticity is regulated by small GTPase Rap1 and its target AF-6. *Neuron*, 48(4), 605-618.
- Xie, Z., Srivastava, D. P., Photowala, H., Kai, L., Cahill, M. E., Woolfrey, K. M., Shum, C. Y., Surmeier, D. J., Penzes, P. (2007). Kalirin-7 controls activity-dependent structural and functional plasticity of dendritic spines. *Neuron*, 56(4), 640-656.

- Xu, H., Jeong, H.-Y., Tremblay, R., Rudy, B. (2013). Neocortical Somatostatin-Expressing GABAergic Interneurons Disinhibit the Thalamorecipient Layer 4. *Neuron*, 77(1), 155-167.
- Xu, X., Callaway, E. M. (2009). Laminar specificity of functional input to distinct types of inhibitory cortical neurons. *J Neurosci*, 29(1), 70-85.
- Yoon, J. H., Maddock, R. J., Rokem, A., Silver, M. A., Minzenberg, M. J., Ragland, J. D., Carter, C. S. (2010). GABA concentration is reduced in visual cortex in schizophrenia and correlates with orientation-specific surround suppression. *J Neurosci*, 30(10), 3777-3781.
- Yoon, J. H., Rokem, A. S., Silver, M. A., Minzenberg, M. J., Ursu, S., Ragland, J. D., Carter, C. S. (2009). Diminished orientation-specific surround suppression of visual processing in schizophrenia. *Schizophr Bull*, 35(6), 1078-1084.
- Young, K. A., Manaye, K. F., Liang, C., Hicks, P. B., German, D. C. (2000). Reduced number of mediodorsal and anterior thalamic neurons in schizophrenia. *Biol Psychiatry*, 47(11), 944-953.
- Yuan, J., Jin, C., Sha, W., Zhou, Z., Zhang, F., Wang, M., Wang, J., Li, J., Feng, X., Yu, S., Wang, J. (2014). A competitive PCR assay confirms the association of a copy number variation in the VIPR2 gene with schizophrenia in Han Chinese. *Schizophr Res*, 156(1), 66-70.
- Yucel, M., Brewer, W. J., Harrison, B. J., Fornito, A., O'Keefe, G. J., Olver, J., Scott, A. M., Egan, G. F., Velakoulis, D., McGorry, P. D., Pantelis, C. (2007). Anterior cingulate activation in antipsychotic-naive first-episode schizophrenia. *Acta Psychiatr Scand*, 115(2), 155-158.